A NIKA2 perspective on the interstellar dust properties of NGC 4254

LARA PANTONI (POSTDOC, UGENT, BELGIUM) ON BEHALF OF NIKA2 COLLABORATION

Overview

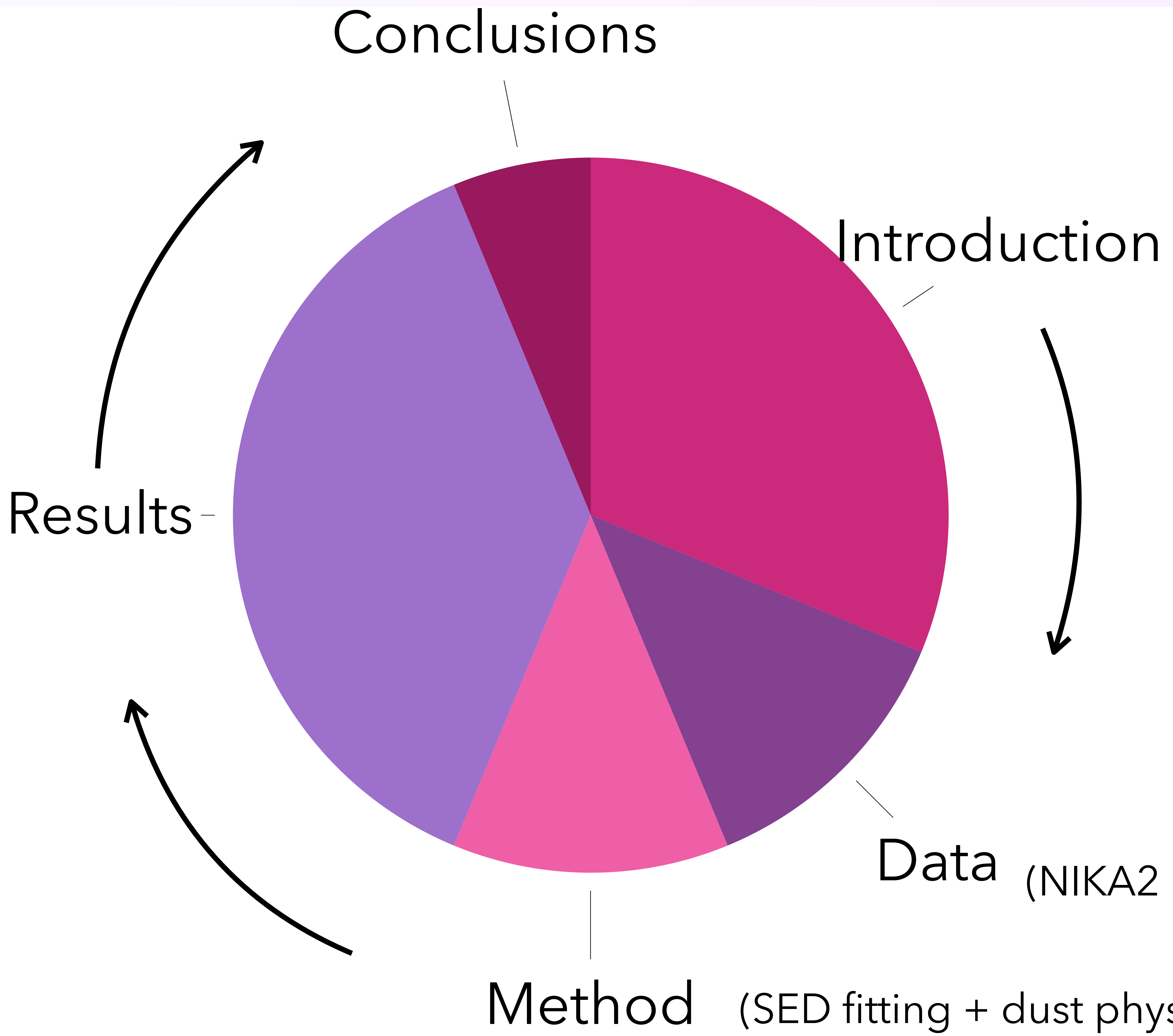

1) Interstellar dust in galaxies;
2) the role of Nearby Galaxies;
3) IMEGIN Large Program.

(NIKA2 maps + ancillary data)

(SED fitting + dust physical model)

1) Global scale;
2) disk, arms, bulge;
3) ~ kpc scale.

Interstellar dust in galaxies

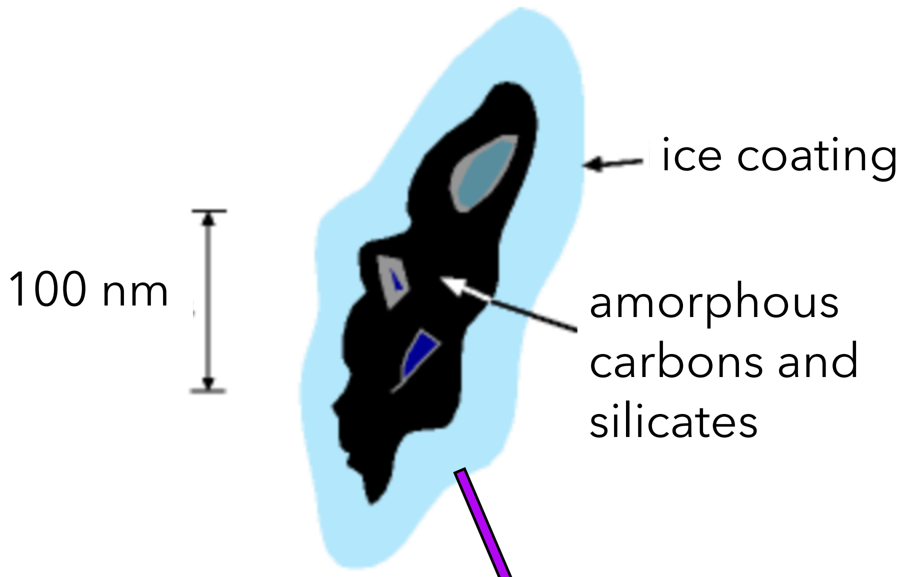

1. Dust grains in the ISM have sizes of **tens of nm** and constitute **~ 1%** of the total **ISM mass**.

2. In the ISM, dust grains undergo a variety of processes which **alter** their **size** distribution, **chemical composition** and **abundance**.

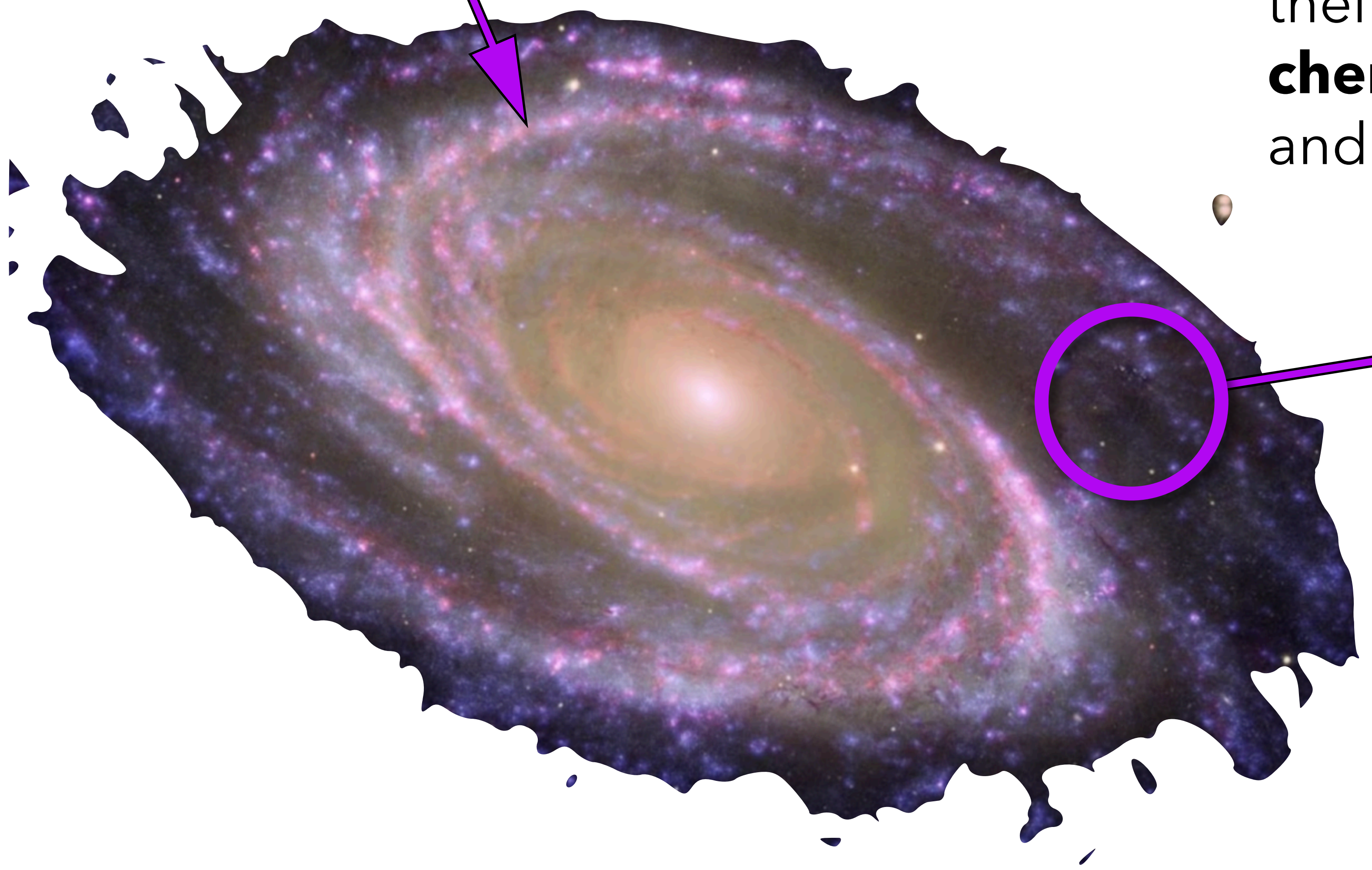

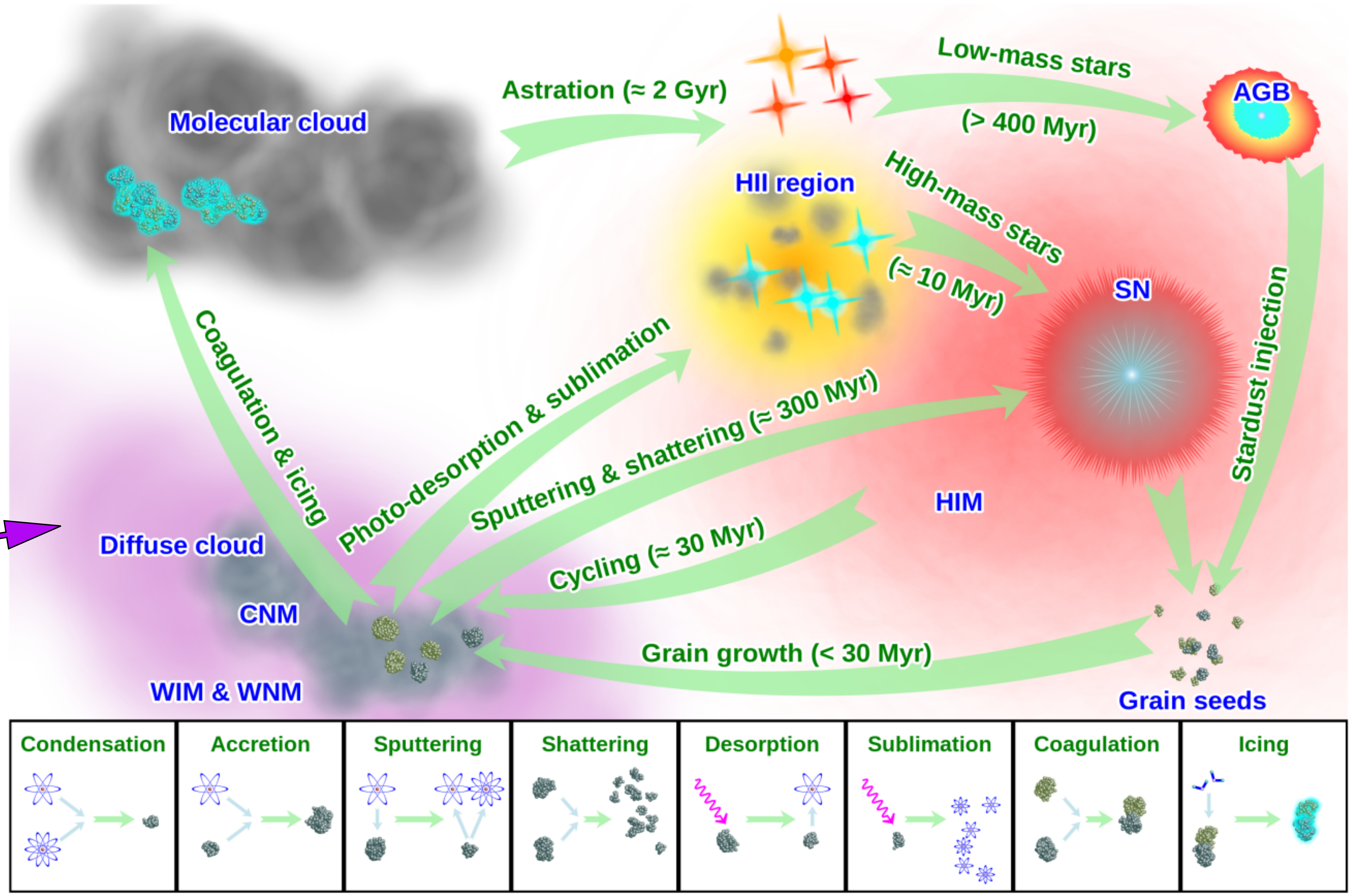

References: Mathis et al. 1977; Galliano et al. 2018; Draine & Hensley 2022

Credits: www.astronomynotes.com; NASA/JPL-CALTECH/ESA/HARVARD-SMITHSONIAN CFA; F. Galliano

Interstellar dust in galaxies

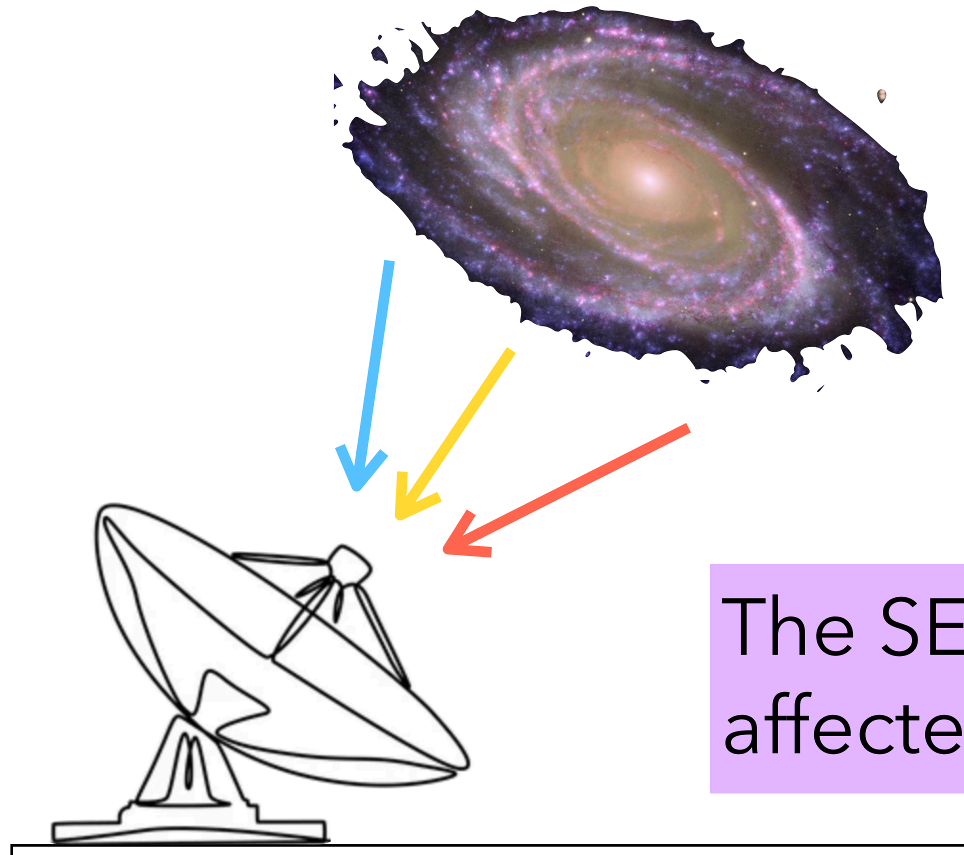

The SED of galaxies is strongly affected by the presence of dust.

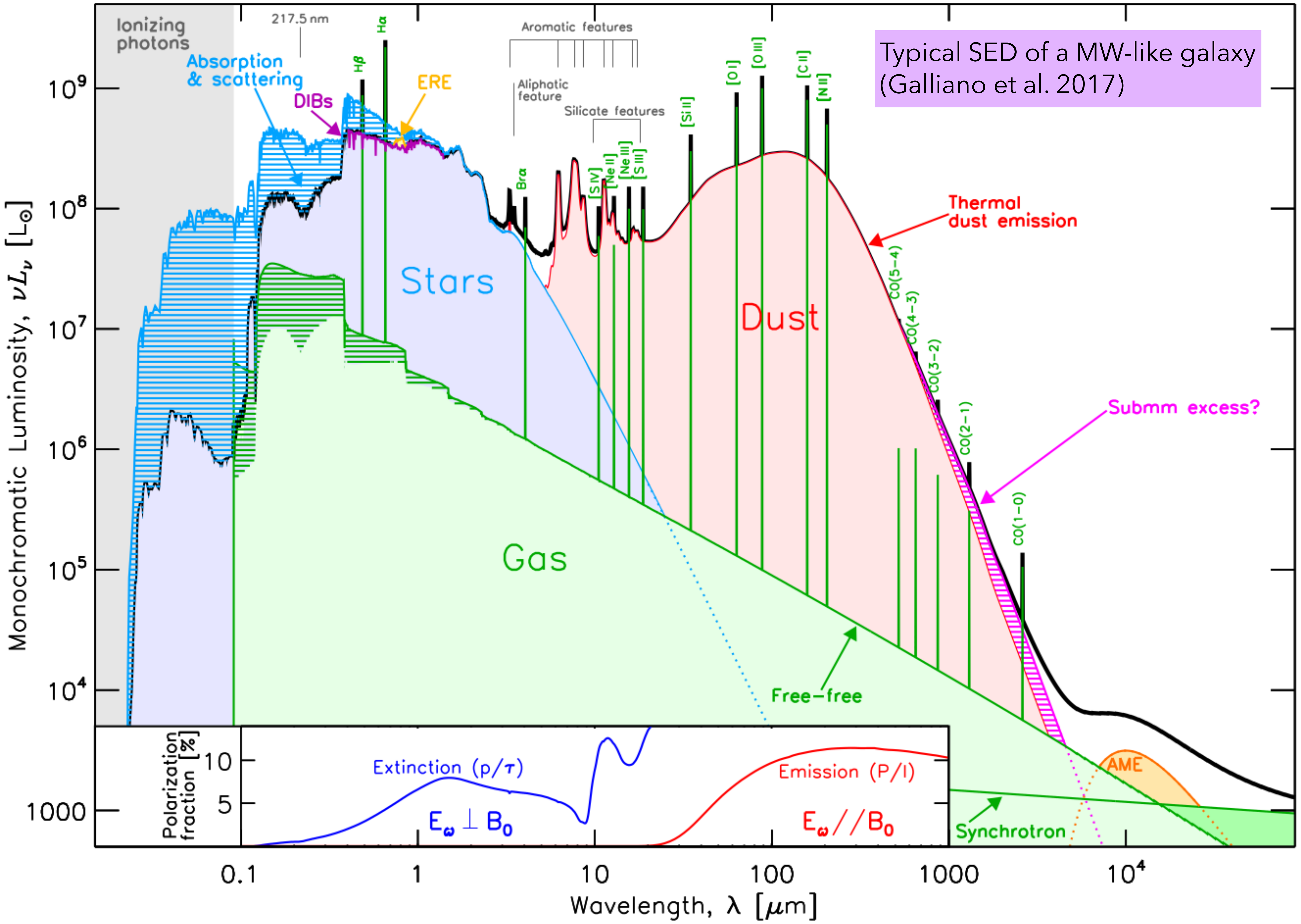

1. Dust grains **absorb** and **re-radiate** ~30% of **stellar power in the IR** (through scattering, absorption, extinction).
2. **Large grains**, which dominate the dust mass budget, are responsible for the **thermal emission** in the **FIR**.
3. **Small grains**, out of thermal equilibrium, are responsible for the **MIR features**.
4. In the mm regime, the **sub-mm excess** and the **AME** are linked to the presence of very cold dust and spinning grains (Galliano+18; Ysard+22).

Credits: NASA/JPL-CALTECH/ESA/HARVARD-SMITHSONIAN CFA

Why Nearby Galaxies?

Most of our knowledge of interstellar dust properties comes from studies of the **Milky Way**.
(Draine 2003a; Galliano, Galametz & Jones 2018)

However these studies are affected by
- confusion along the sightline;
- MW hosting limited range of environmental conditions (e.g. no AGN, limited Z, …).

Instead, **Nearby Galaxies** (< 100 Mpc) can provide **unique constraints** on interstellar dust properties:
(Galliano, Galametz & Jones 2018)

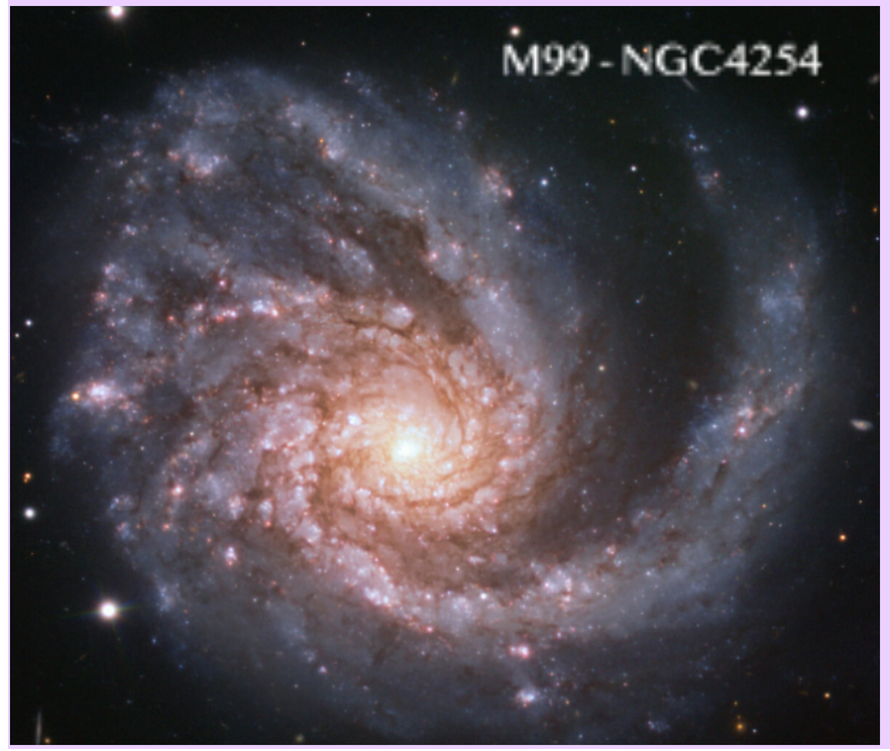

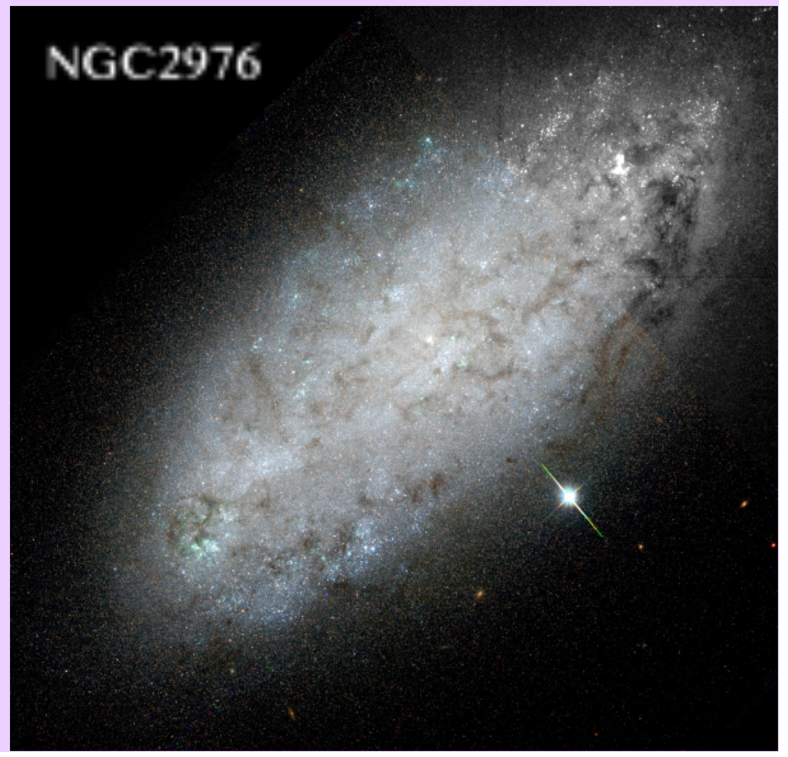

Credits : NASA/ESA Hubble Space Telescope

- face-on galaxies ⟶ clearer sightline.
- edge-on galaxies ⟶ high vertical distances.
- blue dwarfs, bright AGNs, low Z objects ⟶ probe interstellar dust in extreme conditions.
- intermediate step towards understanding interstellar dust and interstellar medium in distant galaxies.

IMEGIN Large Program

IMEGIN (Interpreting the Millimeter Emission of Galaxies with IRAM-30m/NIKA2) is a **NIKA2 Guaranteed Time Large Program** (**~ 200 hours** of observing time) targeting **22 nearby galaxy** (priority A).

Katsioli et al. 2023 (A&A)

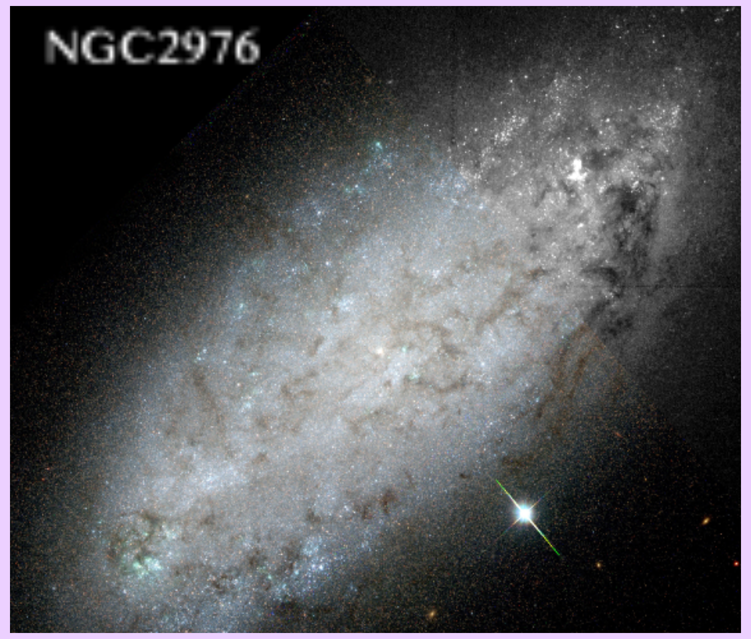

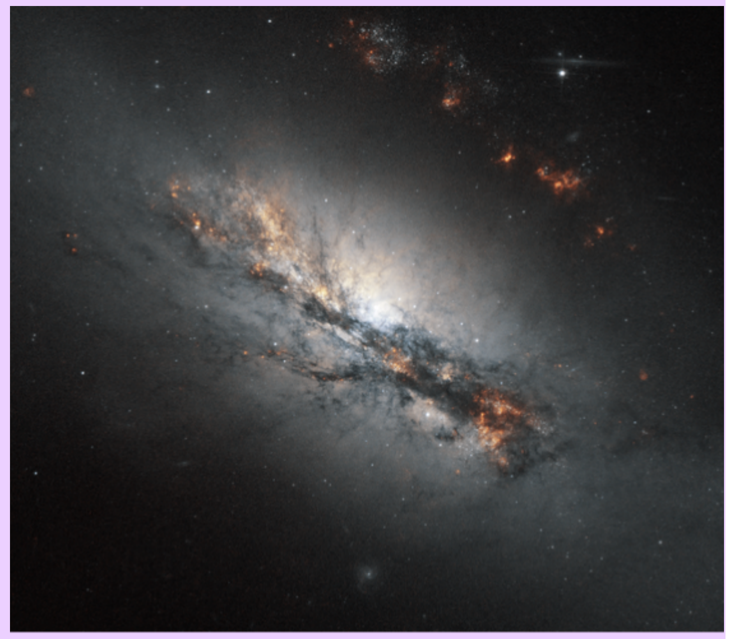

Ejlali et al. 2025 (A&A)

Katsioli et al. 2025 in prep.

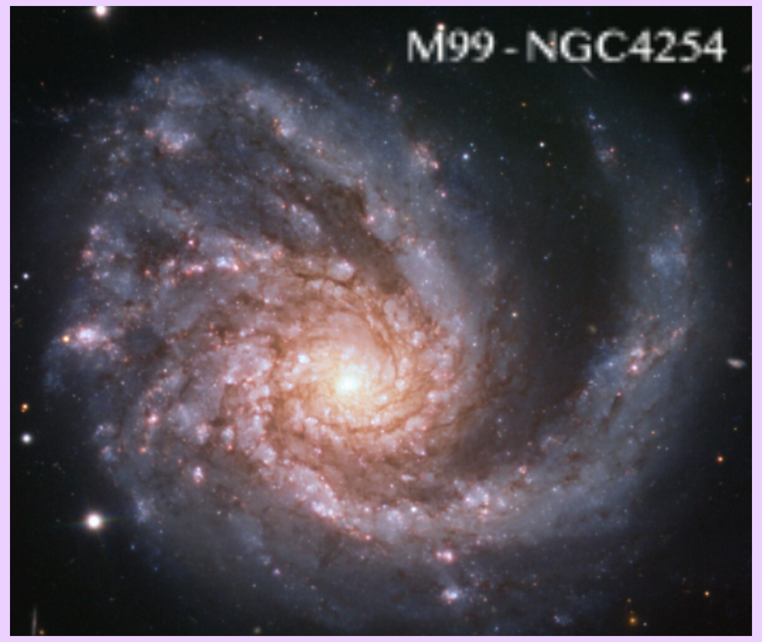

Pantoni et al. 2025 in prep.

+ MORE TO COME!

stay tuned

NIKA2 (IRAM 30m) observes the **1.15** and **2 mm continuum**, with angular resolution of **12''** and **18''** (~ kpc).

It allows us to:

- sample galaxy SED in the mm range;
- study the spatially-resolved mm properties of galaxies.

Main objectives

- Decomposing the mm emission in galaxies in **dust**, **free-free** and **synchrotron** through spatially-resolved SED fitting.
- Constraining the evolution of **dust-to-gas** and **dust-to-stellar mass ratios**.
- Investigating the variations of the microscopic properties of dust (**FIR/mm spectral index, β**).
- Studying the **sub-mm excess** in galaxies.

IMEGIN Large Program

IMEGIN (Interpreting the Millimeter Emission of Galaxies with IRAM-30m/NIKA2) is a **NIKA2 Guaranteed Time Large Program** (**~ 200 hours** of observing time) targeting **22 nearby galaxy** (priority A).

Pantoni et al. 2025 in prep.

NGC 4254 (M 99)

- Face-on galaxy
- Milky-Way like
- No AGN
- Elongated arm which extends up to 15 kpc
- D(L) = 14.4 Mpc
- 1 kpc = 14.3″

We characterize the dust and the ISM of this galaxy through spatially-resolved SED fitting (from NIR to radio regime).

NIKA2 maps of NGC 4254

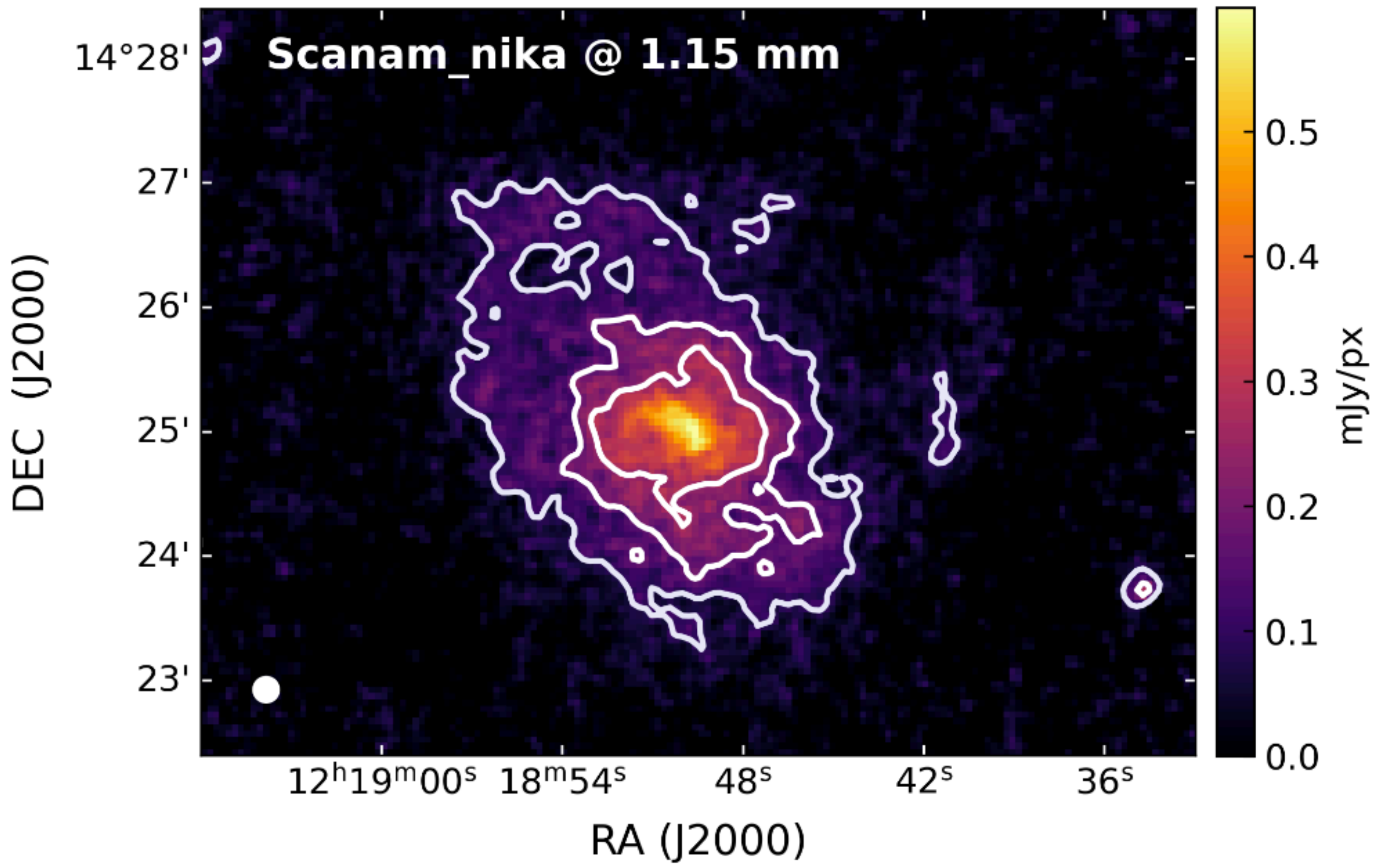

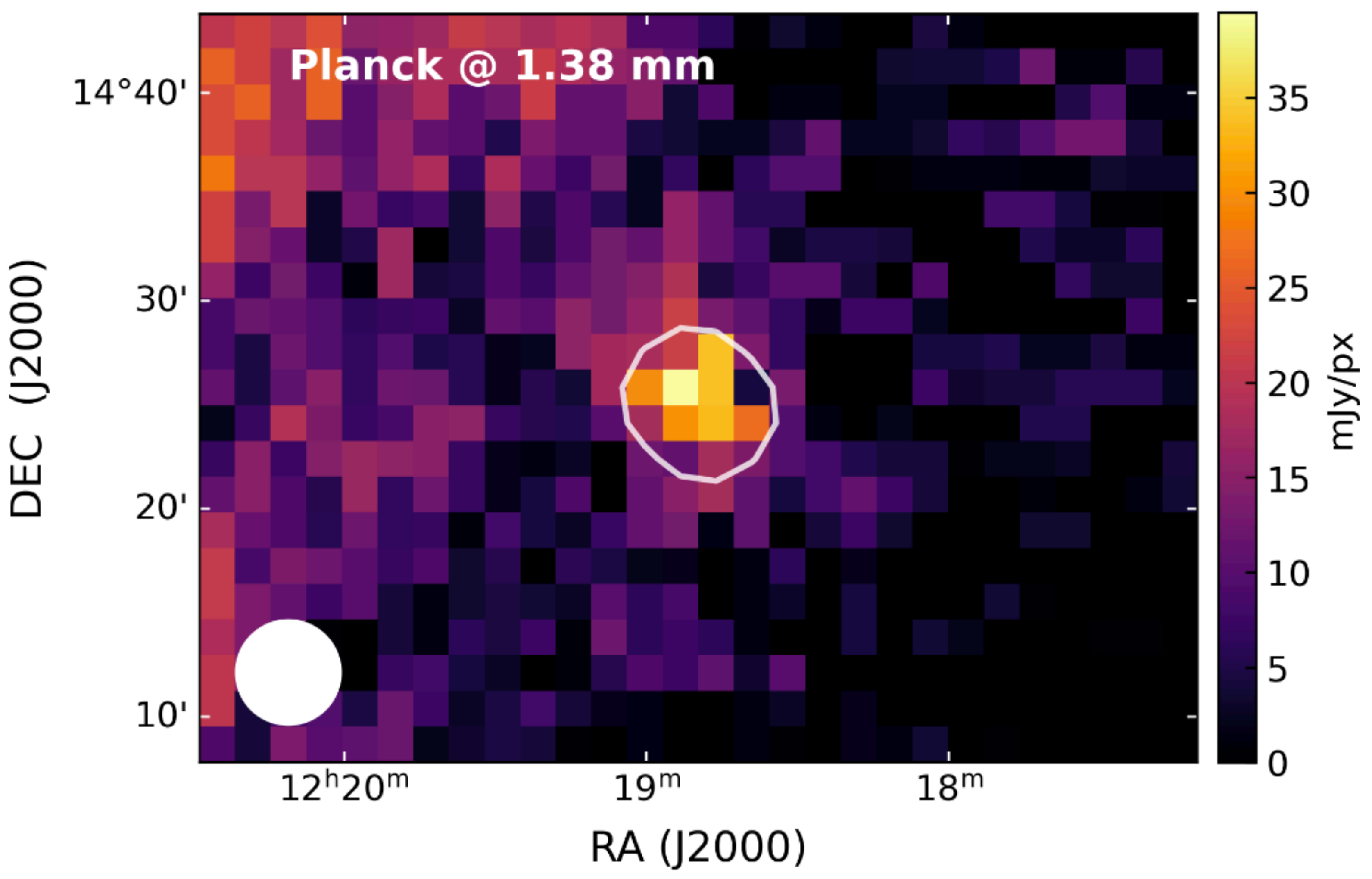

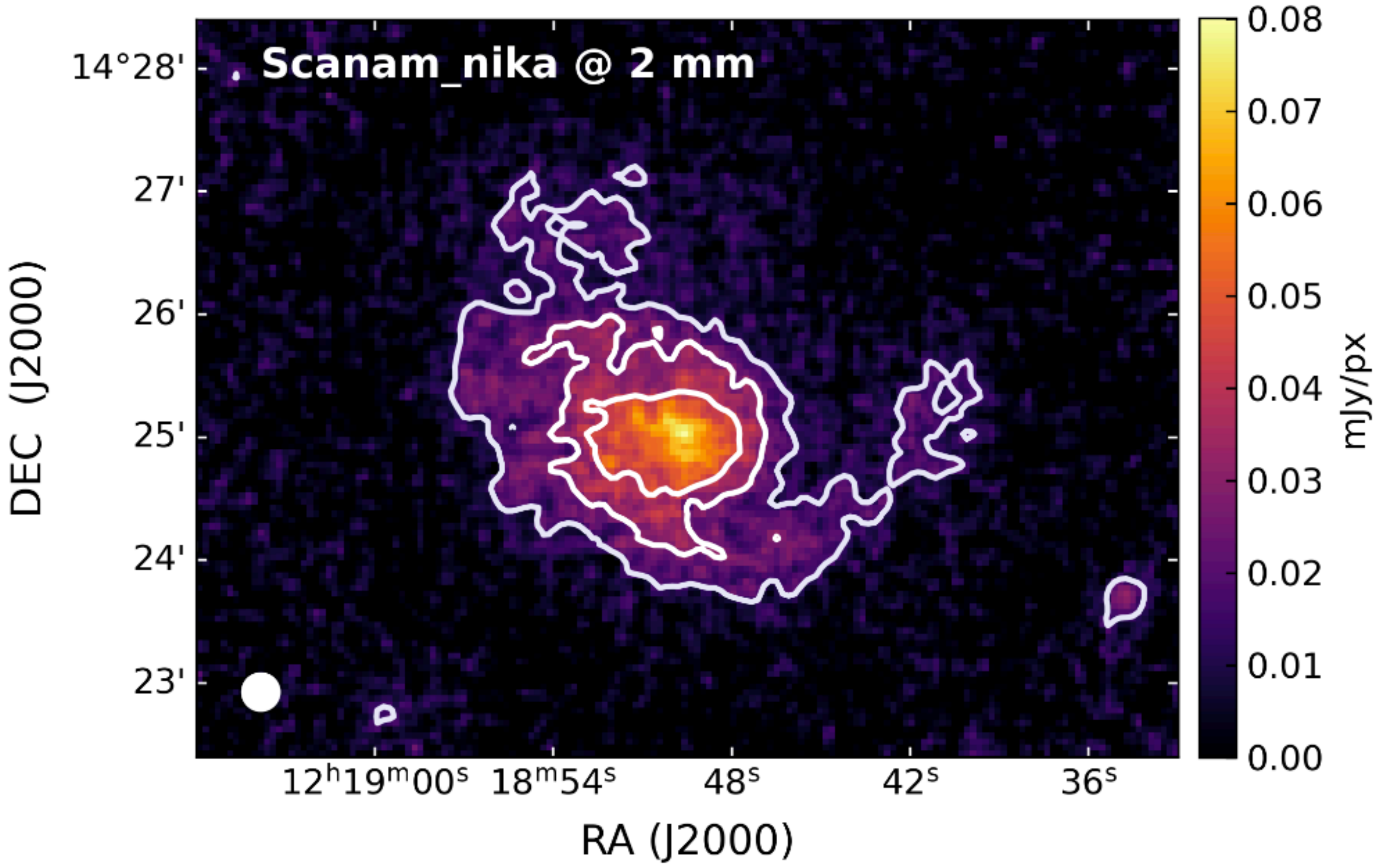

- Impressive **improvement** in terms of **angular resolution** compared to Planck.
- The NIKA2 maps suffer from large scale filtering. We have quantified and included this effect (**up to 2%** in the **bulge**, **10%** in the **arms**, **20%** in the **inter-arms**) in the uncertainty budget

Ancillary data

- The NIR to FIR images of NGC 4254 are taken from the **DustPedia archive**, for a total of **11 maps** with angular resolution comparable with NIKA2 (**from 0.6″ to 36″**).
- The radio maps at 3 cm and 6 cm are **VLA+Effelsberg** (15″) from Chemin+16; **VLA only** at 20 cm (5″; private).

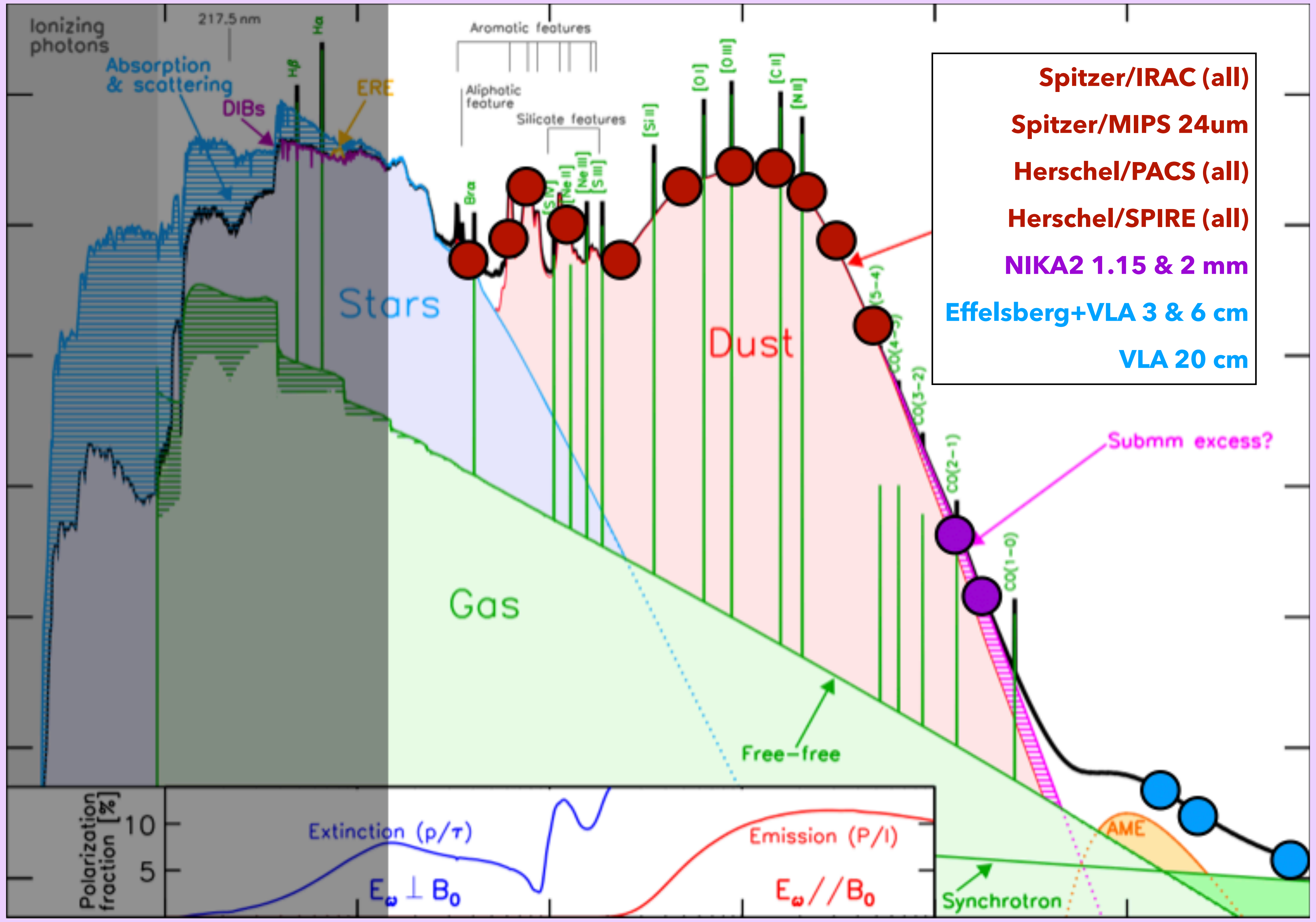

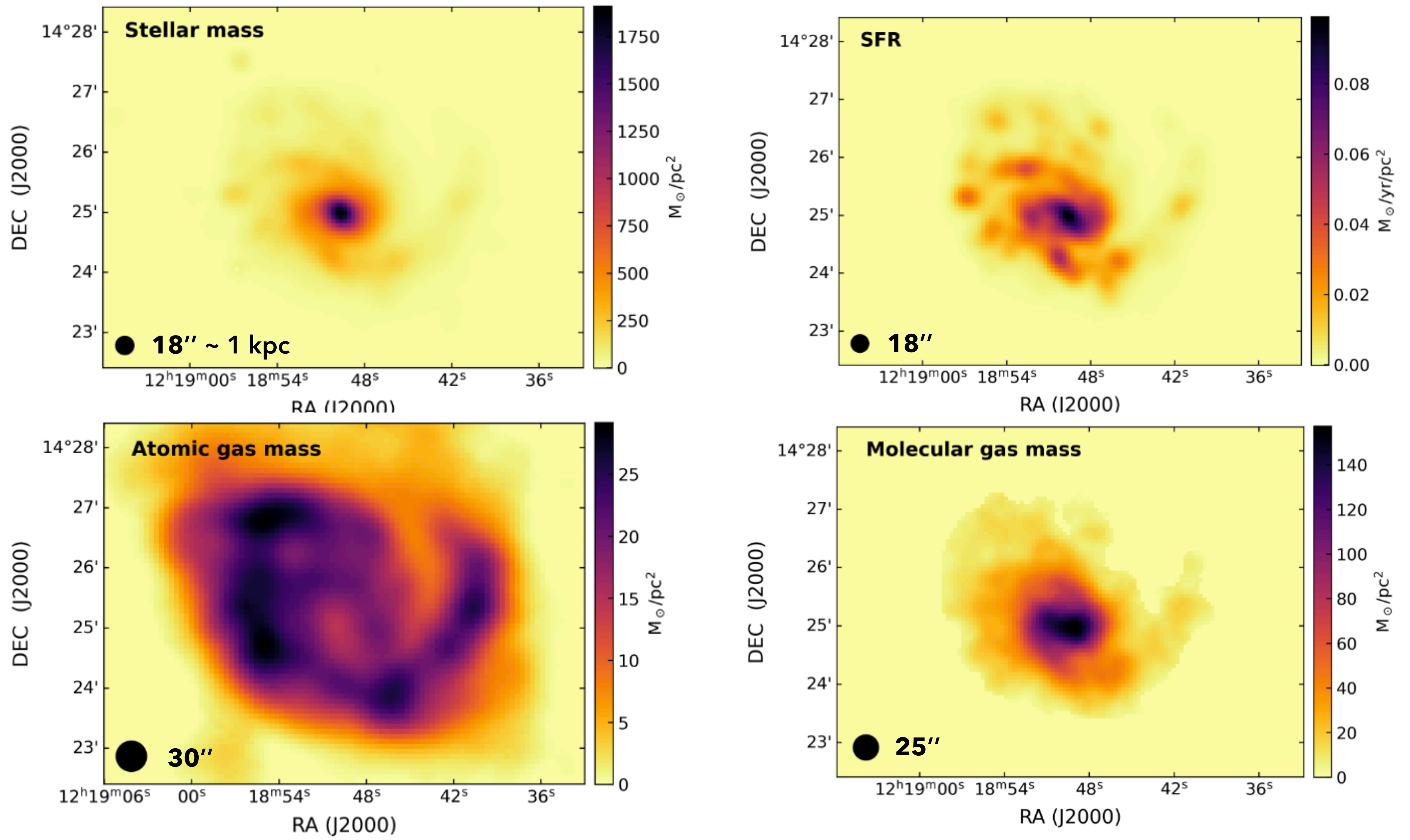

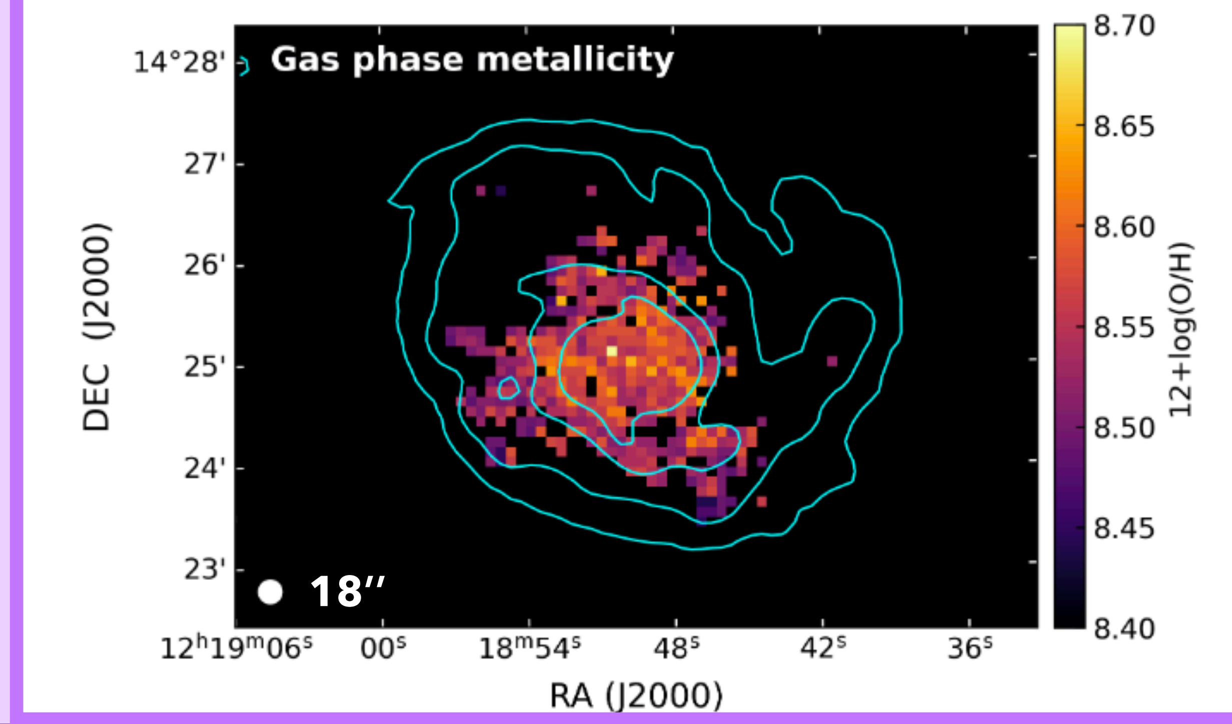

- IRAC+GALEX and Leroy+08 calibrations;
- CO(1-0) and HI from EMPIRE and VIVA VLA;
- Metallicity measurements by PHANGS/MUSE and DeVis+19.

SED fitting: HerBIE and THEMIS

- We use **HerBIE** **(Galliano 2018)** to fit the dust SED of NGC 4254.

  HerBIE is a hierarchical bayesian SED fitting code: the **prior distributions** are not set before running, basing on some assumptions, but **inferred from the data**.

  We use: 1. a non-uniformly illuminated dust mixture (free parameters : $\mathbf{M_{dust}}$, **<U>**, $\mathbf{q_{AF}}$);
  2. the NIR emission by stellar populations (BB of T = 50 000 K and free **L**);
  3. includes free–free and synchrotron continua (radio; free parameters : $\boldsymbol{\alpha_{sync}}$, $\boldsymbol{f_{ff}}$, $\mathbf{L_{radio}}$).

  HerBIE returns the pdf, the map of dust parameters and their uncertainties.

- HerBIE incorporates the **dust model THEMIS** **(Jones et al. 2017)**.

  THEMIS dust mixture consists of core-mantle amorphous carbon and silicate grains. The corresponding HerBIE parametrization divides them in four families, depending on **their size and composition**.

  In HerBIE parametrization, $\boldsymbol{f_{Sil}}$ **= 0.83** and **β = 1.79**.

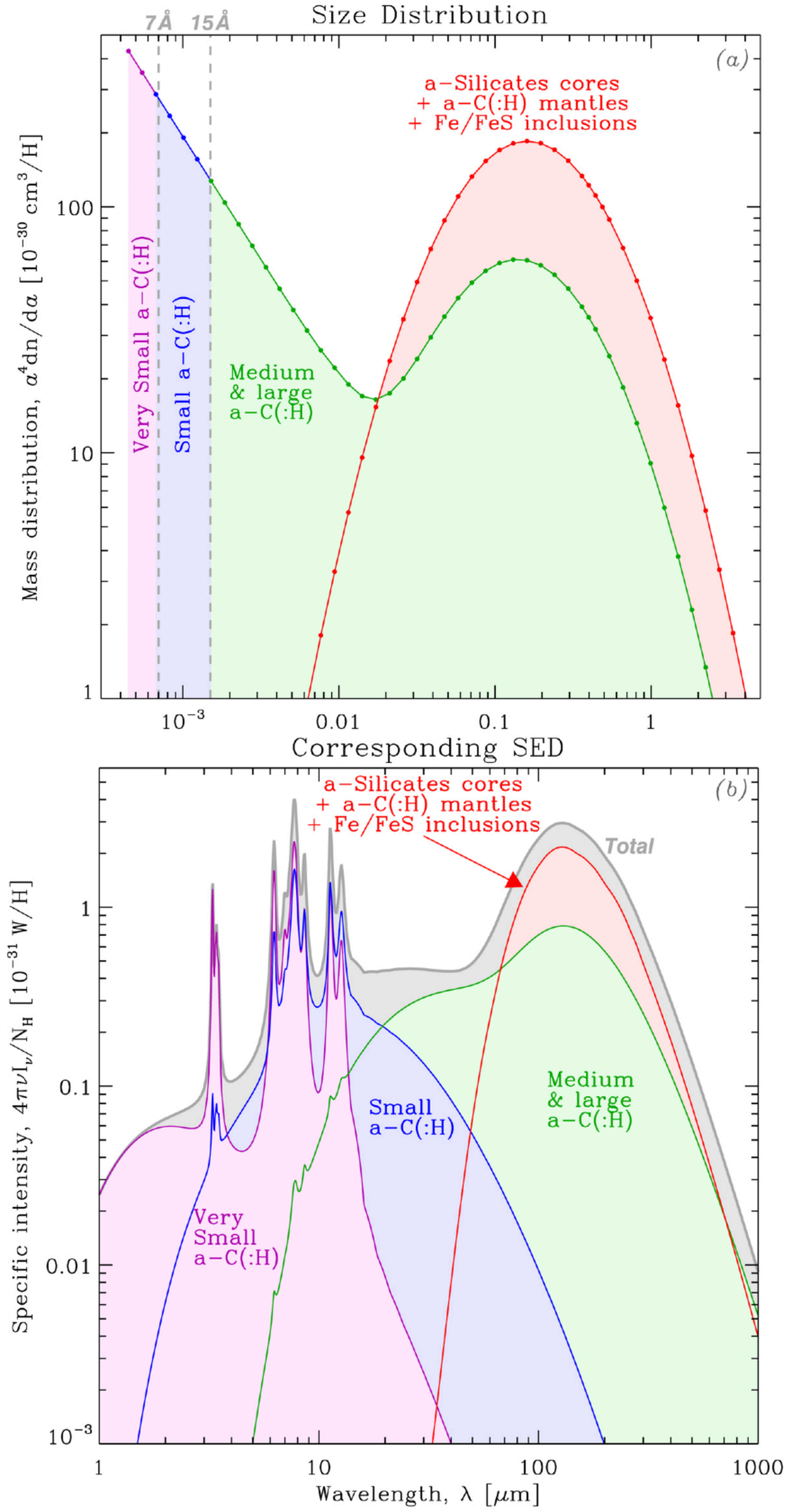

SED fitting: spatial scales

1. **Global** SED fitting.

2. SED fitting of the fluxes **integrated** within the main morphological components of the galaxy: **disk, spiral arms and bulge** (basing on PHANGS environmental masks by Querejeta et al. 2021), matching NIKA2 2mm resolution (18″ ~ 1.25 kpc).

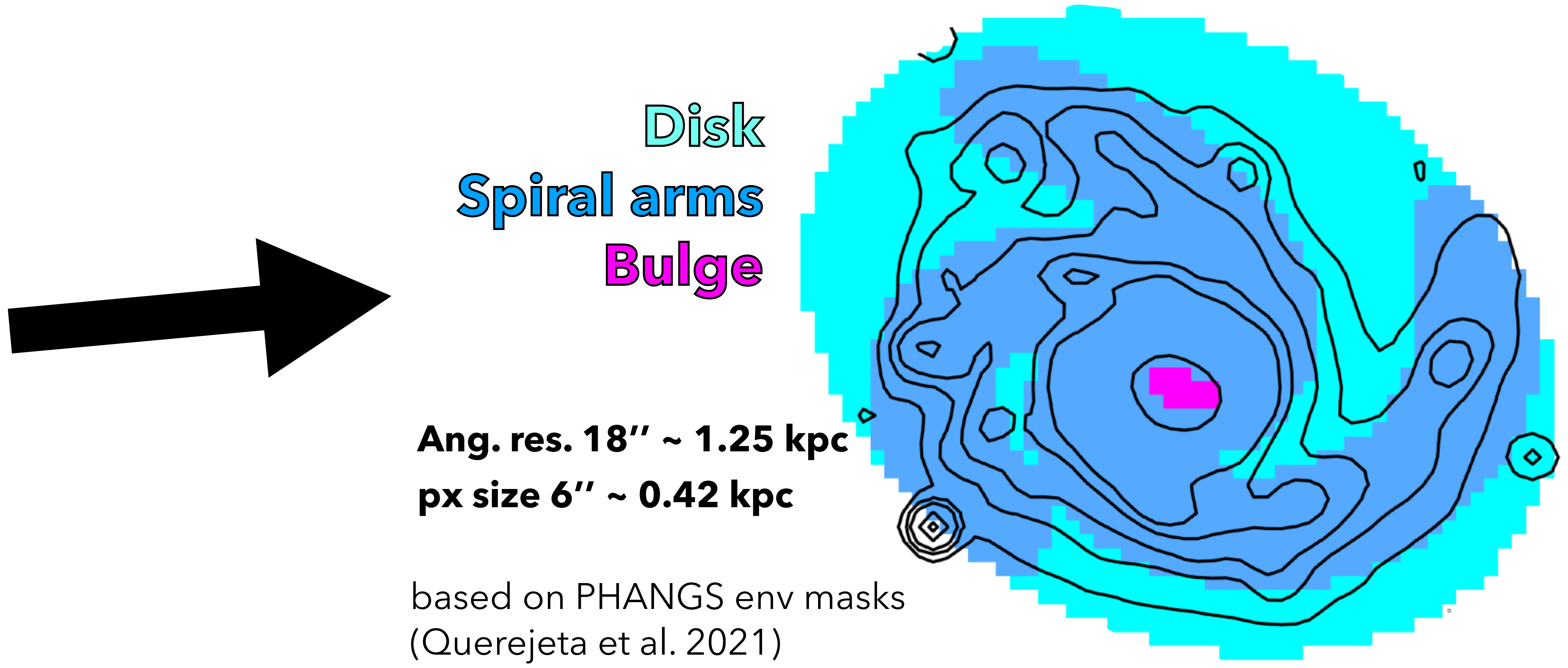

3. **Pixel-by-pixel** SED fitting at 25″ resolution (matching SPIRE 350 um) and pixel size of 8″ ~ 0.56 kpc.

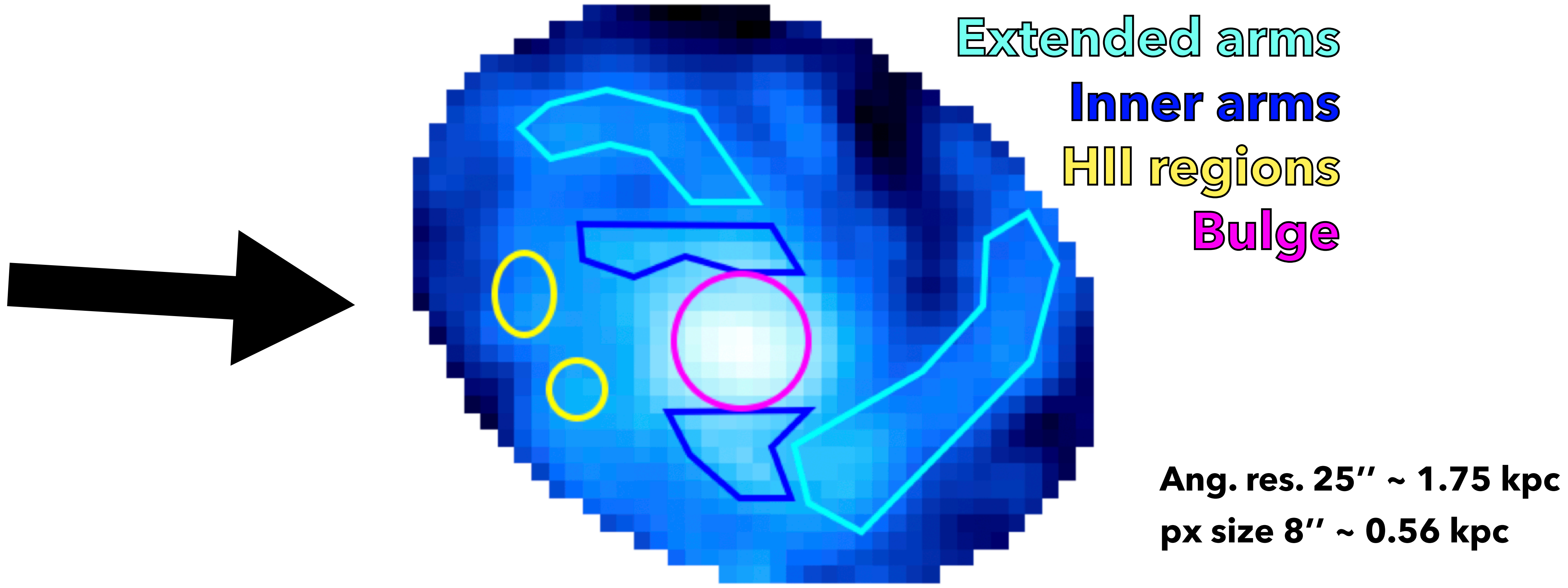

A global view of the dust in NGC 4254

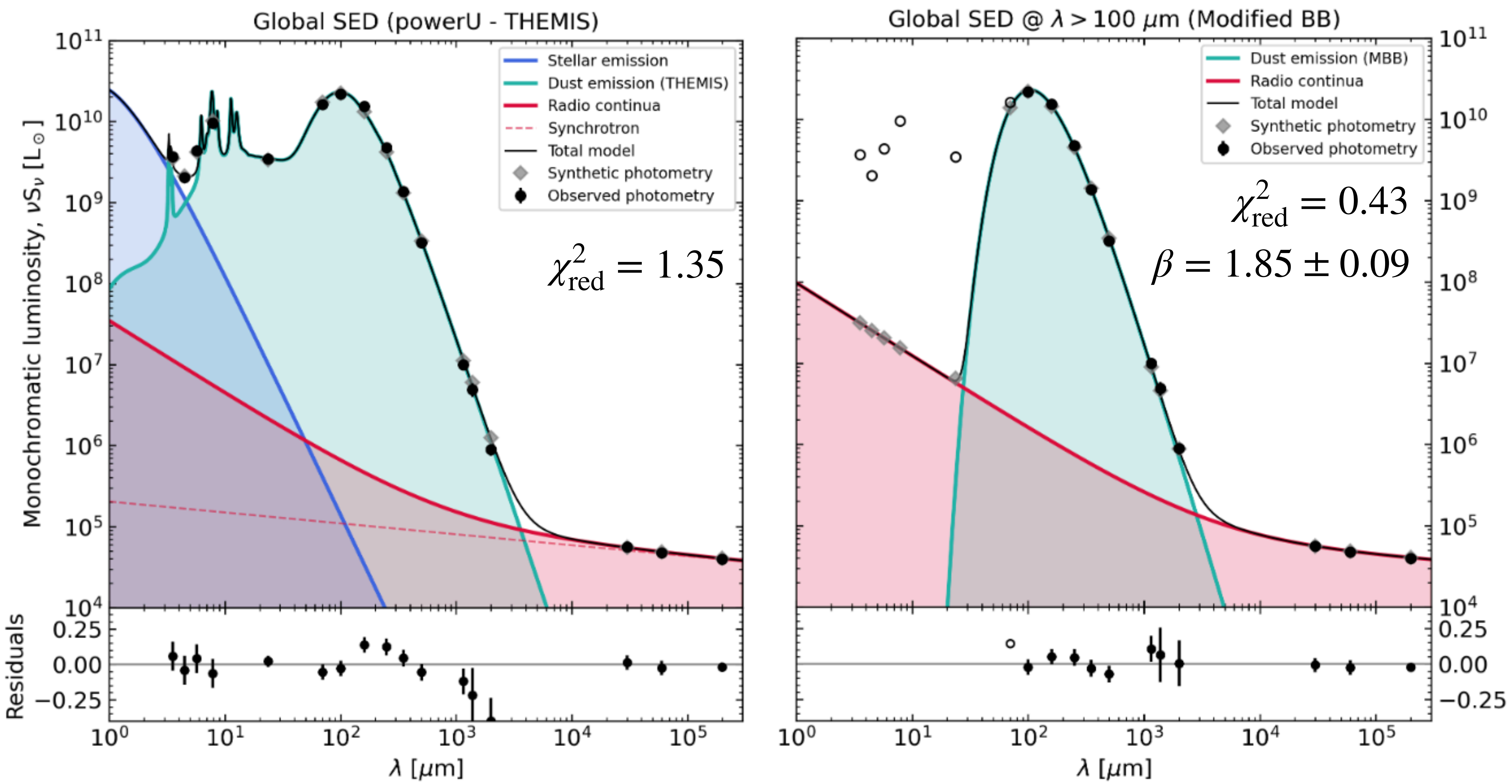

Parameter	HerBIE value (powerU - THEMIS)	Units
$M_{\rm dust}$	$(3.2 \pm 0.2) \times 10^7$	$M_\odot$
$q_{\rm AF}$	15 ± 1	%
$L_\star$	$(3.8 \pm 0.7) \times 10^{10}$	$L_\odot$
$\langle U \rangle$	5.6 ± 0.6	$\langle U \rangle_\odot$
$L_{\rm radio}$	$(7.0 \pm 0.6) \times 10^4$	$L_\odot$
$\alpha_{\rm sync}$	0.87 ± 0.04	
$f_{\rm FF}$	15 ± 12	%

	1.15 mm	2 mm	5 mm	1 cm
DUST	99%	91%	20%	2%
RADIO	1%	10%	80%	98%
ff	52%	40%	23%	15%
sync	48%	60%	77%	85%

The steeper FIR slope we find for the integrated SED of NGC 4254 may result from the contribution to the total dust emission of **colder and denser regions** than the typical conditions observed in diffuse ISM of the MW (which sets the THEMIS value).

β in Disk, Arms and Bulge

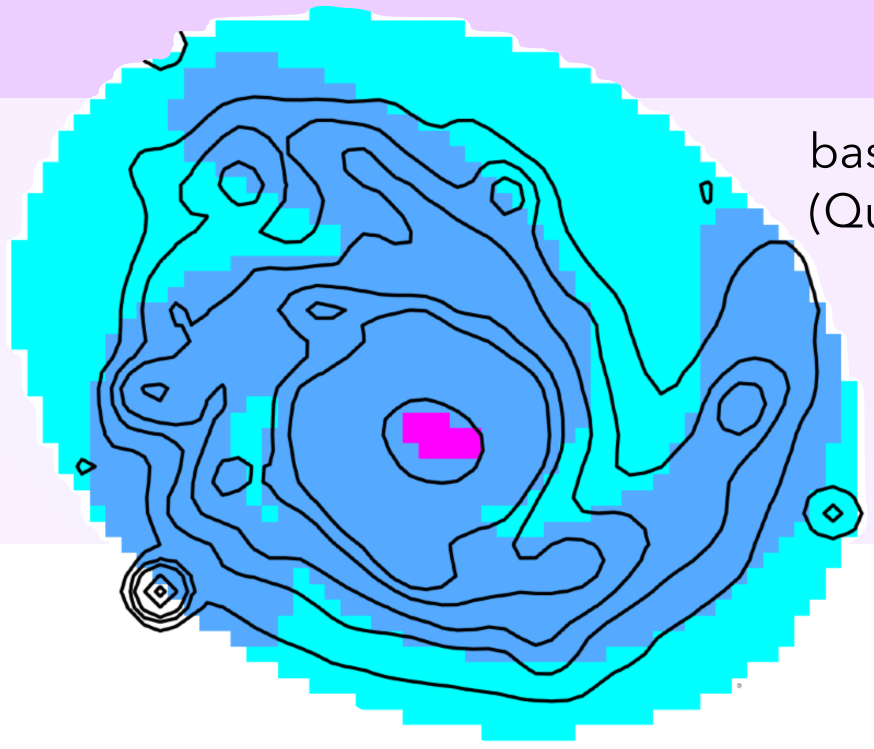

based on PHANGS env masks (Querejeta et al. 2021)

Ang. res. 18″ ~ 1.25 kpc
px size 6″ ~ 0.42 kpc

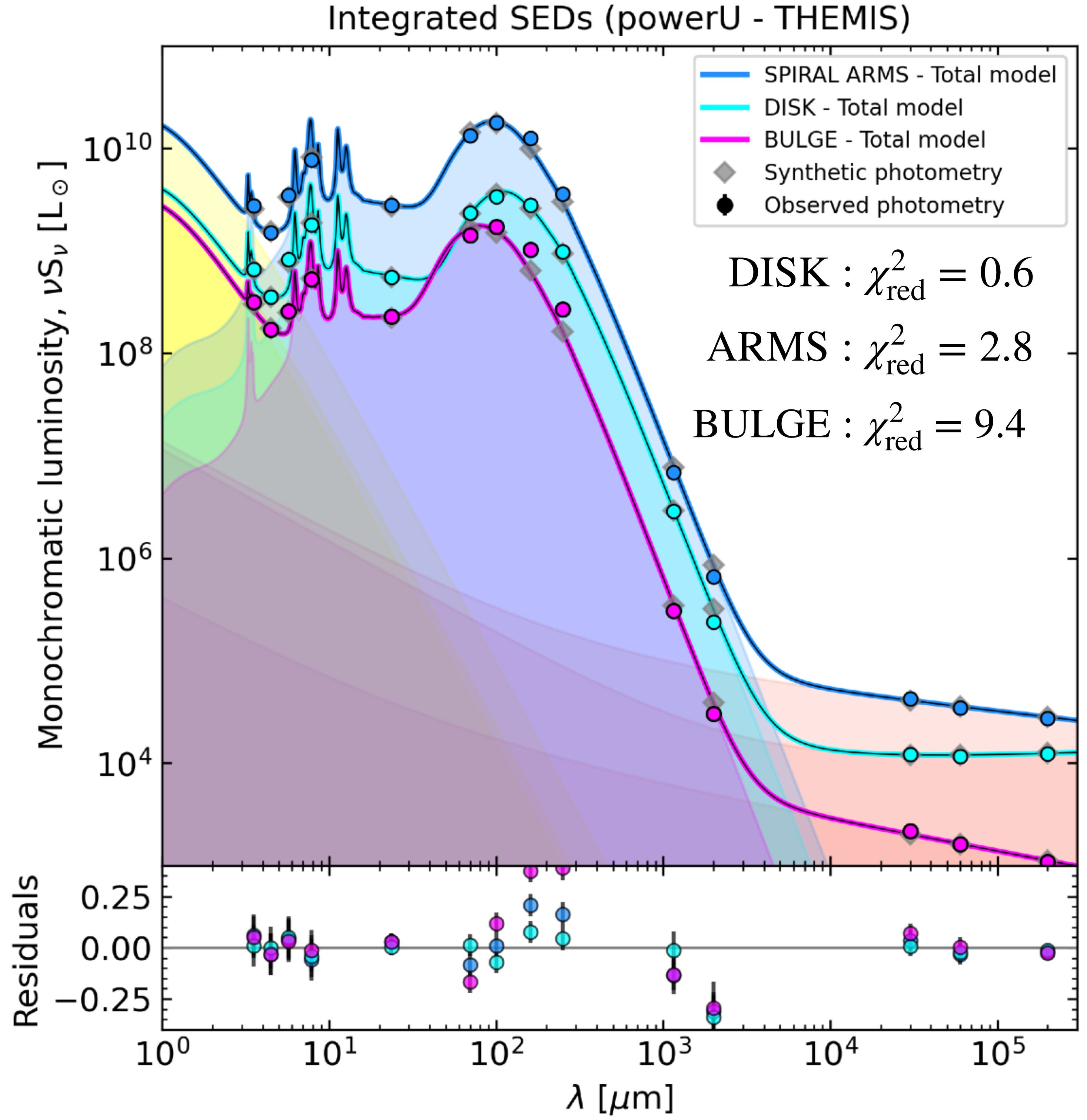

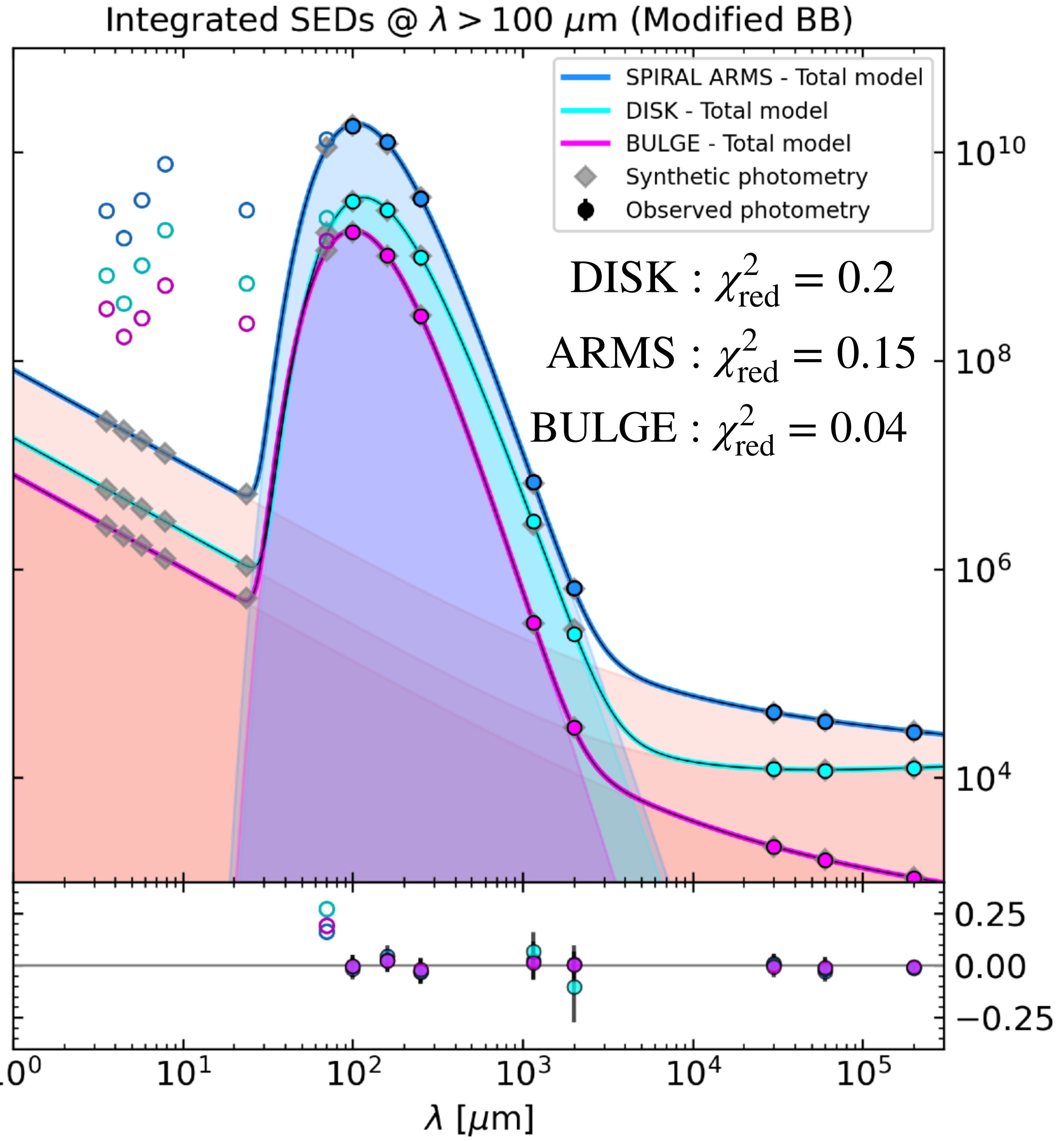

$$\beta^{\rm MBB}_{\rm DISK} = 1.72 \pm 0.09$$

$$\beta^{\rm MBB}_{\rm ARMS} = 1.92 \pm 0.08$$

$$\beta^{\rm MBB}_{\rm BULGE} = 2.27 \pm 0.09$$

Consistent with THEMIS value (i.e. 1.79), which is the typical value for diffuse ISM in the MW.

Steeper FIR slopes: dust grains are highly reprocessed in spiral arms and bulge: drastic change in their size distribution and chemical composition.

- **dense regions:** coagulation into aggregates; accretion of aliphatic-rich amorphous carbon mantles (Köhler+15; Ysard+16)
- **vicinity of stars:** loosing (or reducing the thickness) of the dehydrogenated carbonaceous mantles of large grains (e.g. through photo-desorption, sublimation or sputtering; Köhler+14; Ysard+15).
- changing in the relative abundance of carbonaceous and silicate large grains (set by THEMIS to $f_{\rm Sil}$ = **0.83**)

Spatially-resolved β variations

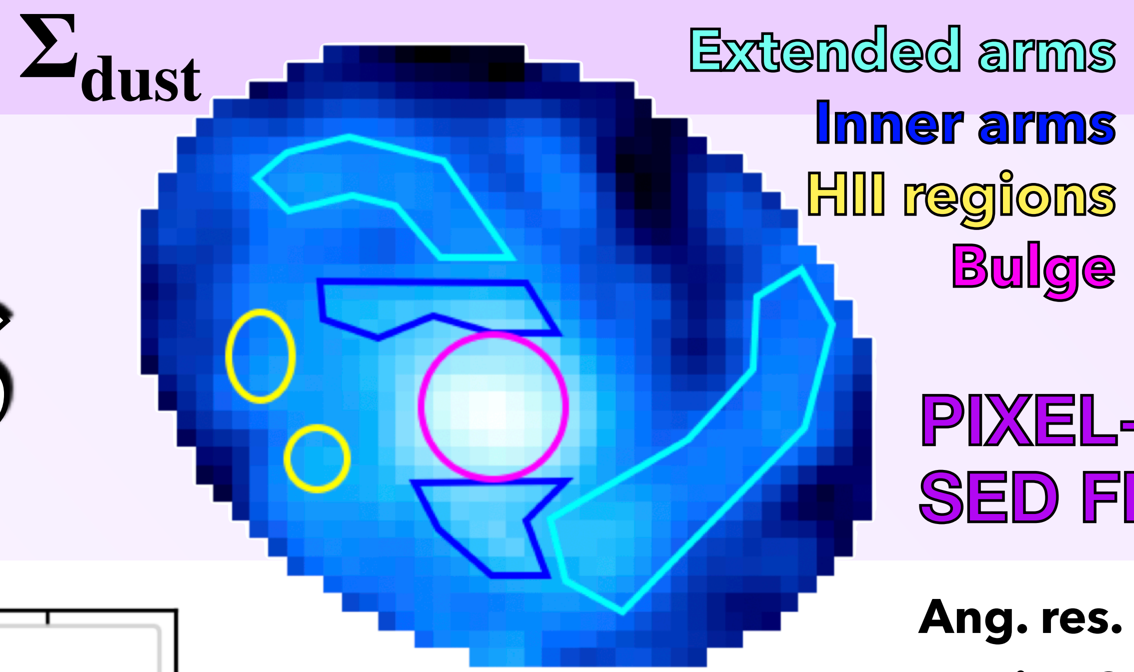

PIXEL-BY-PIXEL SED FITTING

Ang. res. 25'' ~ 1.75 kpc
px size 8'' ~ 0.56 kpc

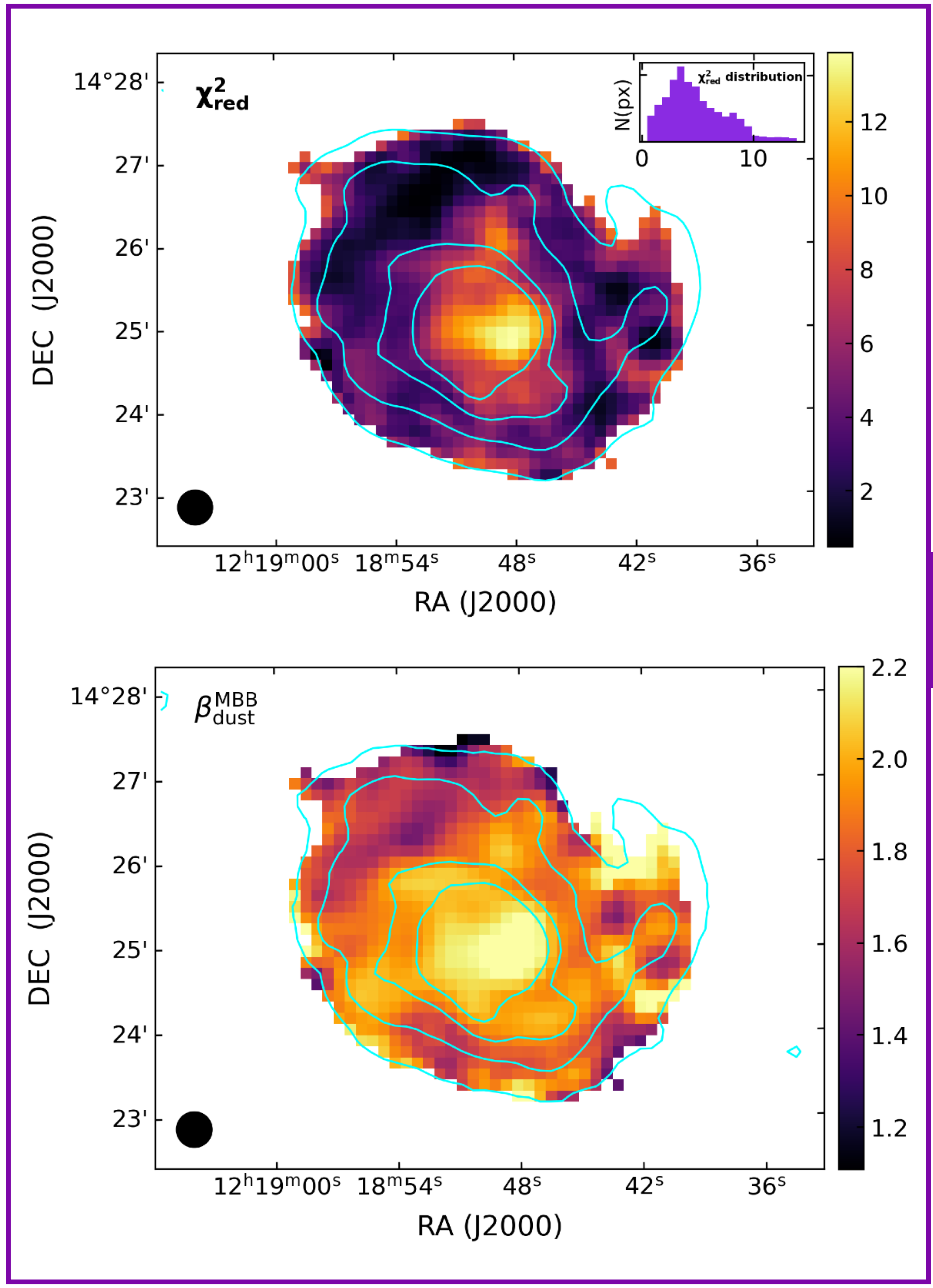

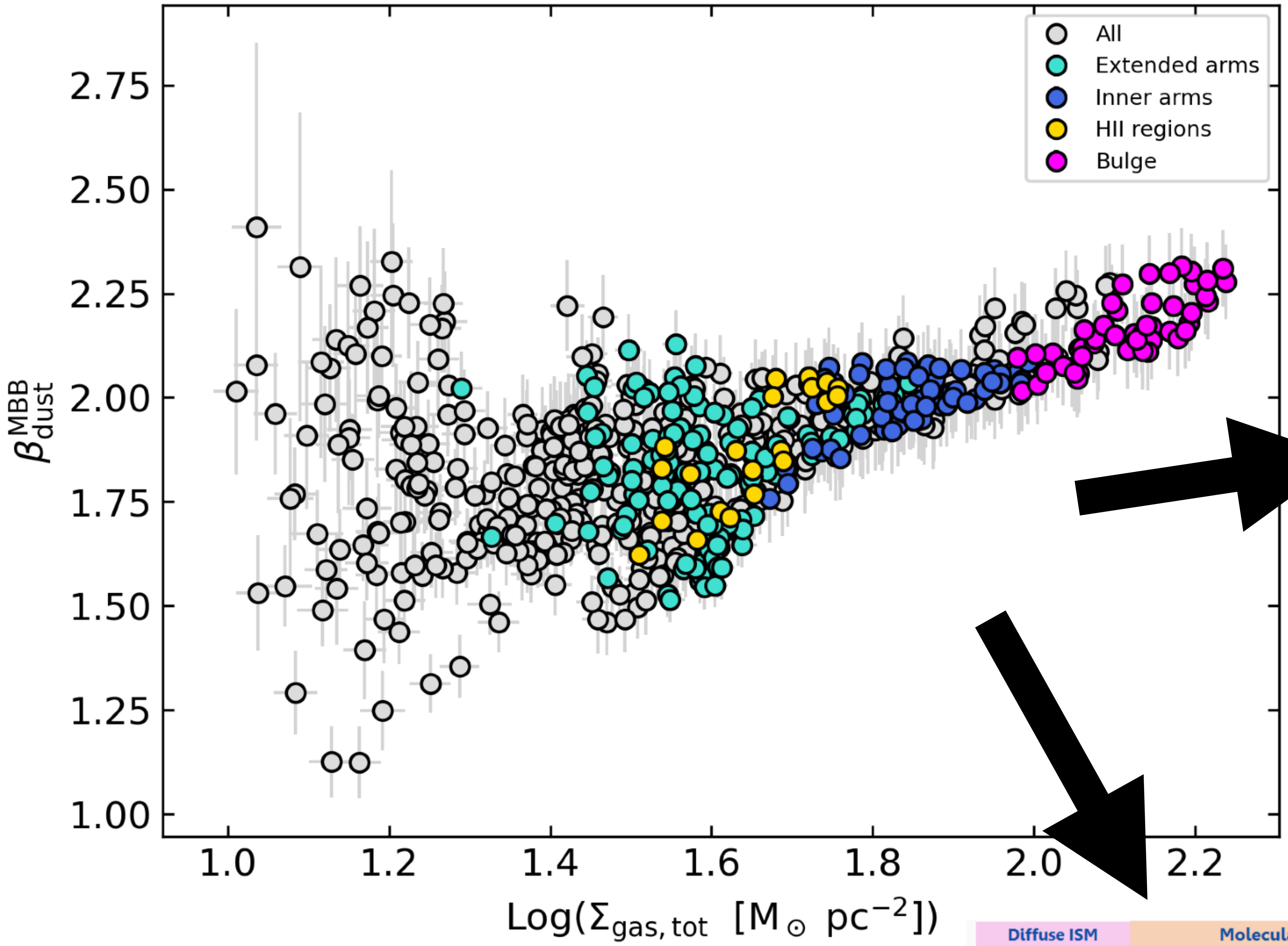

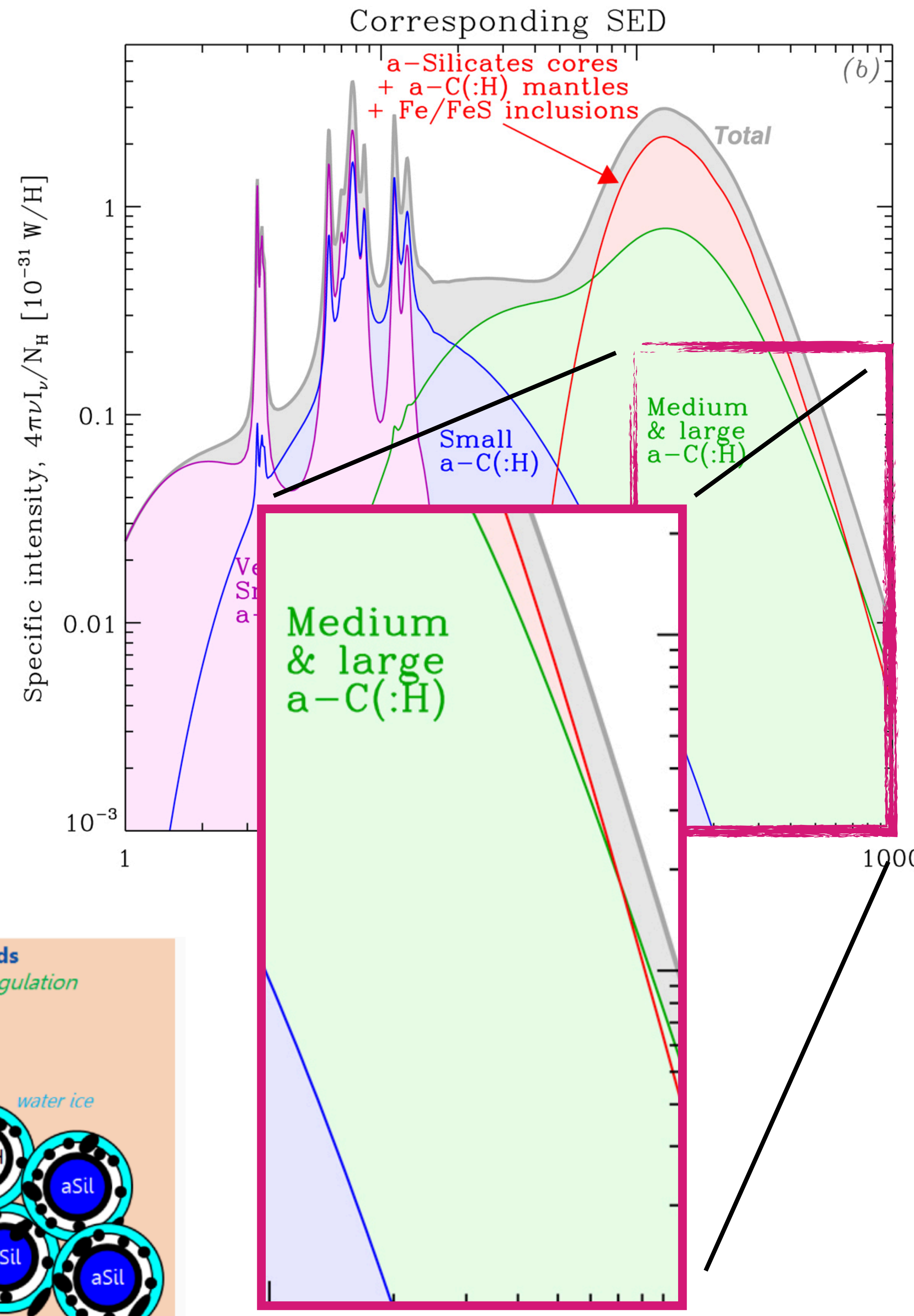

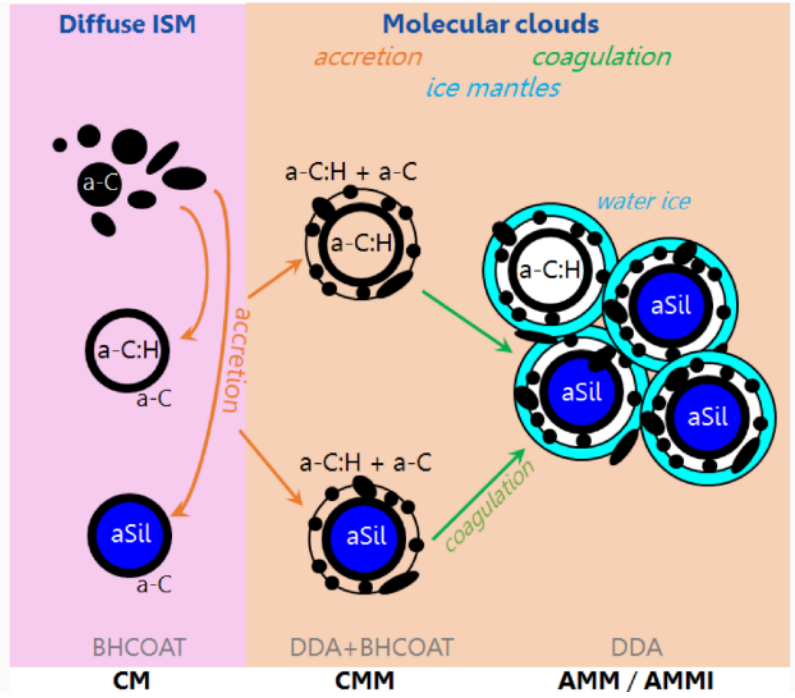

Spatially-resolved dust / ISM properties

1. Typical q_{AF} shows an **inverse trend** with $\langle U \rangle$:

Small grains are historically known to be efficiently destroyed if exposed to hard interstellar radiation fields

(e.g., Boulanger et al. 1988;Puget & Leger 1989; Contursi et al. 2000).

q_{AF}	Disk	16 ± 1	%
	Spiral arms	15 ± 1	
	Bulge	10 ± 1	
$\langle U \rangle$	Disk	3.1 ± 0.3	$\langle U \rangle_\odot$
	Spiral arms	6.8 ± 0.7	
	Bulge	18 ± 2	

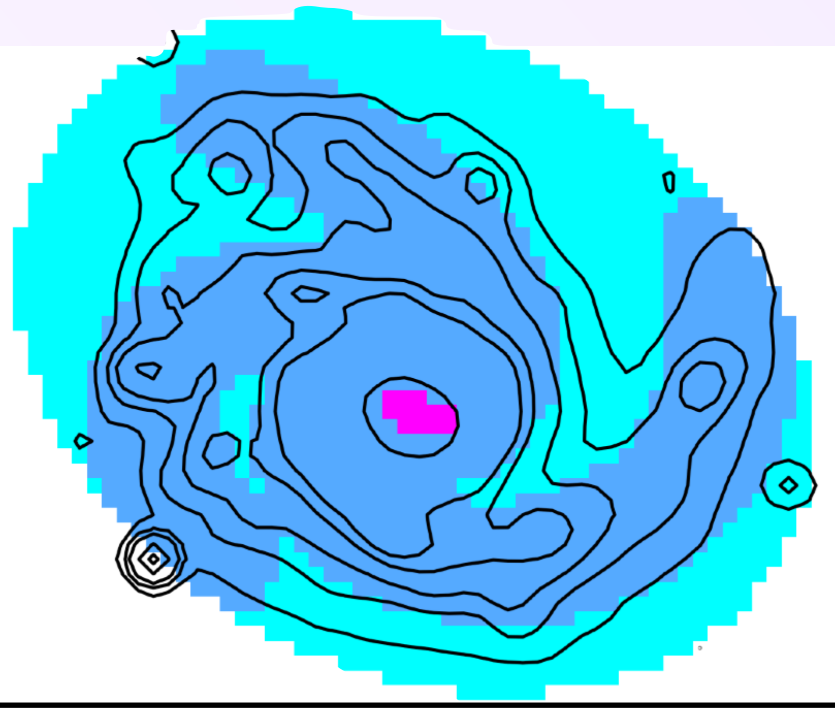

INTEGRATED SED FITTING

Ang. res. 18″ ~ 1.25 kpc

px size 6″ ~ 0.42 kpc

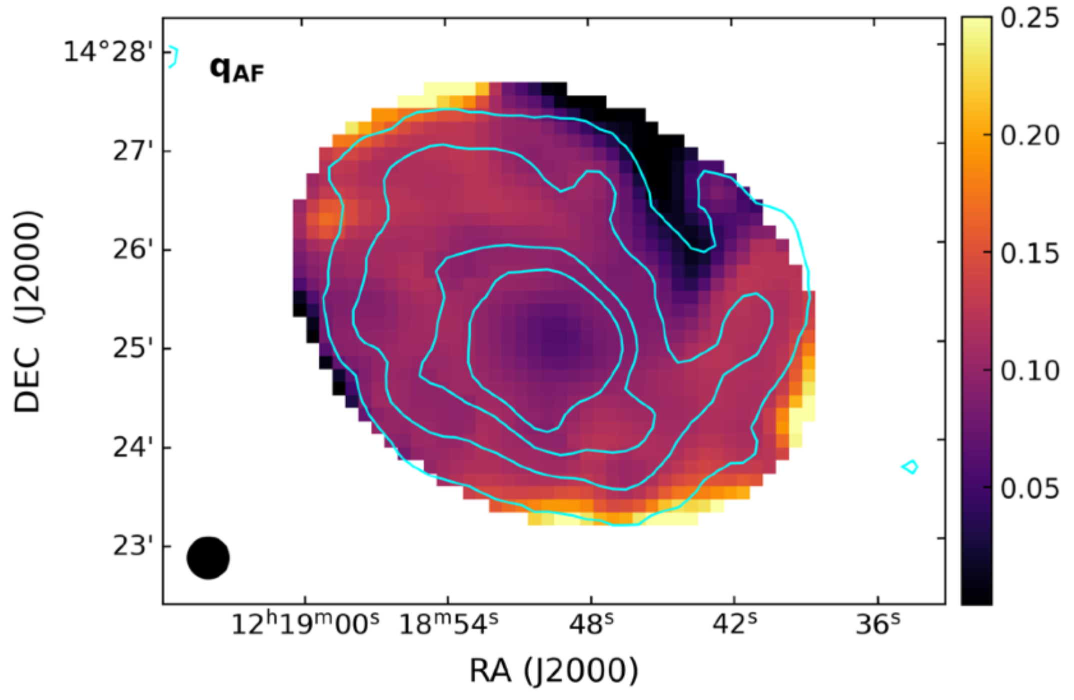

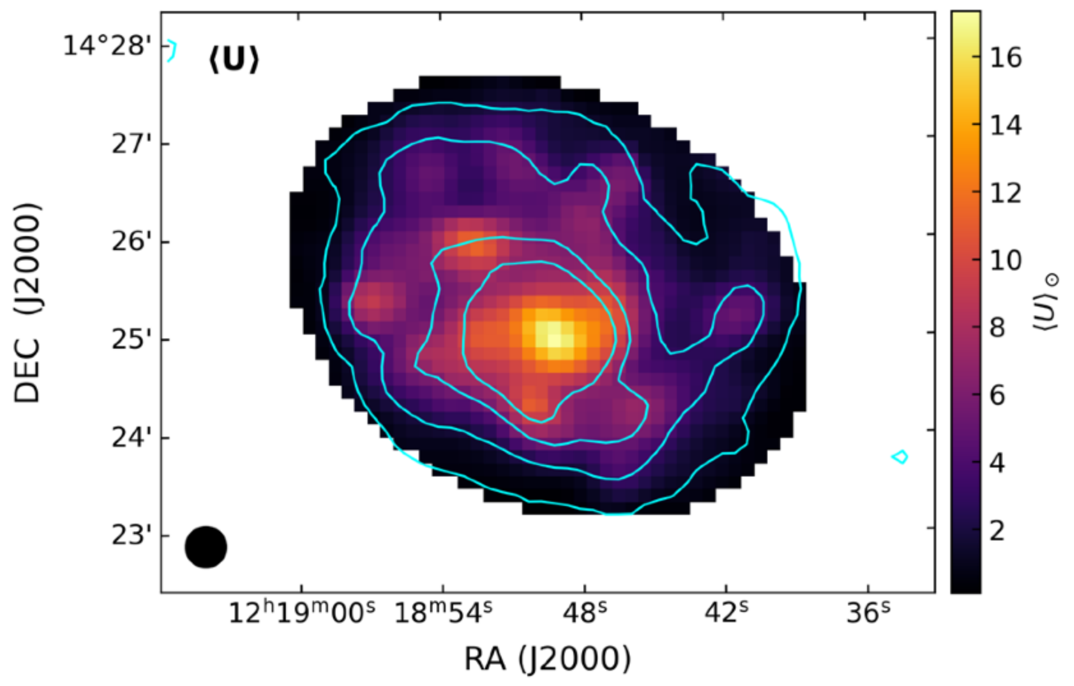

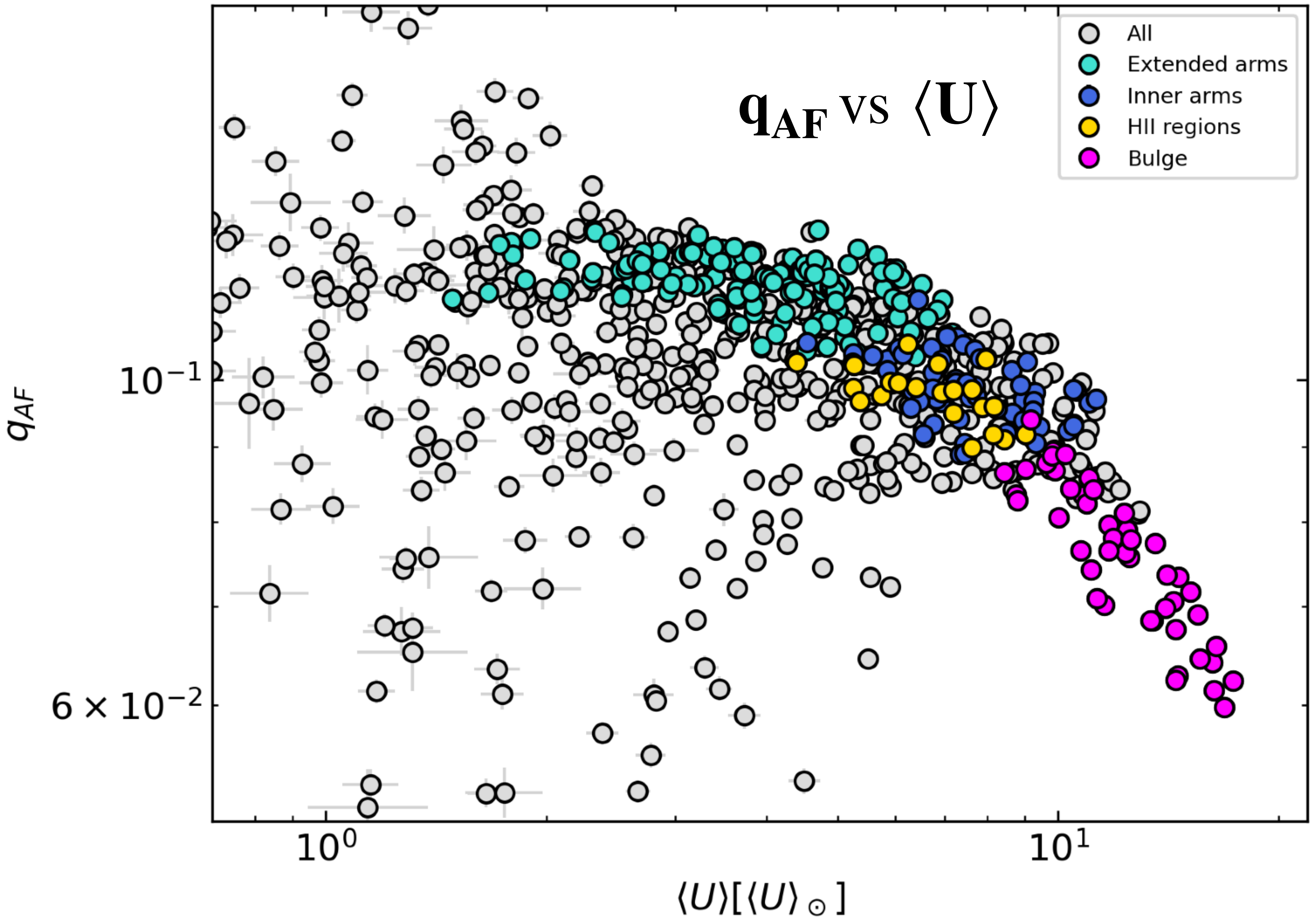

PIXEL-BY-PIXEL SED FITTING

Ang. res. 25″ ~ 1.75 kpc

px size 8″ ~ 0.56 kpc

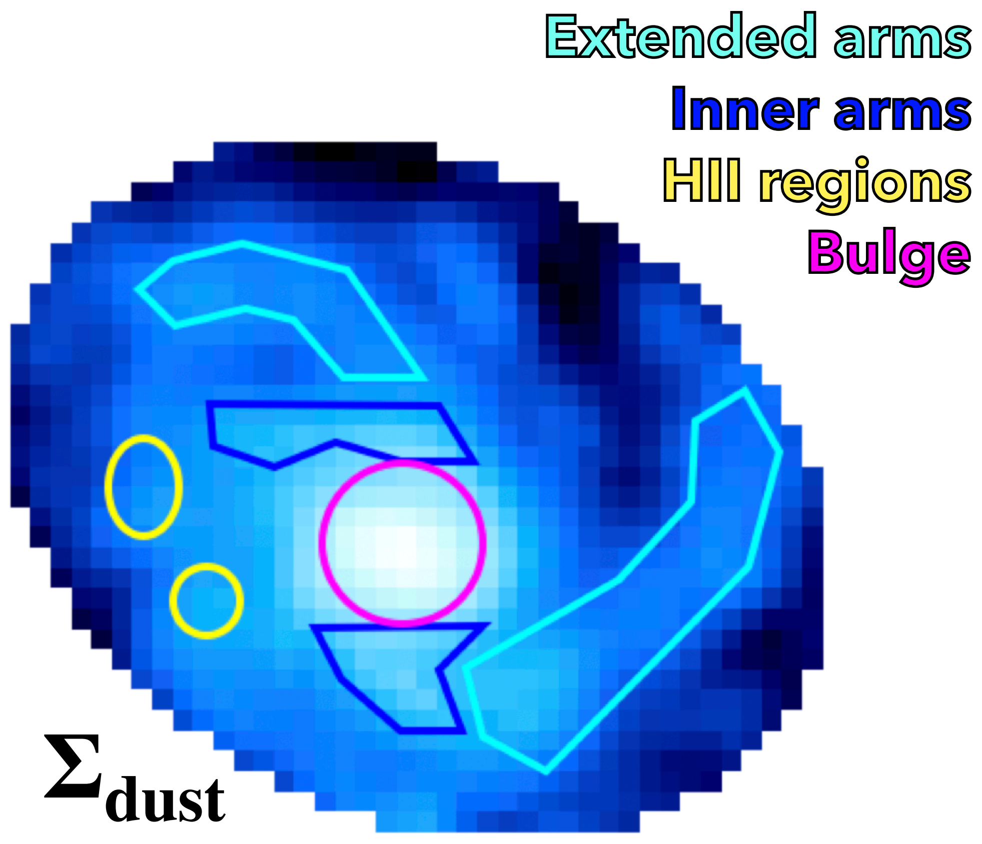

Spatially-resolved dust / ISM properties

2. Systematic variation of the **synchrotron spectral index**

(consistent with Gajović+24; Fletcher +11)

Disk: older, lower-energy electrons, tracing **older stellar populations**.

Arms + bulge: the flatter indices are consistent with **younger stellar population**.

α_{sync}	Disk	1.06 ± 0.05
	Spiral arms	0.82 ± 0.03
	Bulge	0.70 ± 0.03

STEEPENING : *aging of Cosmic Ray Electrons*

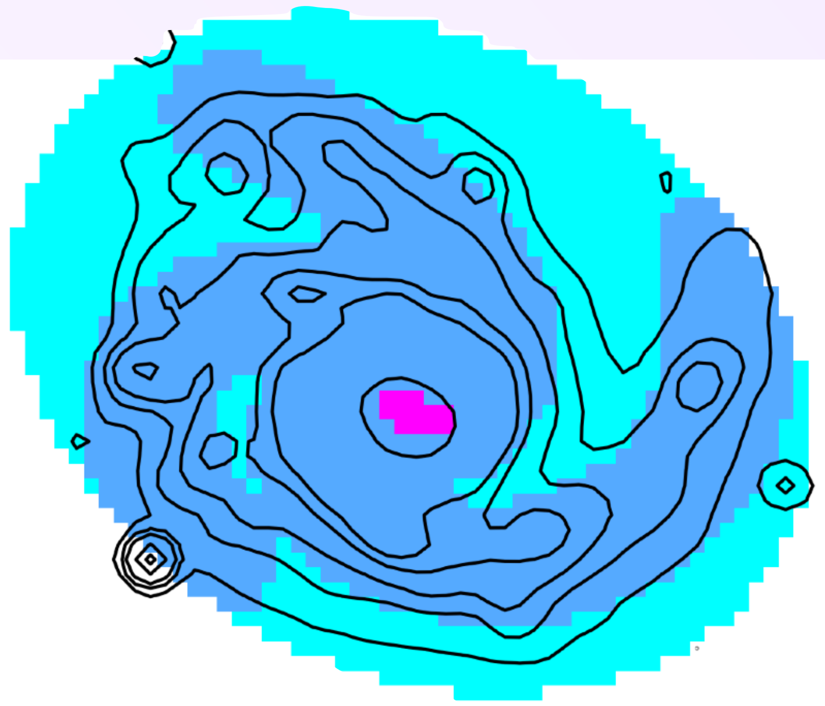

INTEGRATED SED FITTING

Ang. res. 18″ ~ 1.25 kpc

px size 6″ ~ 0.42 kpc

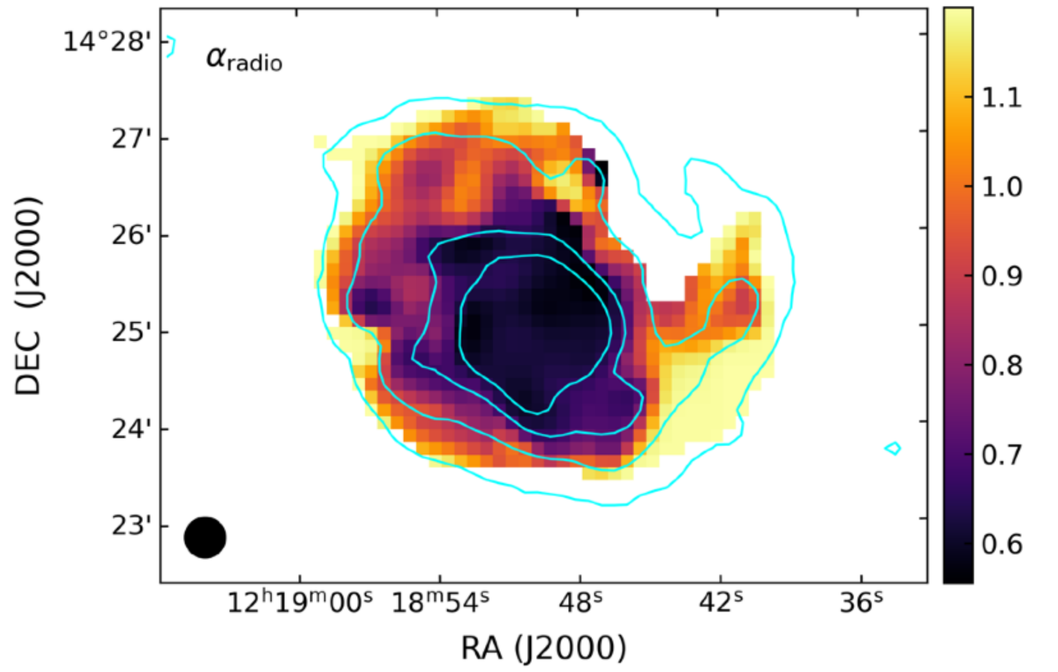

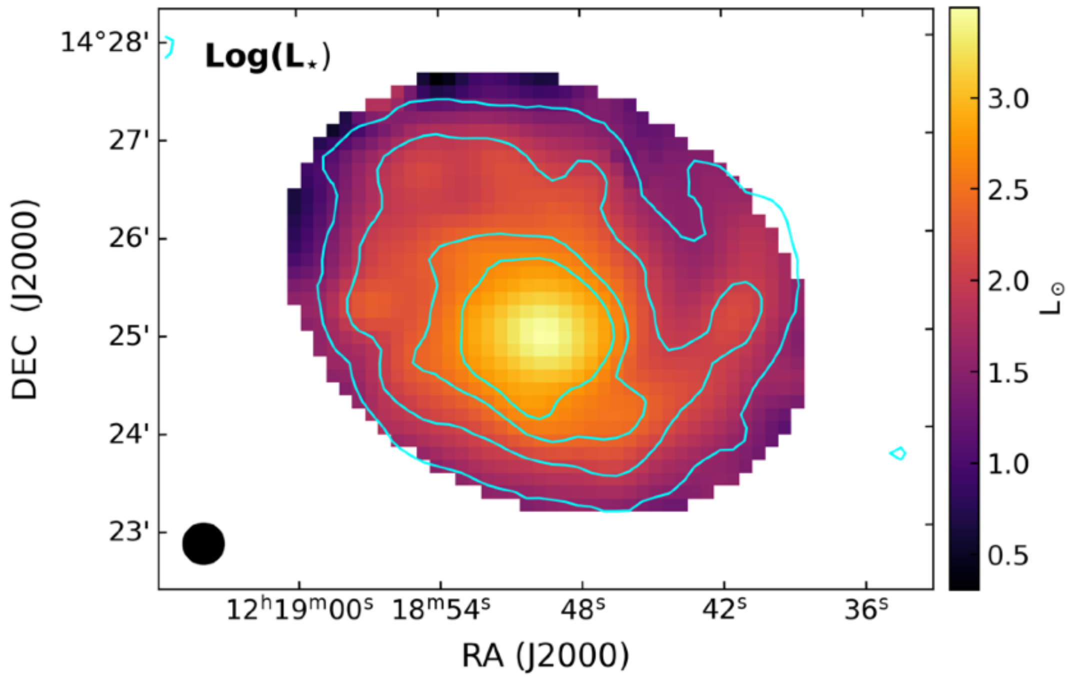

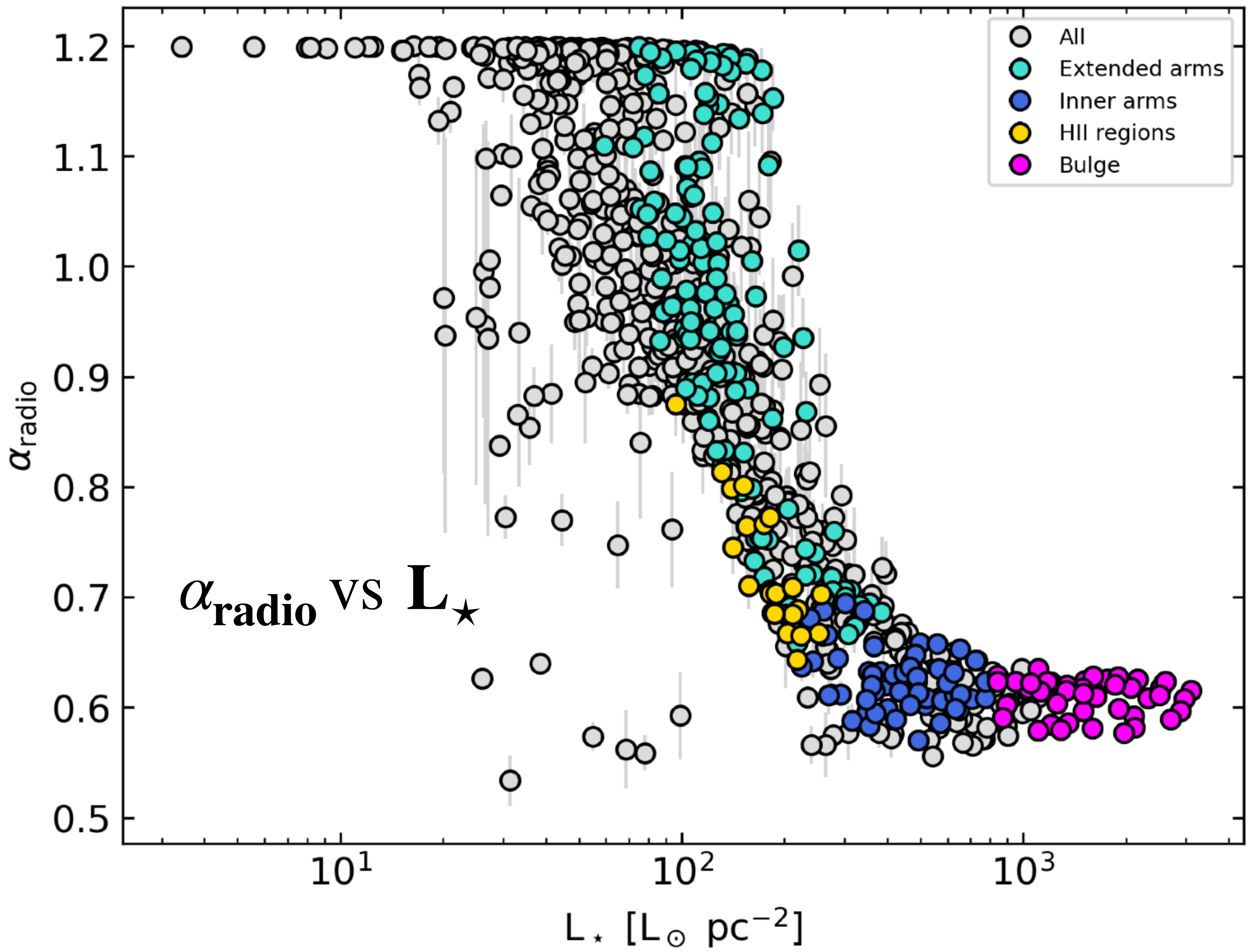

PIXEL-BY-PIXEL SED FITTING

Ang. res. 25″ ~ 1.75 kpc

px size 8″ ~ 0.56 kpc

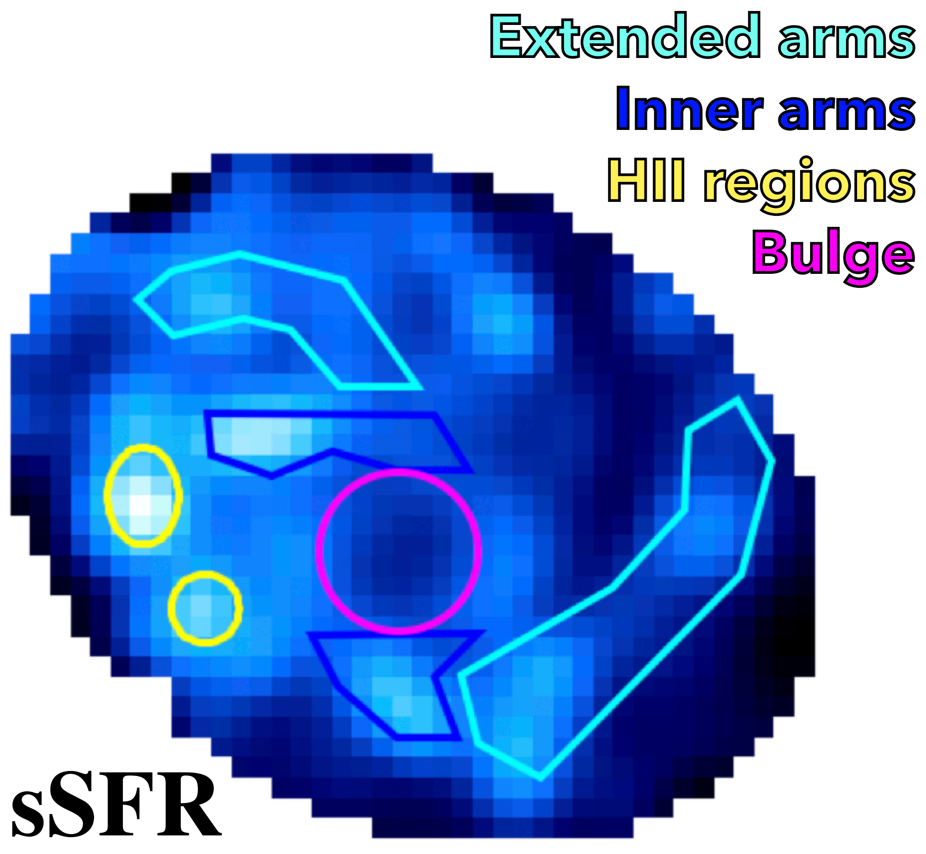

Spatially-resolved dust / ISM properties

3. Typical SRF densities, gas and dust reservoirs show that the **bulk of star formation activity** in NGC 4254 happens in the **bulge**, **spiral arms** and **HII regions.**

   HII regions and spiral arms are **more efficient in converting molecular gas into stars and in forming new stars**, showing the shortest τ_depl and the highest sSFR.

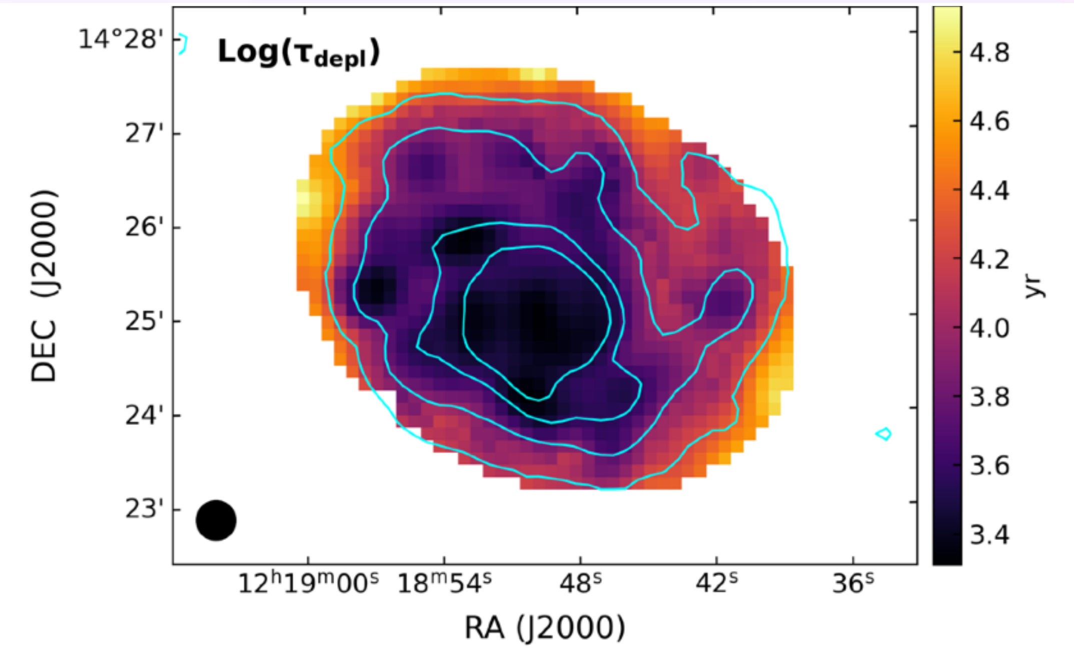

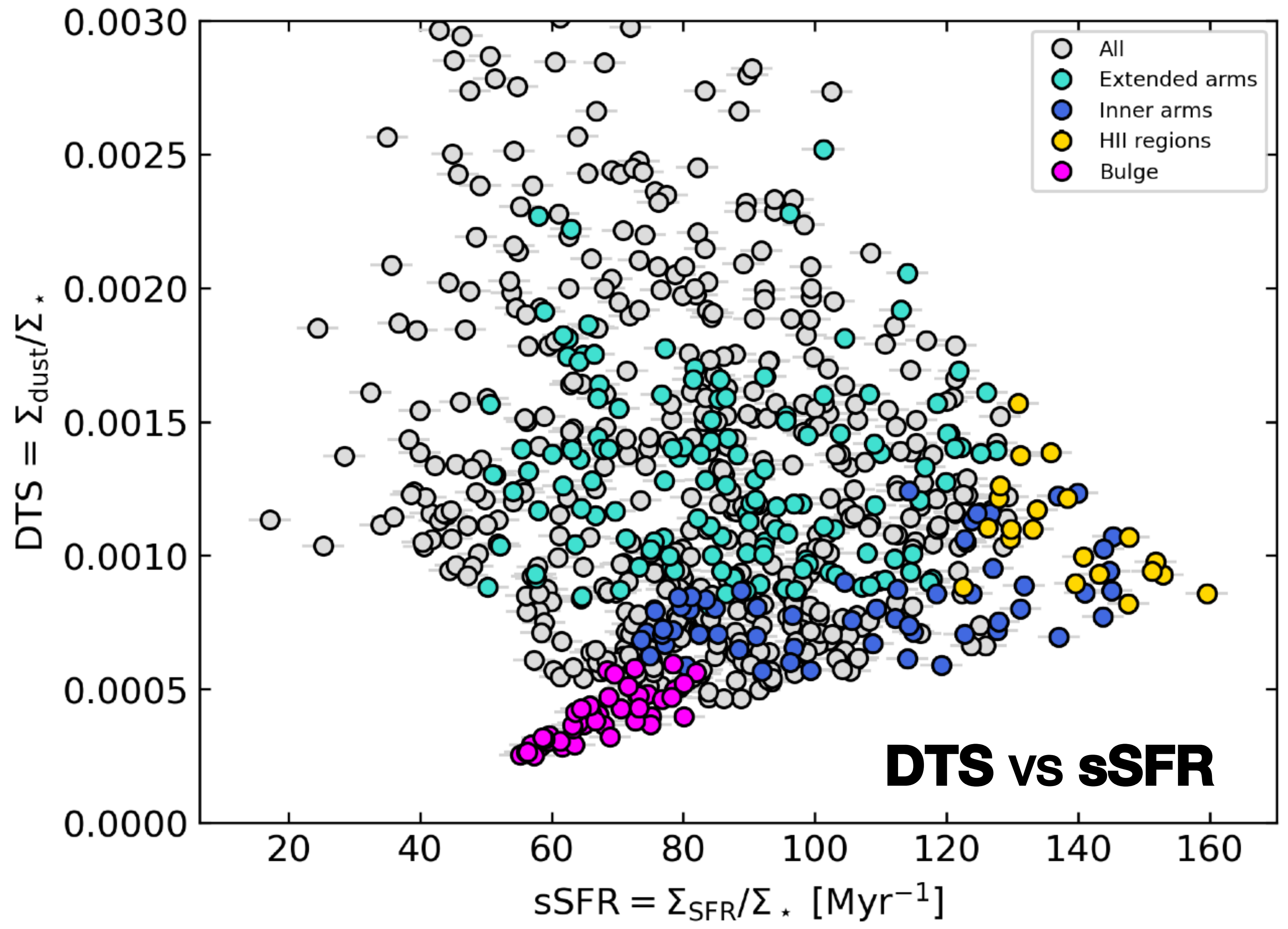

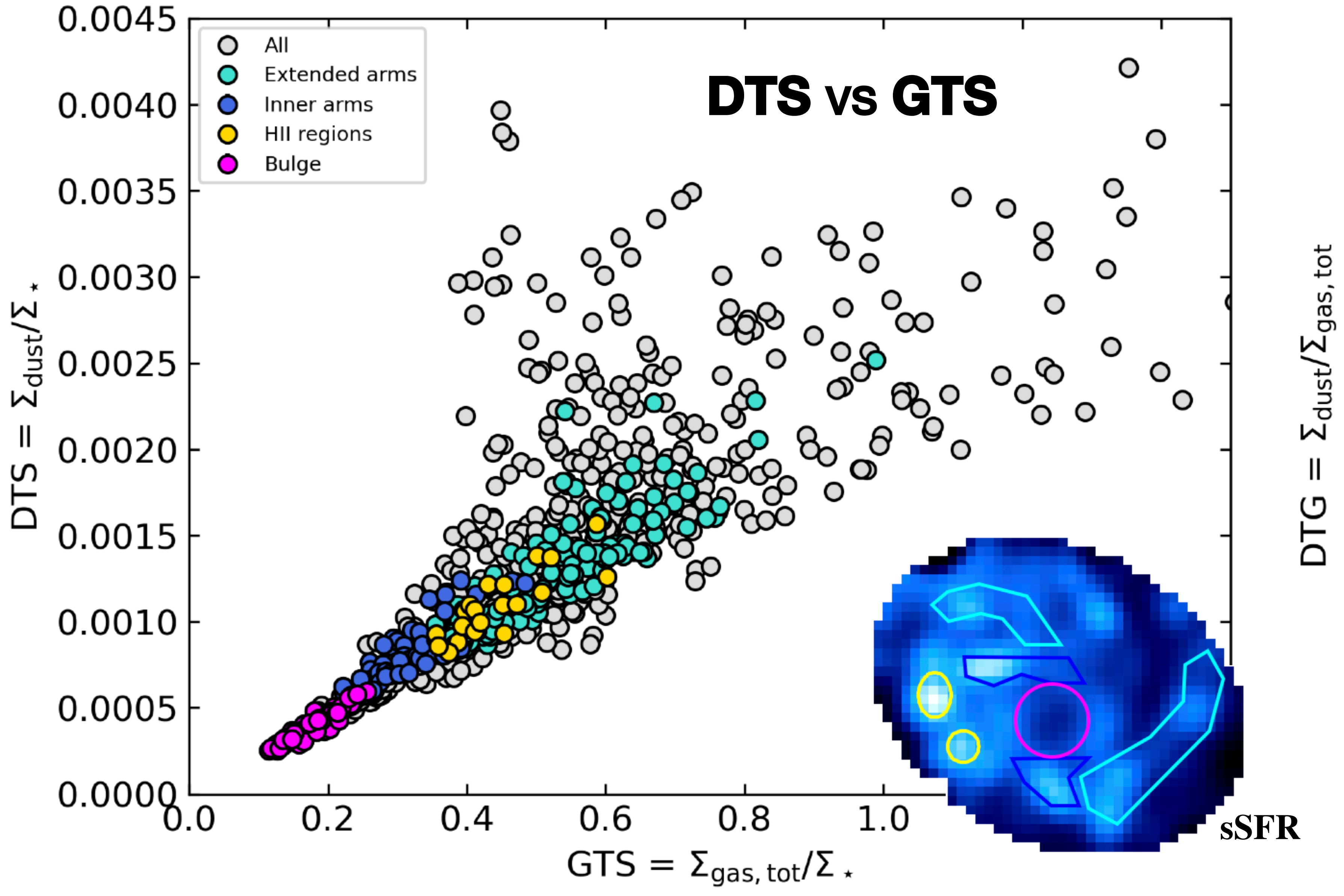

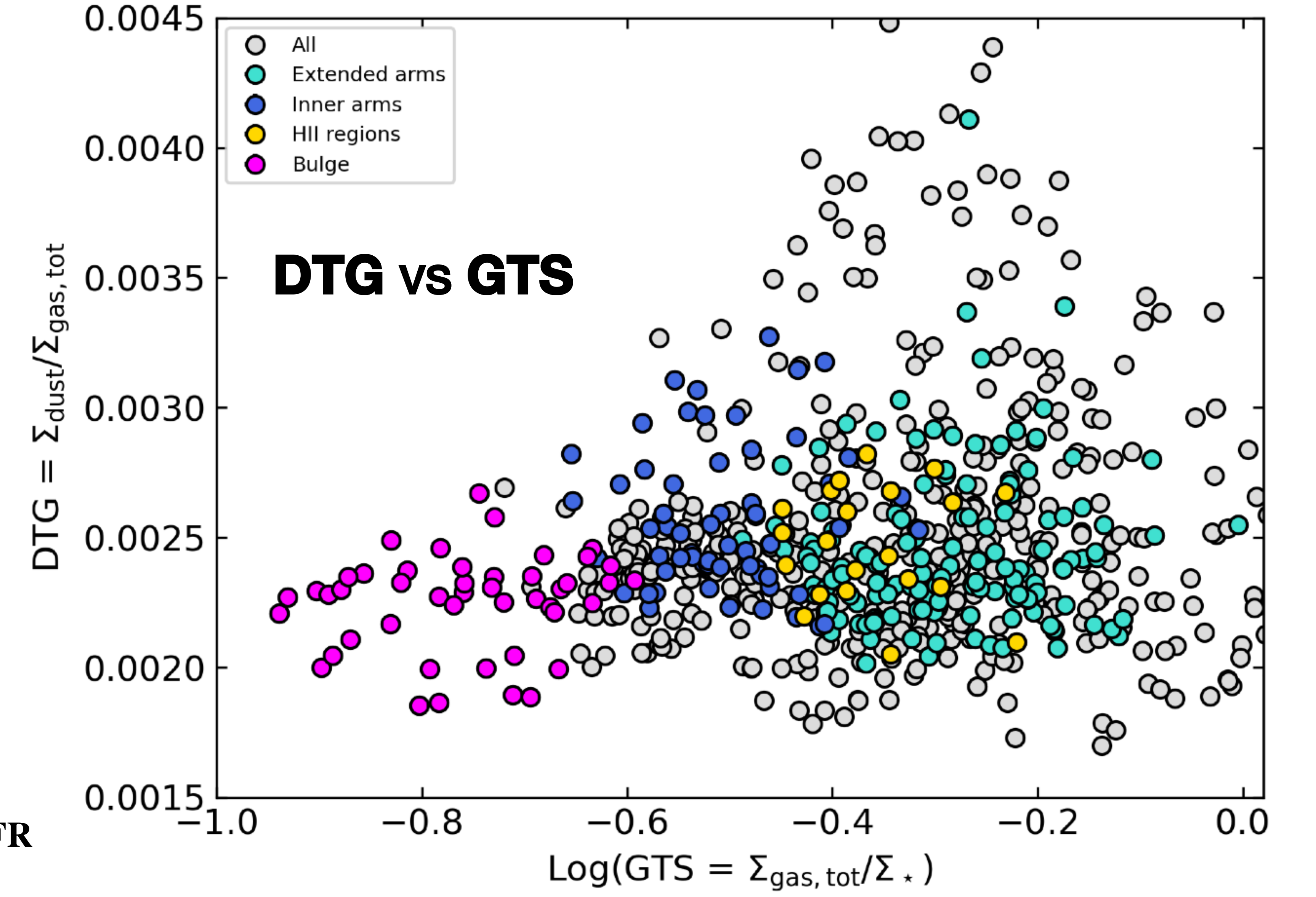

PIXEL-BY-PIXEL SED FITTING

Ang. res. 25'' ~ 1.75 kpc

px size 8'' ~ 0.56 kpc

Spatially-resolved dust / ISM properties

3. Typical SRF densities, gas and dust reservoirs show that the **bulk of star formation activity** in NGC 4254 happens in the **bulge**, **spiral arms** and **HII regions.**

   HII regions and spiral arms are **more efficient in converting molecular gas into stars and in forming new stars**, showing the shortest τ_depl and the highest sSFR.

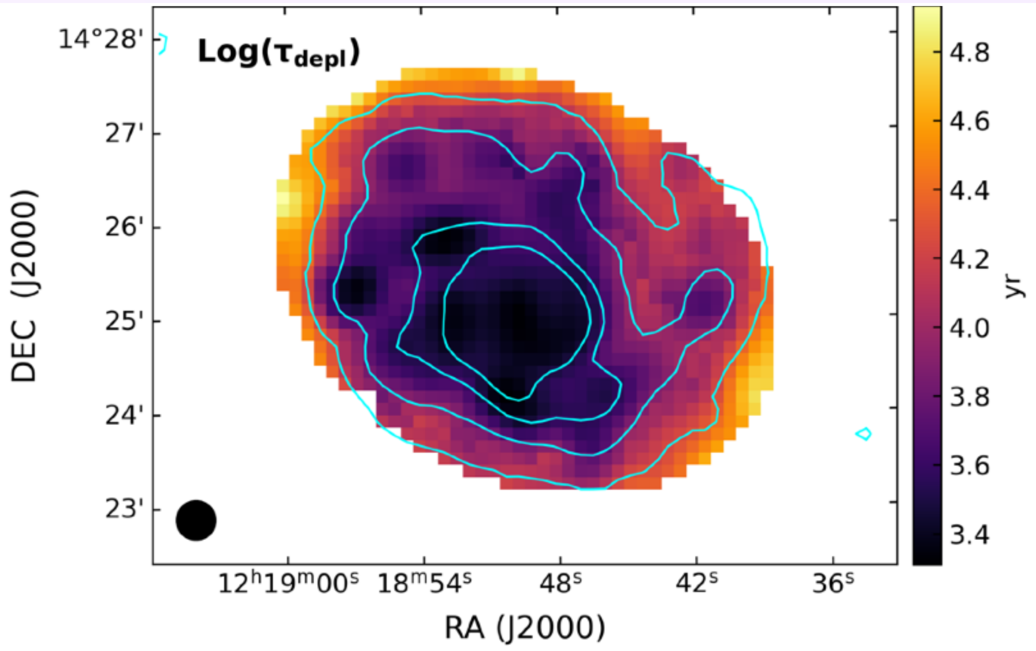

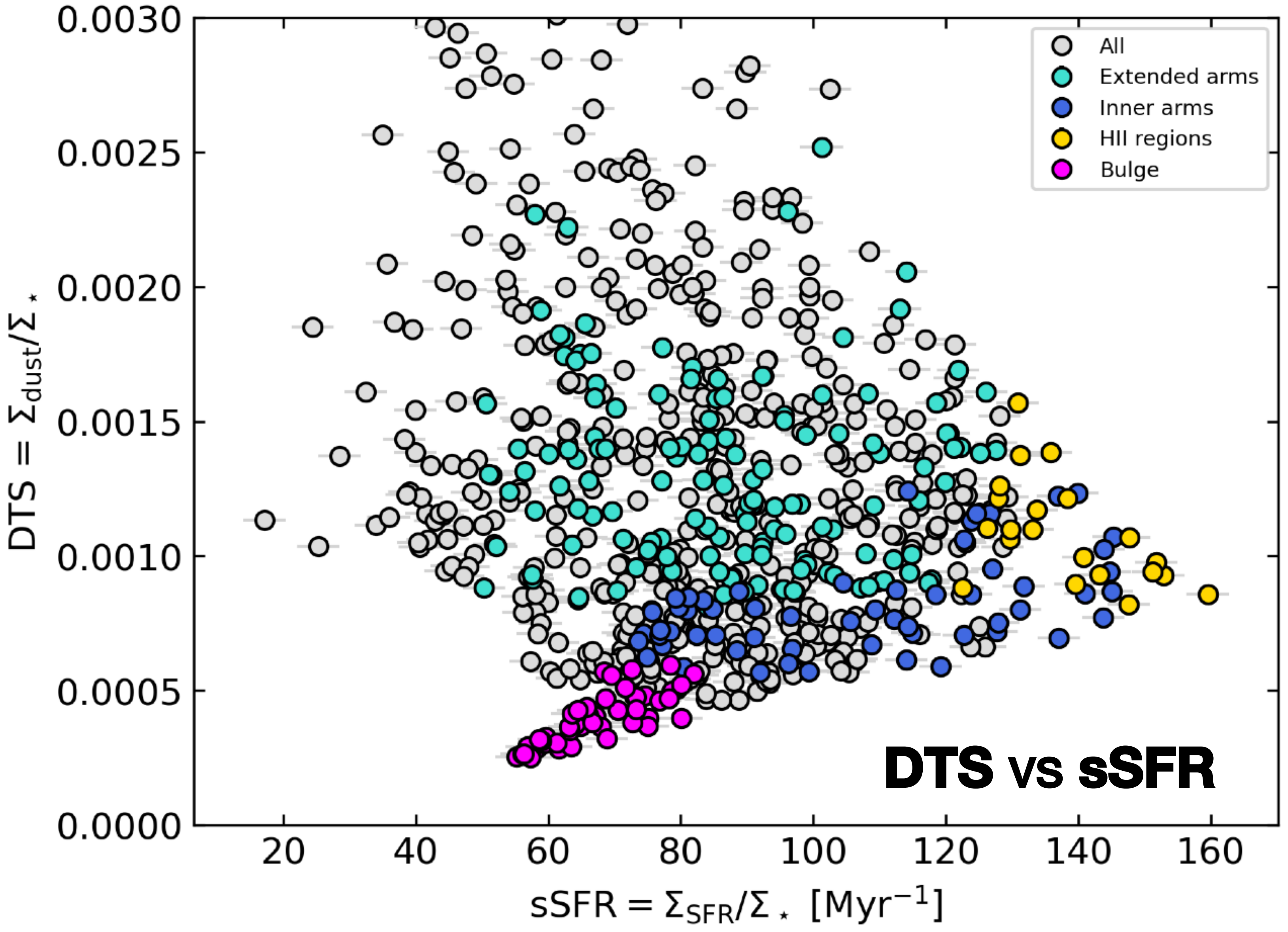

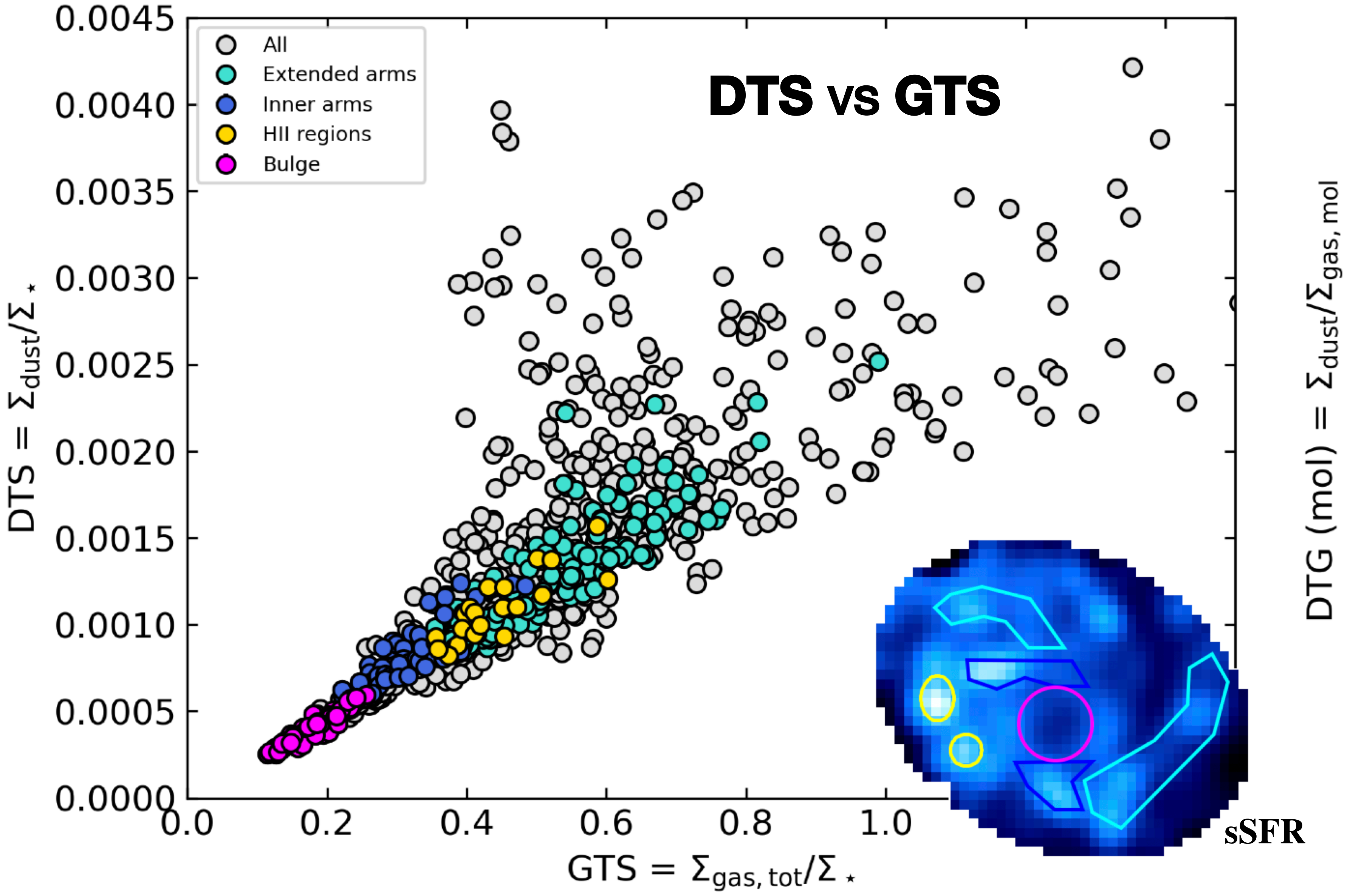

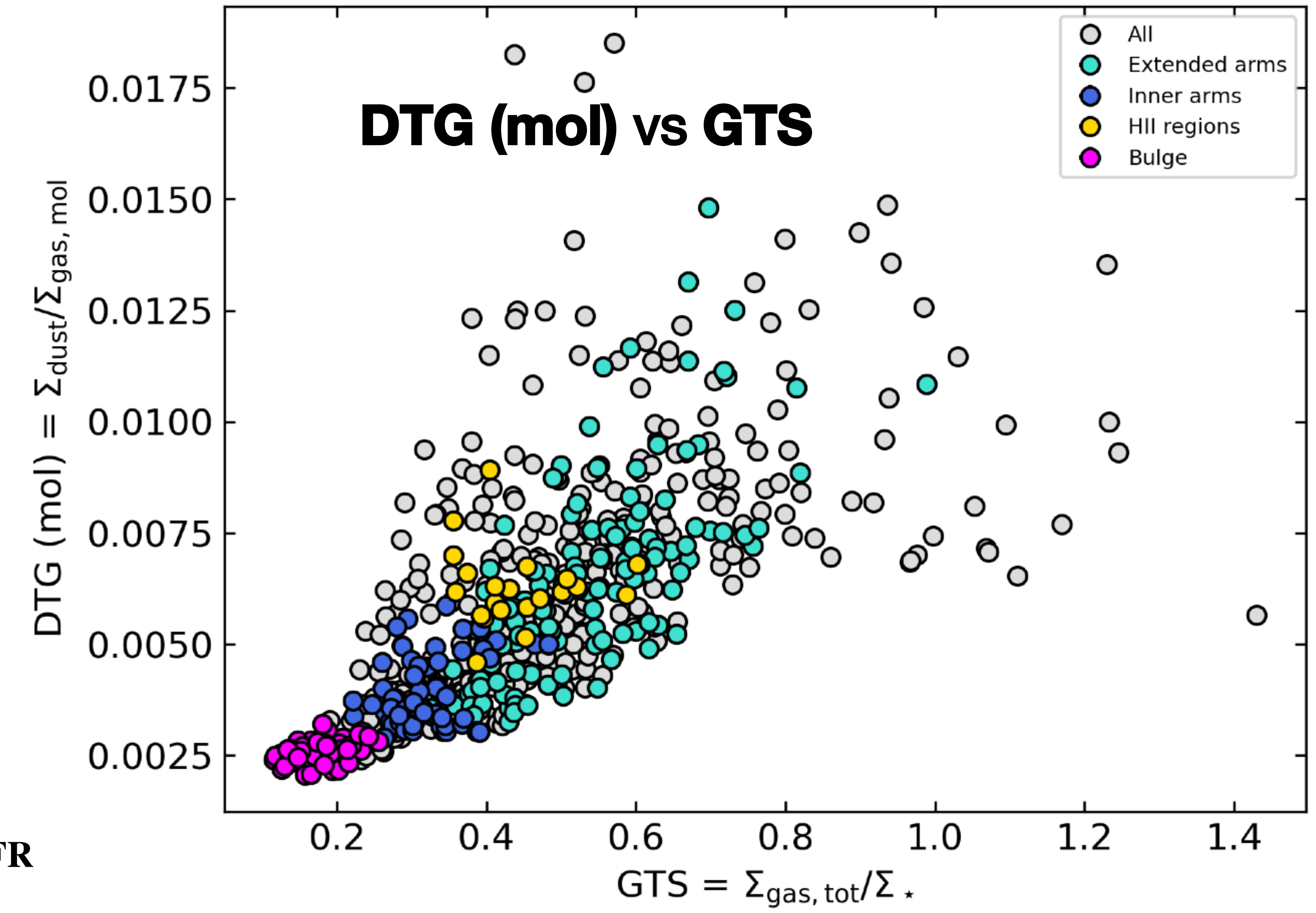

PIXEL-BY-PIXEL SED FITTING

Ang. res. 25″ ~ 4.05 kpc

px size 8″ ~ 1.35 kpc

Spatially-resolved dust / ISM properties

3. Typical SRF densities, gas and dust reservoirs show that the **bulk of star formation activity** in NGC 4254 happens in the **bulge**, **spiral arms** and **HII regions.**

   HII regions and spiral arms are **more efficient in converting molecular gas into stars and in forming new stars**, showing the shortest τ_depl and the highest sSFR.

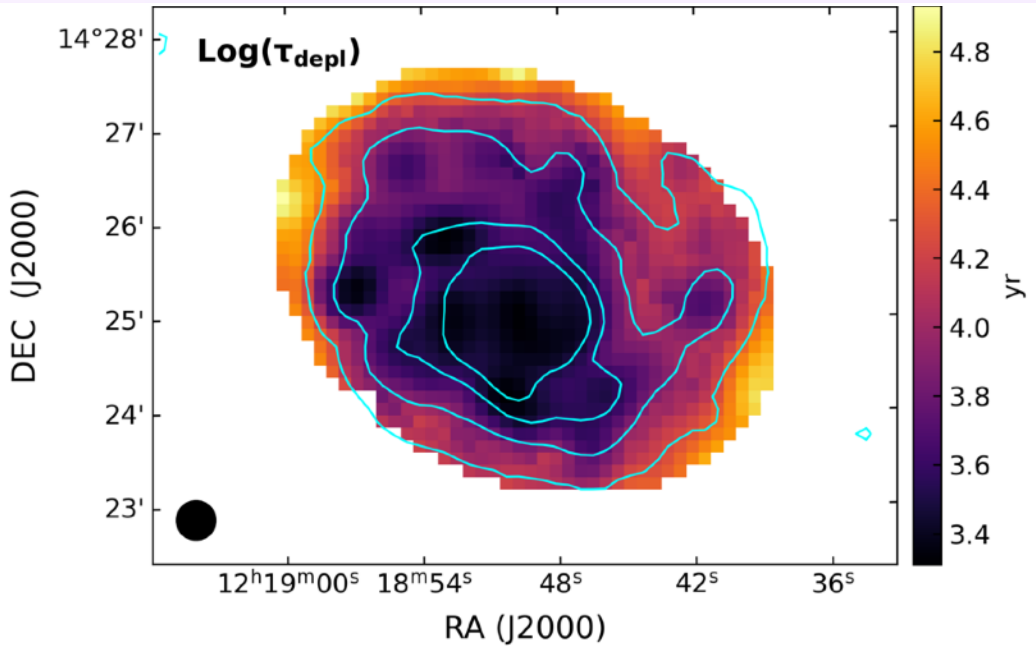

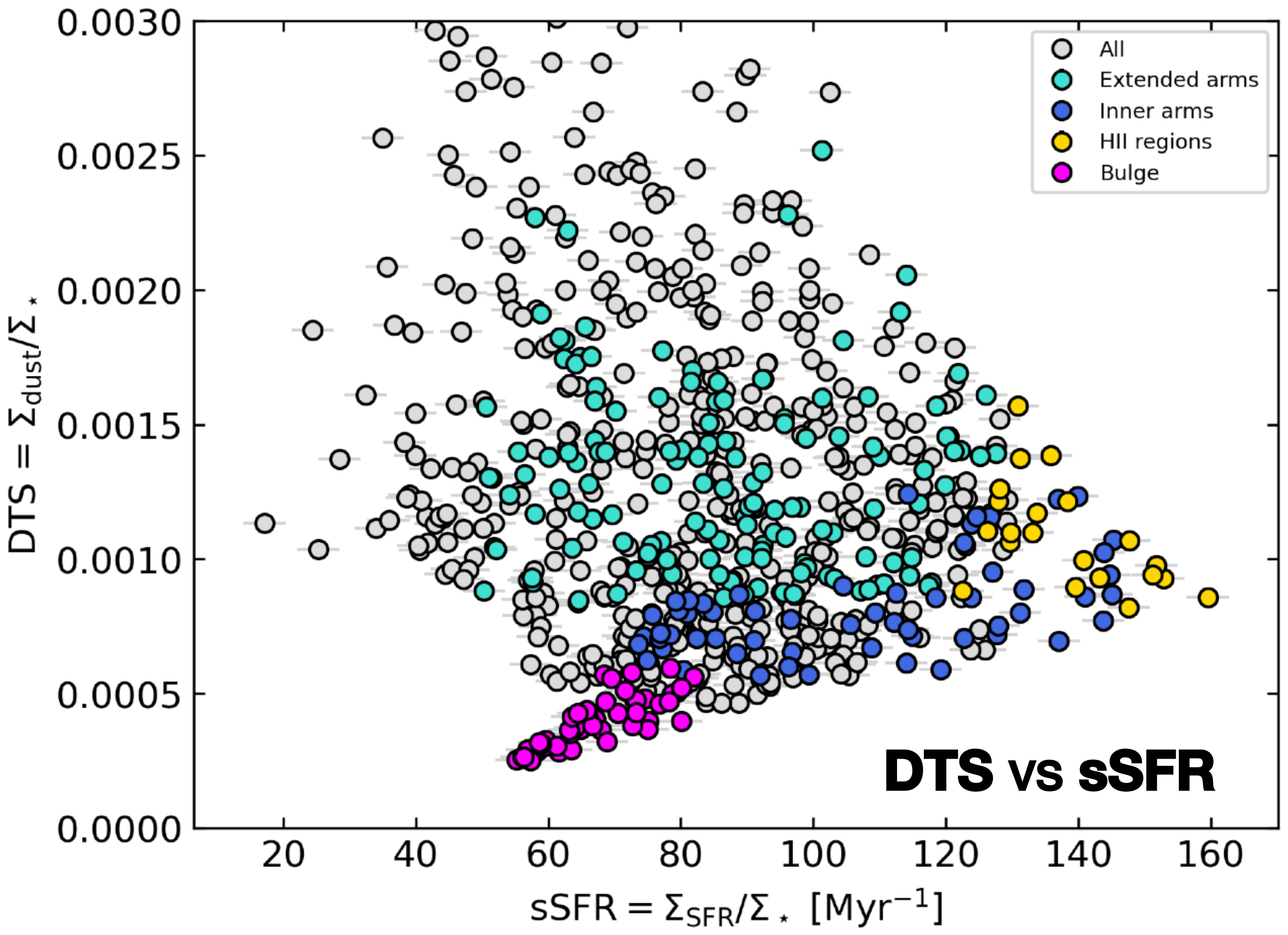

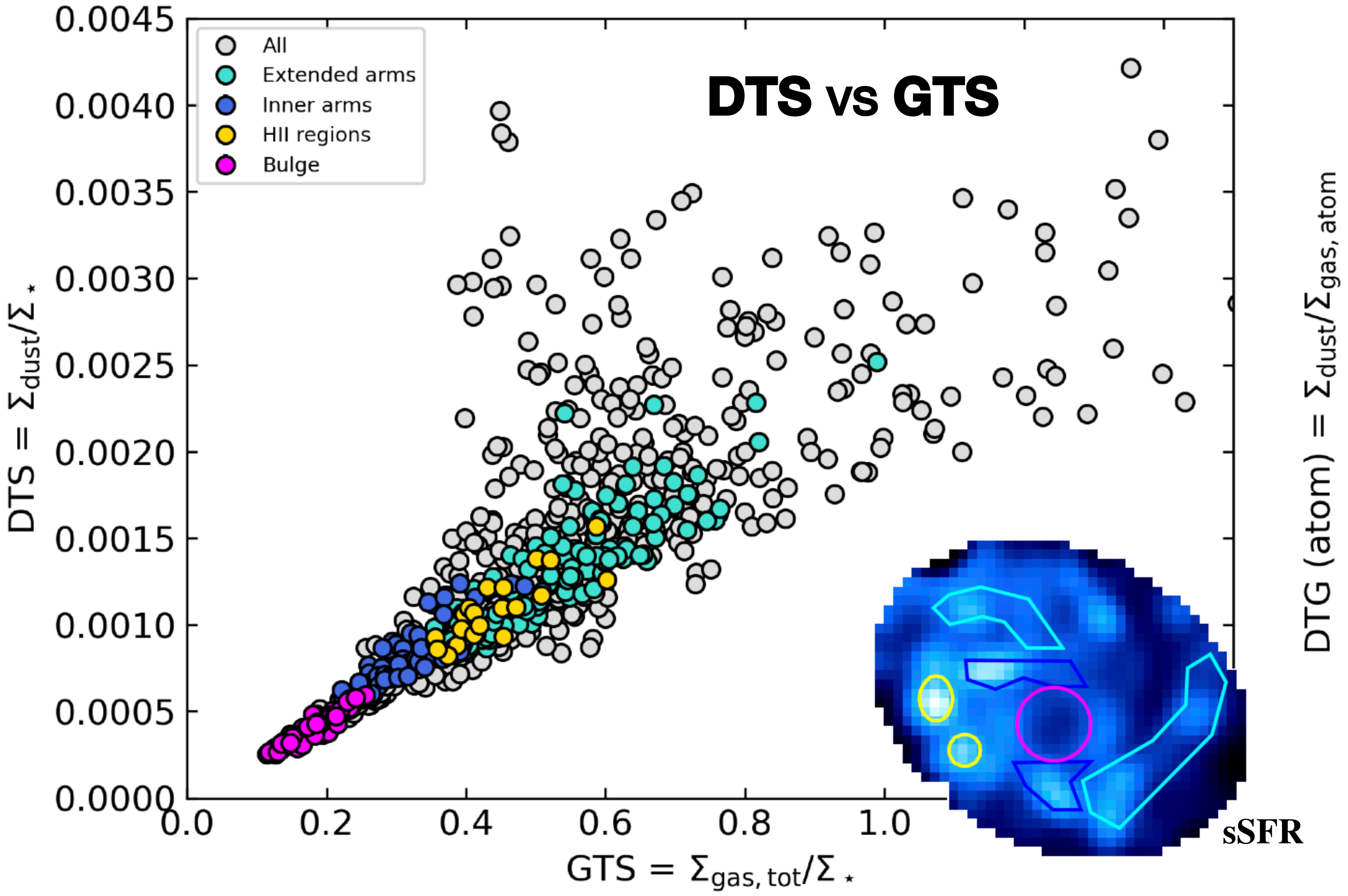

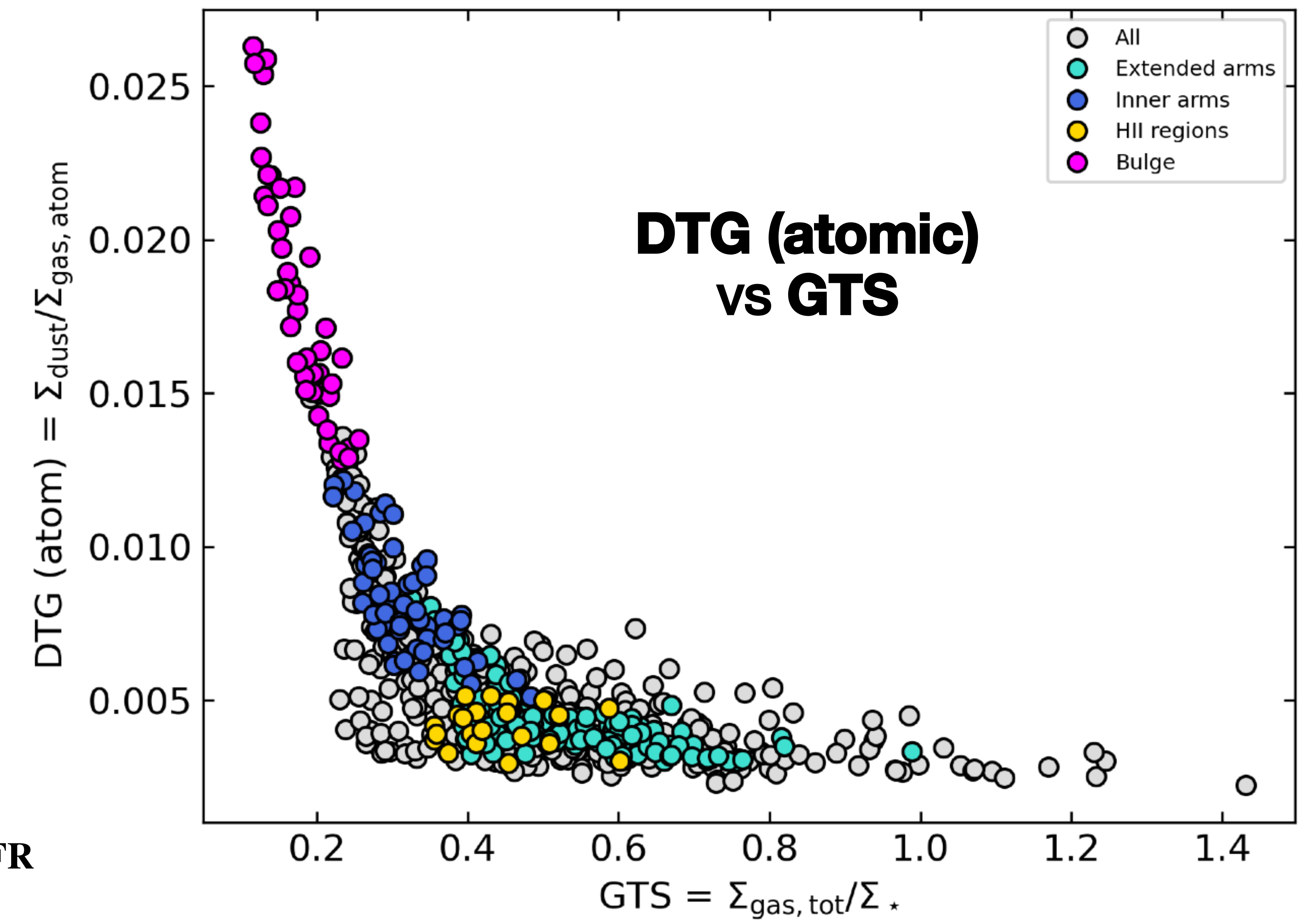

PIXEL-BY-PIXEL SED FITTING

Ang. res. 25'' ~ 4.05 kpc

px size 8'' ~ 1.35 kpc

Summary and Conclusions

Focusing on NGC4254, I have shown that our method

- allows us to get the most important **dust parameter** maps (e.g., dust mass, beta, mean ISRF, fraction of small grains) and the **resolved scaling relations** with the other **ISM components**;
- is **effective** in retrieving the typical correlations between free parameters;
- allows us to **put constraints on dust evolution** in the diverse local environments within a galaxy (i.e., HII regions, arms, bulge, disk).

NIKA2 maps were essential for modeling the dust millimeter emission at kpc scale.

Main results:

- Significant **steepening of the FIR dust spectral** index going into **denser star-forming regions** (β~2) where dust grains are highly reprocessed (coagulation + loss of carbonaceous mantle);
- Small grains are efficiently destroyed in ambients with hard interstellar radiation field (sublimation + desorption).
- Dust correlate well with **sSFR** in dense environment and with **gas** in all environments; the **gas *dustiness*** is broadly constant with specific gas mass, but changes significantly when considering the molecular or atomic phase.
- Flat radio spectral indices are linked to recent star formation activity.

ACKNOWLEDGEMENTS
S. Madden, F. Galliano, M. Baes, J. Tedros, H. Roussel, C. Kramer, G. Ejlali, S. Katsioli, X. Desert, A. Jones, N. Ysard, M. Smith, M. Xilouris, A. Hughes, A. Nersesian, and NIKA2 collab.

Backup slides

Molecular gas and r21

Transition	Telescope	λ_{rest} [mm]	θ_{res}^{FWHM} [″]	Pixel size [″]
CO(2 – 1) [a]	IRAM–30m	1.3	13.4	2
CO(1 – 0) [b]	IRAM–30m	2.6	25.6	4
HI [c]	VLA	210	30	5

Table 3. Spectral line intensity maps used to compute the gas surface density of NGC4254 and correct the millimeter continuum for CO line emission contamination.

[a] HERACLES program (Leroy et al. 2009).
[b] EMPIRE program (Jiménez-Donaire et al. 2019).
[c] VIVA VLA Atlas (Chung et al. 2009).

< r21 > = 0.7 +\- 0.2

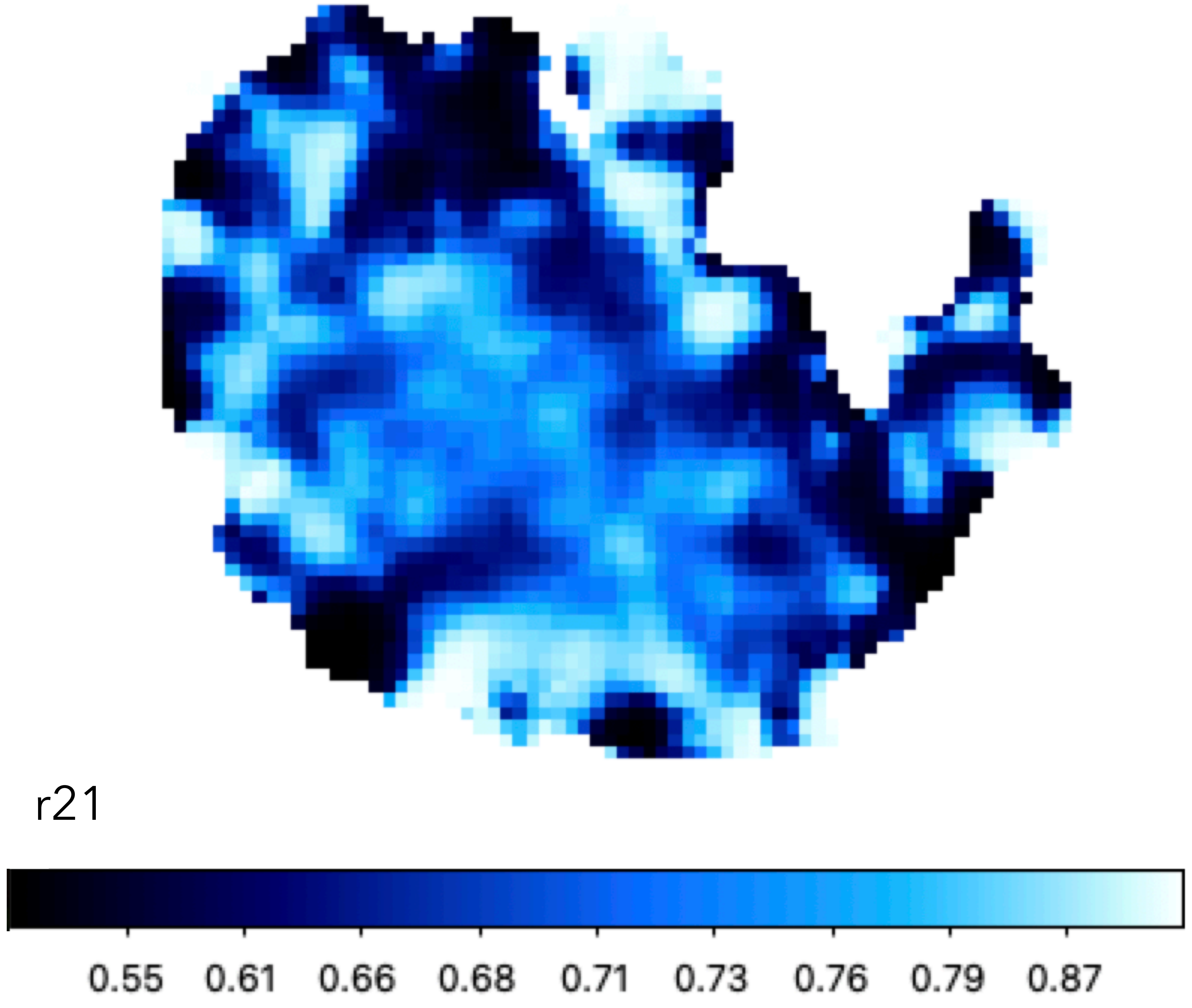

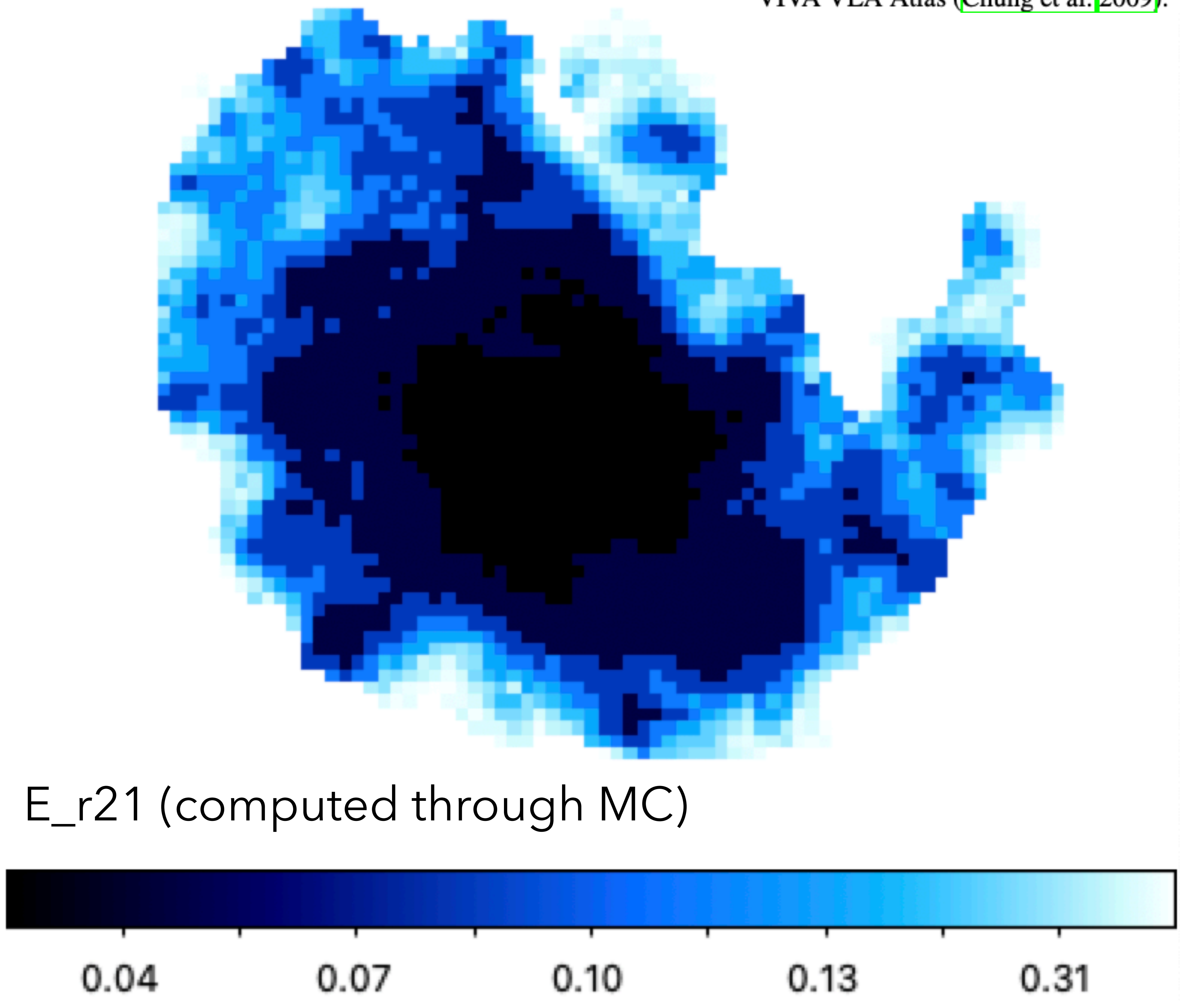

Metallicity map

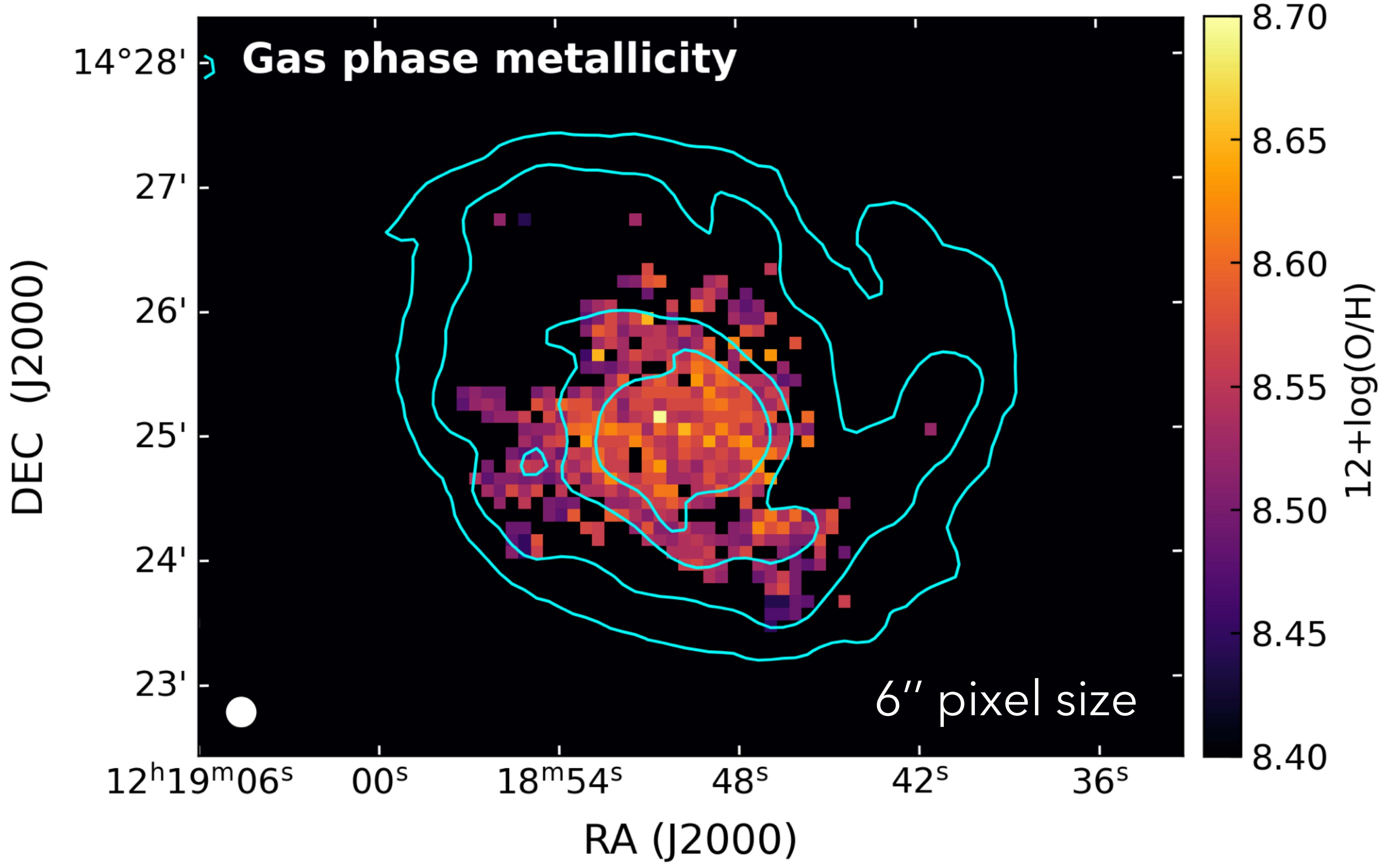

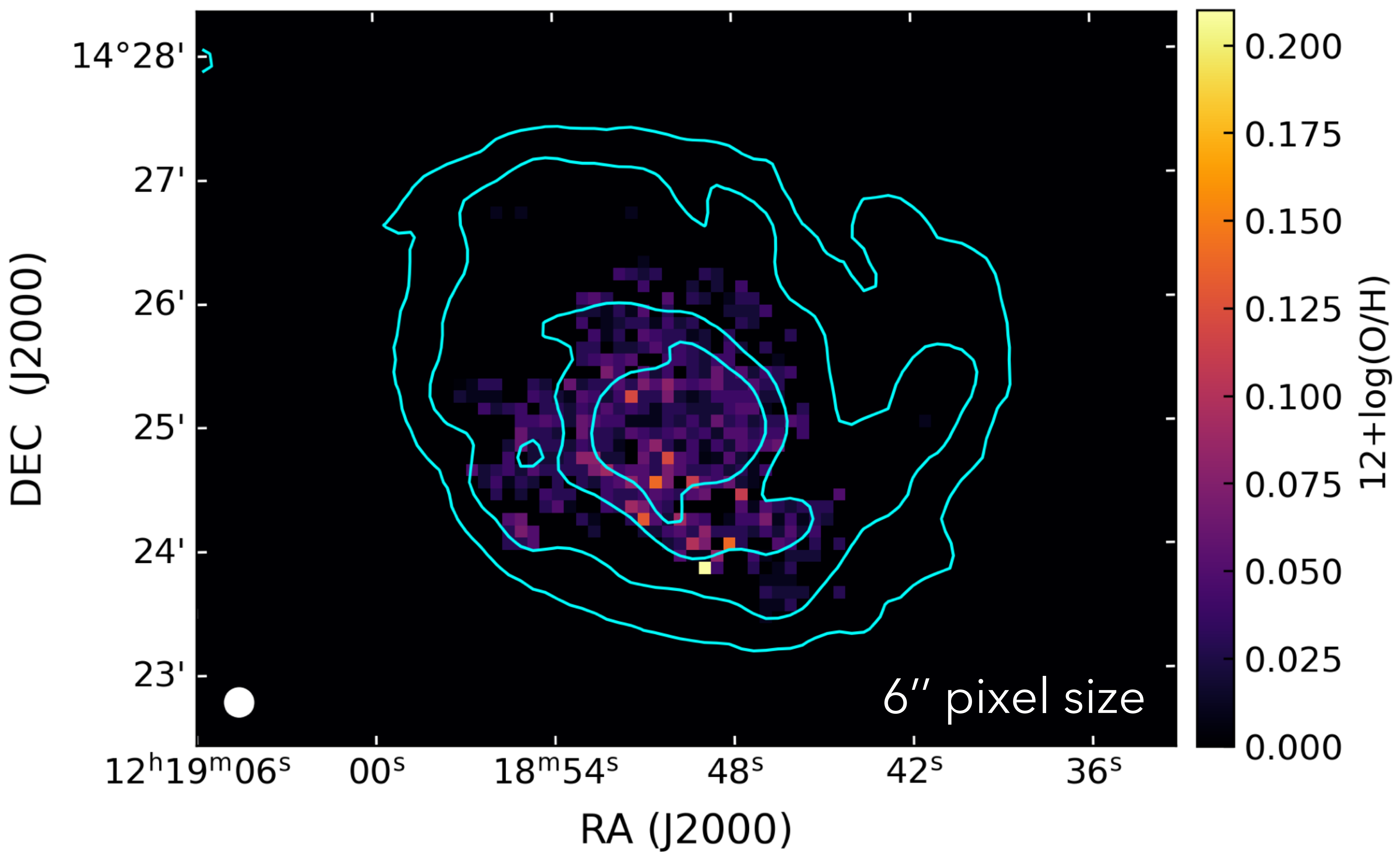

Gas-phase metallicity measurements in approximately 1900 HII regions from:

- **PHANGS-MUSE** (Kreckel et al. 2019);
- **De Vis et al. (2019**; DustPedia collaboration).

Metallicity were calibrated using the S calibration by Pilyugin & Grebel (2016).

Data homogenization

The multi-λ maps have **different size, spatial resolution, pixel size, orientation, units.**
In order to perform the pixel-by-pixel SED fitting, we need to **homogenize these quantities**.

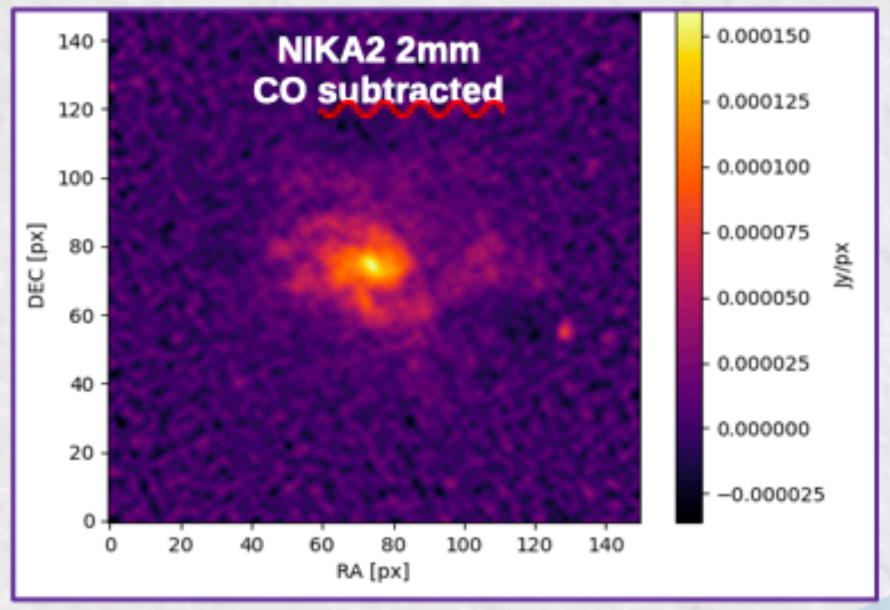

0) - **Large-scale filtering is included in the uncertainty budget.**
- **CO(2-1) is subtracted** from NIKA2 1.15 mm map.
(Drabek et al. 2012)

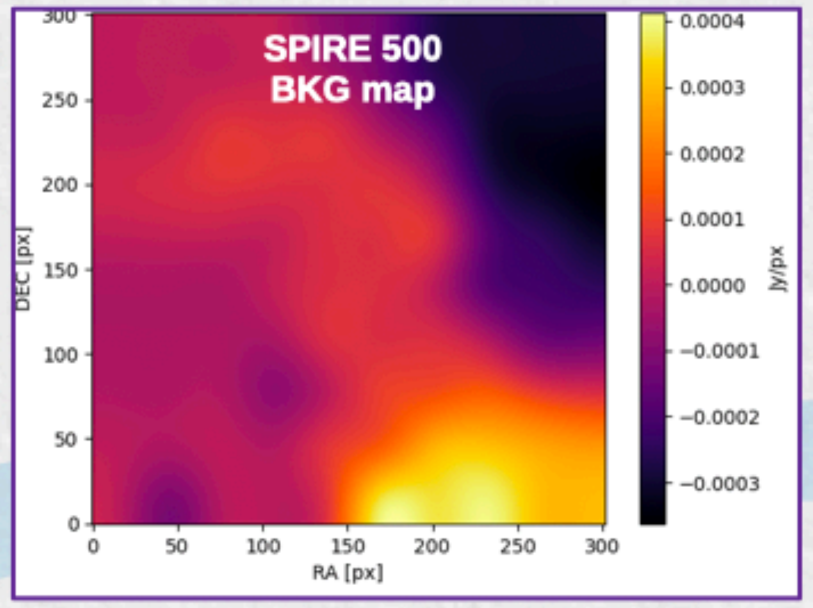

1) Emission in the **background and foreground** is **modelled** and **subtracted.**

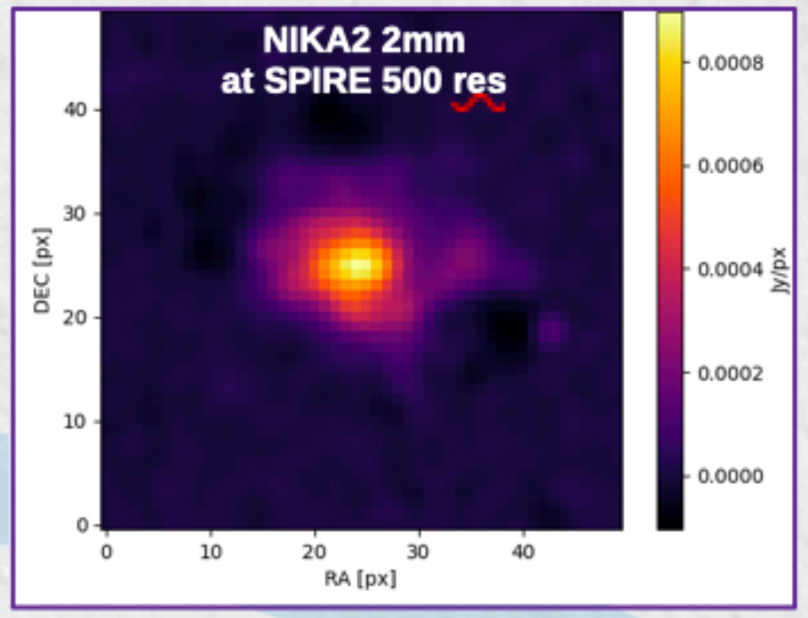

2) **Maps** are **convolved** to the **same resolution, pixel size** and **orientation.**
(Aniano et al. 2011)

3) **Uncertainties** are **propagated** using the **Monte Carlo method.**

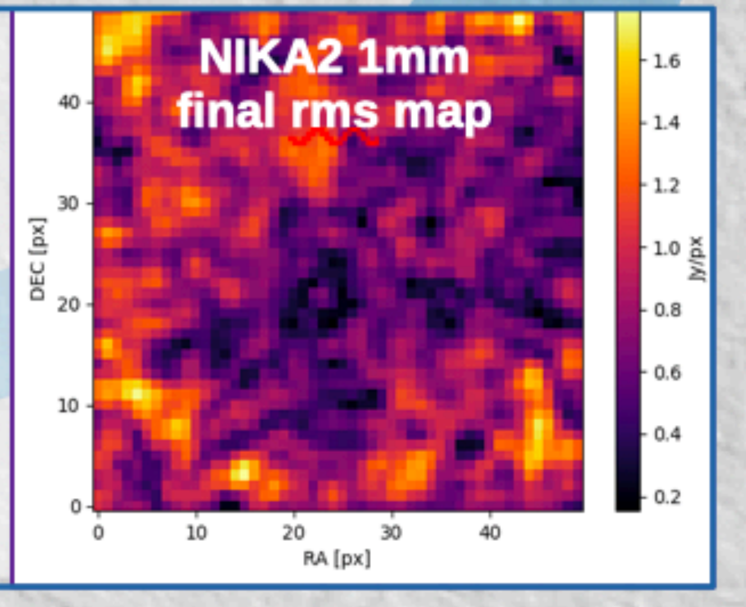

These steps are implemented in the **Homogenization of IMEGIN Photometry** post-processing pipeline (**HIP**; **Pantoni et al. in prep.**)

PIIC, Scanam_nika maps & ACT+Planck

- **PIIC data reduction v1**: significant lost in integrated flux, i.e. 0.4 ± 0.03 Jy, compared to Planck 1.38 mm (extrapolated to 1.15 mm with beta=2), i.e. 0.64 Jy.
- **Scanam_nika latest released**: global flux, i.e. 0.65 ± 0.04 Jy, matches the Planck 1.38 mm flux.
- **Planck** does not detect the galaxy at 2mm. **ACT+Planck** map show negative flux densities within the SPIRE 500 um 5sigma contour. **Scanam_nika** global flux at **2 mm**, i.e. 0.092 ± 0.016 Jy, is larger than the flux measure on ACT+Planck, i.e. 0.070 ± 0.001 Jy, even if there is evidence of a few % of filtering.

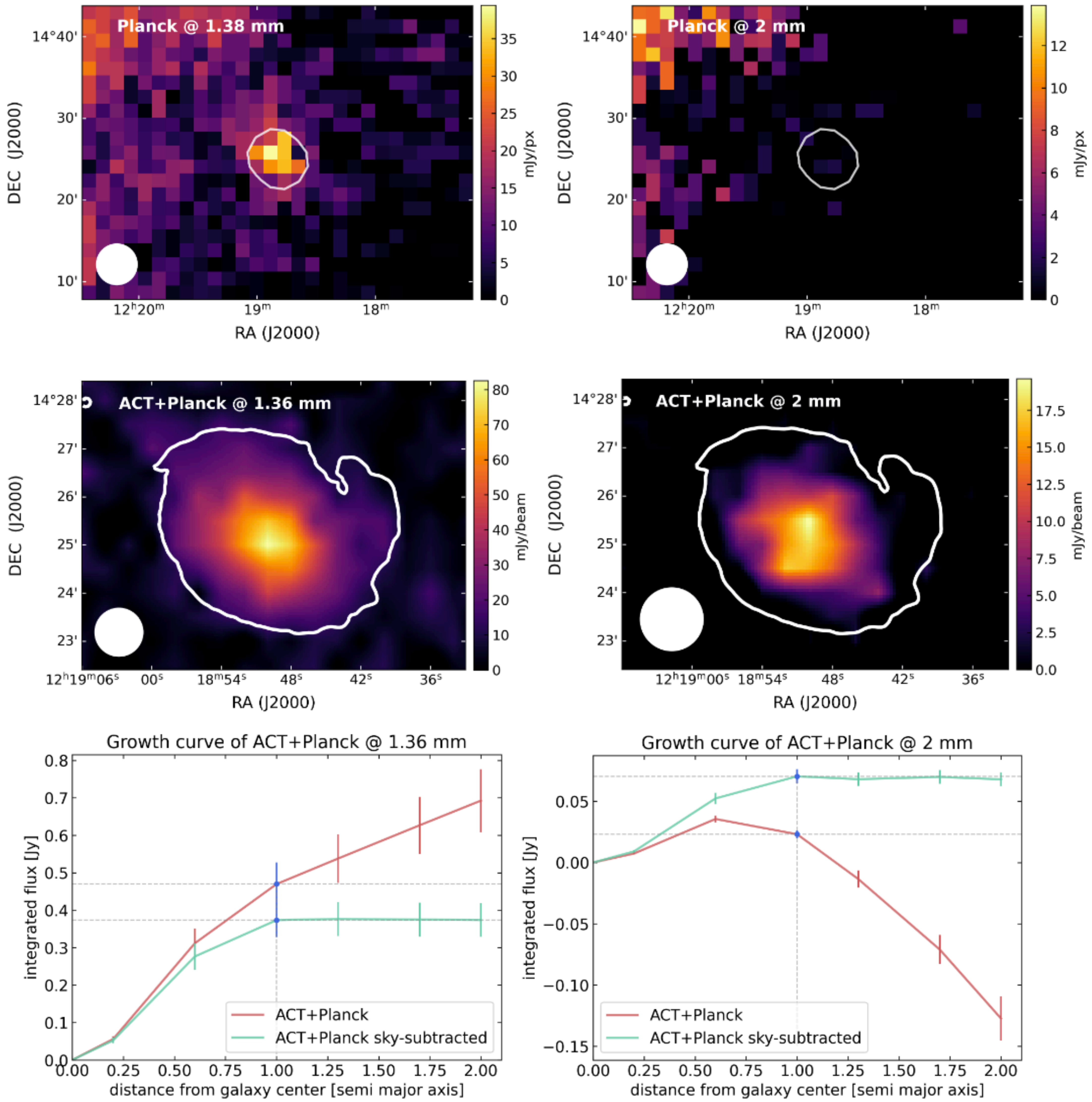

Note: Planck+ACT are background subtracted.

Scanam_nika maps: filtering

- Scanam_nika maps are affected by filtering (**up to 20%**).

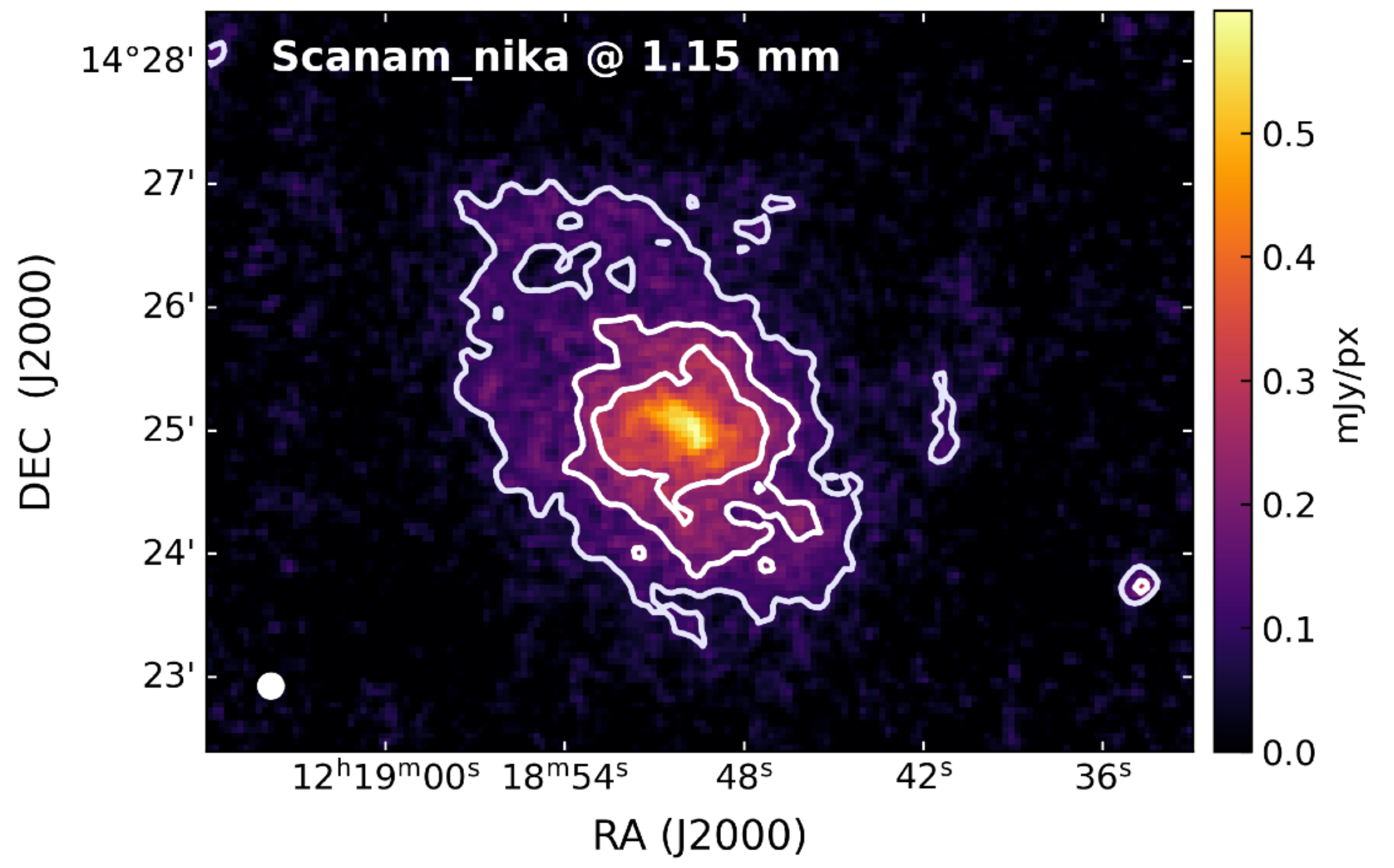

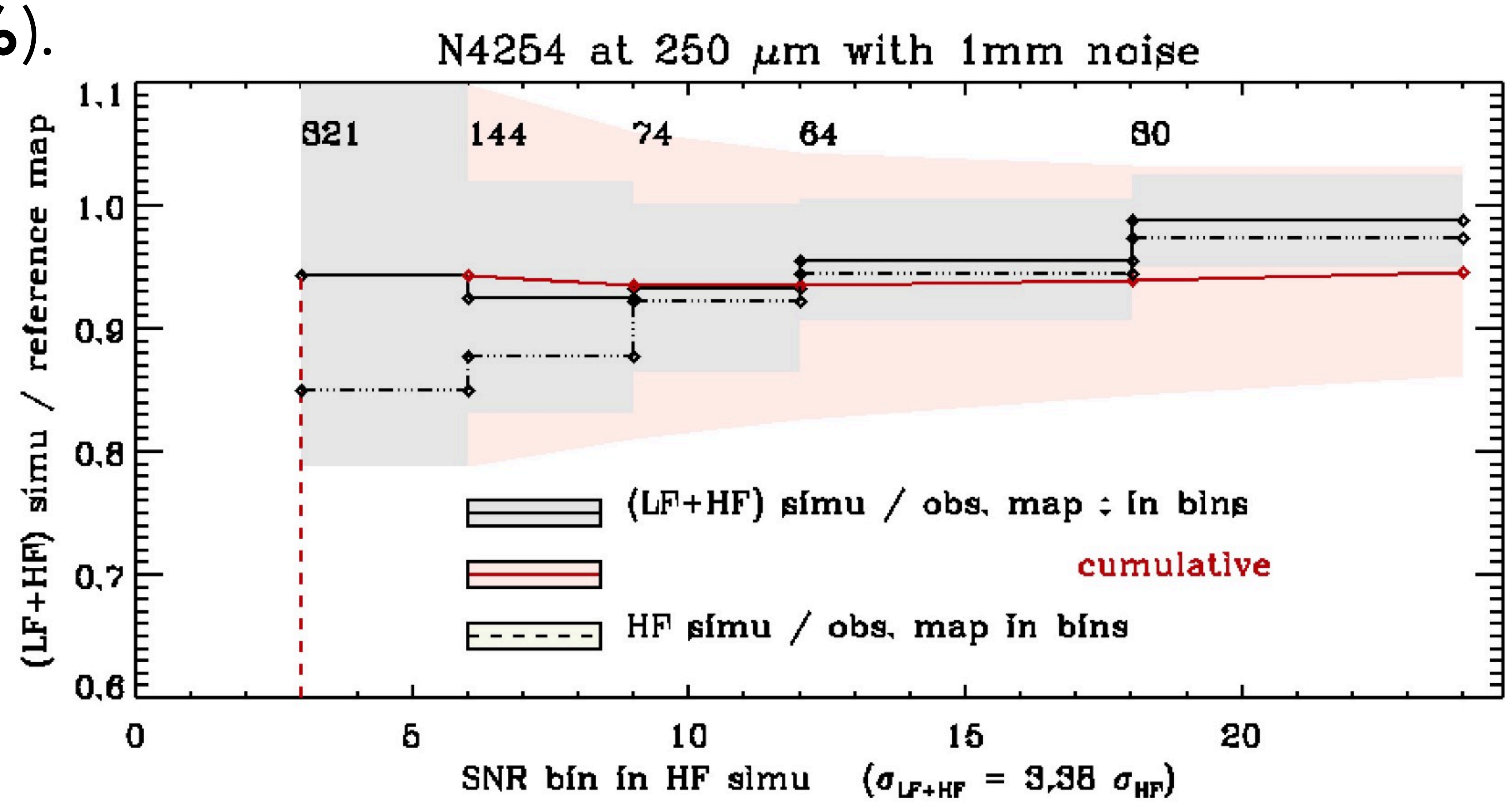

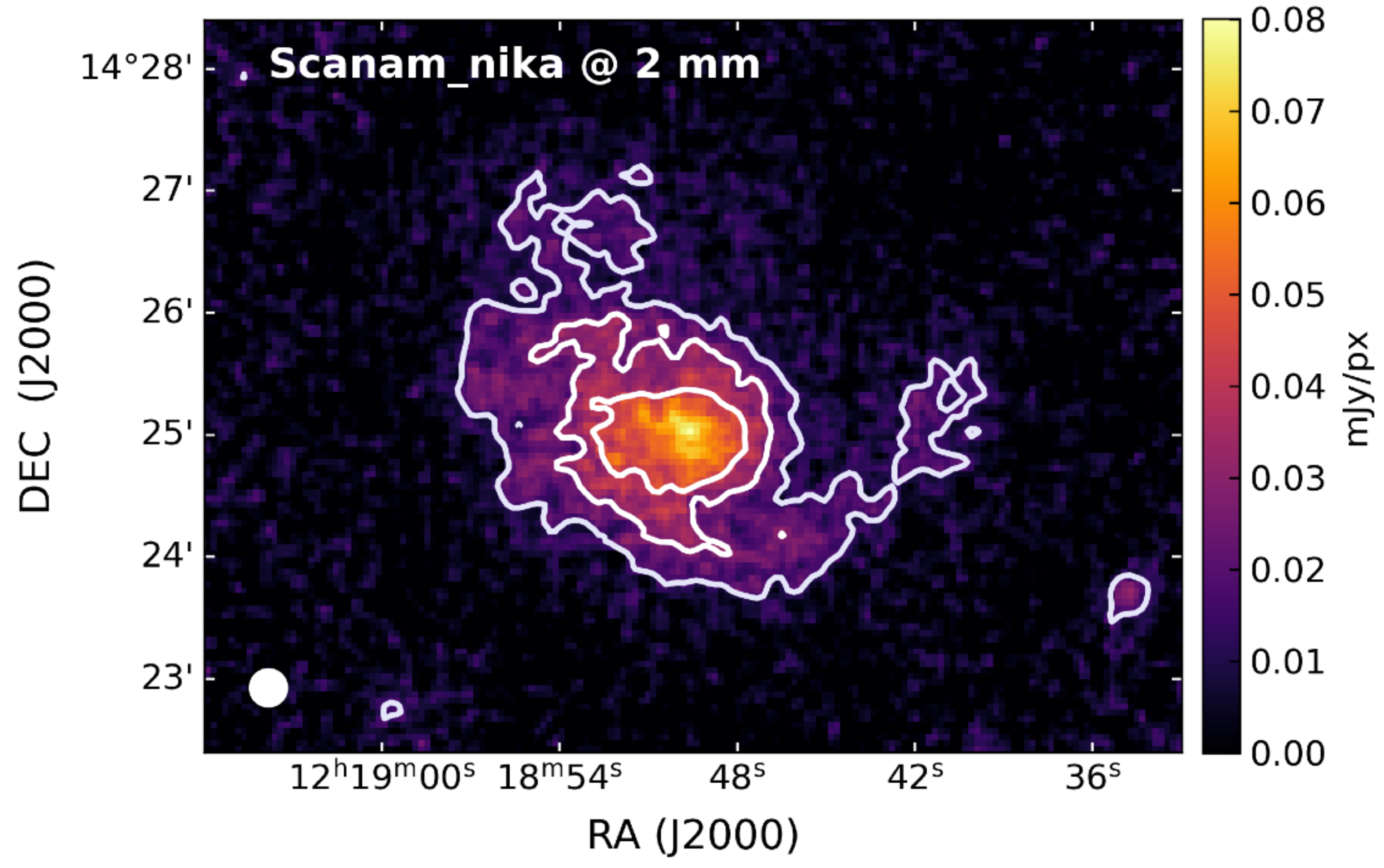

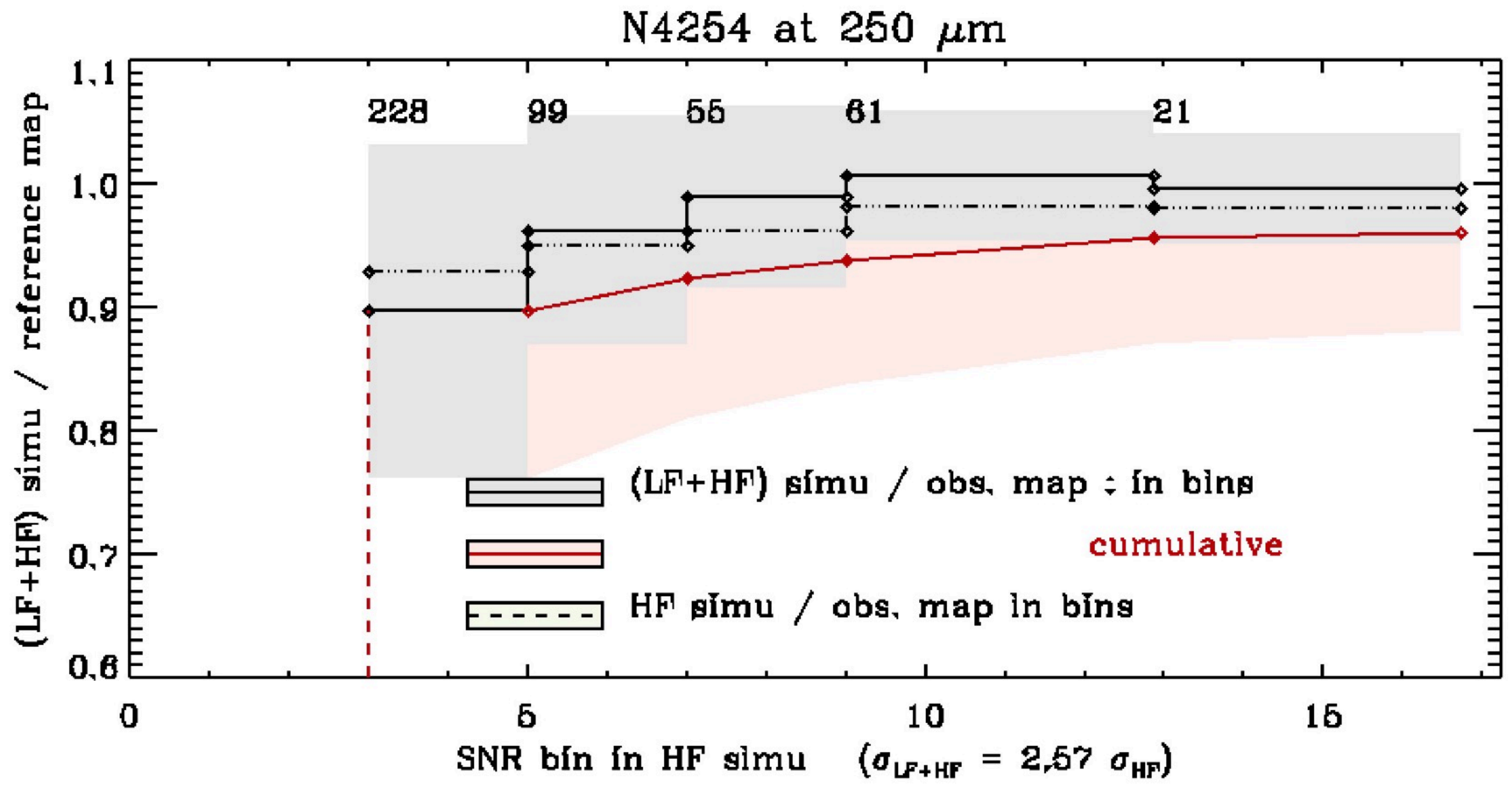

Scanam_nika maps: filtering

- How to include this evidence in our **uncertainty** budget?

GLOBAL SCALE

On **global scale** (within the ellipse we use to measure the global photometry), the relative uncertainties are **4%** at 1.15 mm and **8%** at 2 mm.

1.15 mm Error = 4% of the global flux

2 mm Error = 8% of the global flux

Spiral arms, disk, bulge

Within the galaxy **spiral arms, disk and bulge**, relative uncertainties are **5%** (spiral arms and disk) and **1%** (bulge) at 1.15 mm; **7%** (spiral arms), **16%** (disk) and **2%** (bulge) at 2 mm.

1.15 mm Error = 5% of the spiral arms flux
= 5% of the disk flux
= 1% of the bulge flux

2 mm Error = 7% of the spiral arms flux
= 16% of the disk flux
= 2% of the bulge flux

Scanam_nika maps: filtering

- How to include this evidence in our **uncertainty** budget?

GLOBAL SCALE (1.15 mm)

Error = 5% of the global flux

added in quadrature to the statistical error (sky_rms in Scanam_nika header).

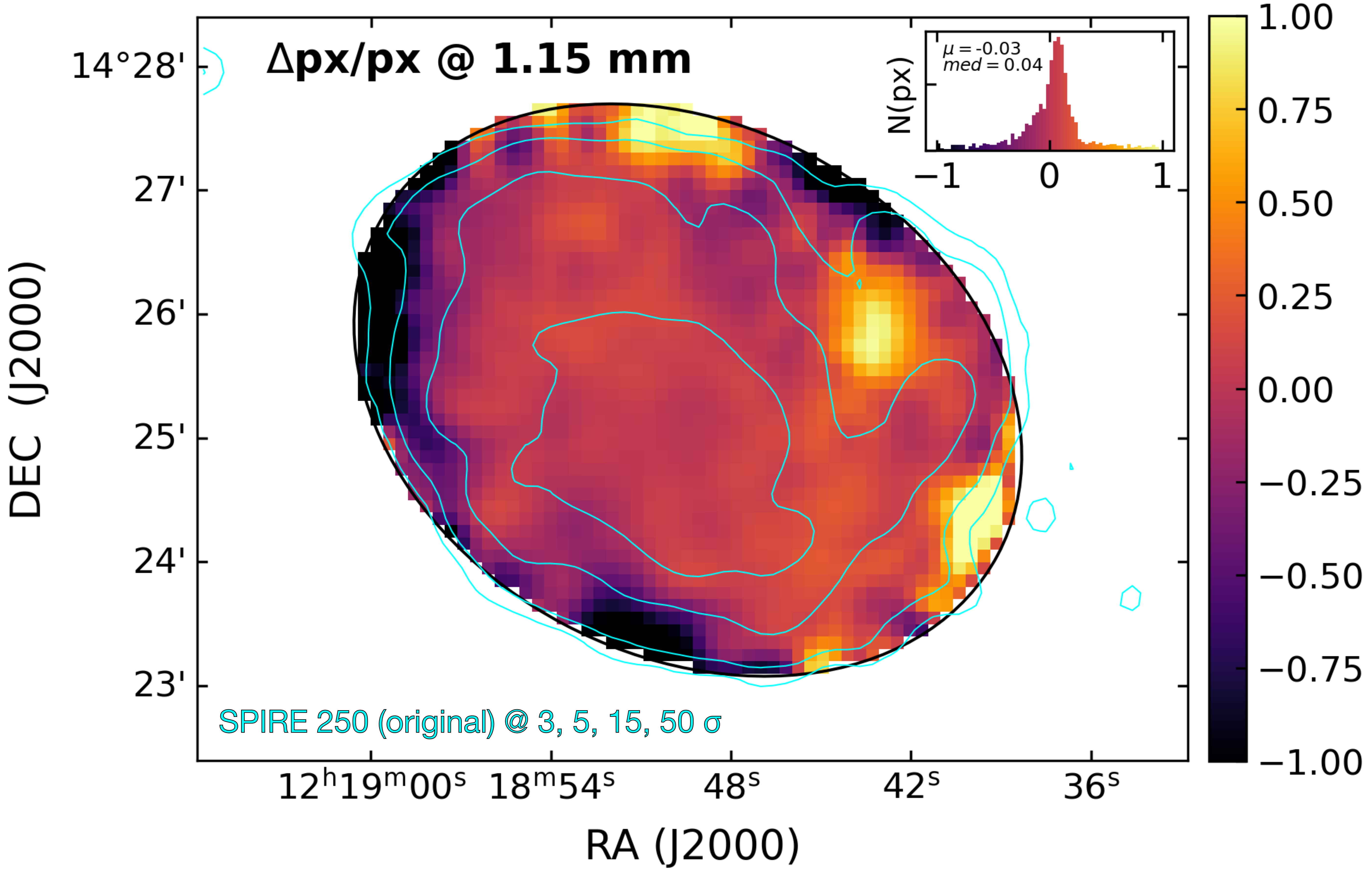

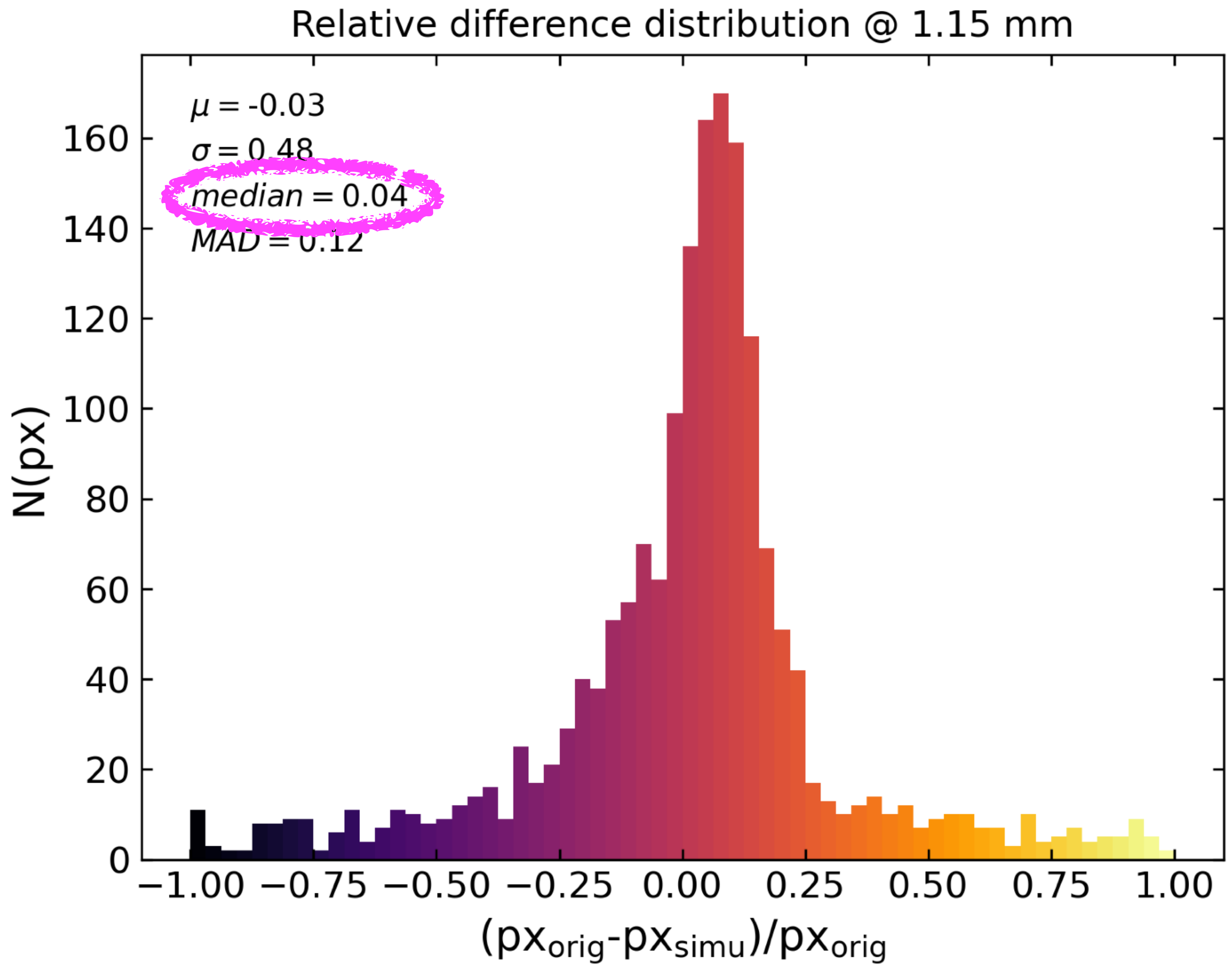

Scanam_nika maps: filtering

- How to include this evidence in our **uncertainty** budget?

GLOBAL SCALE (2 mm)

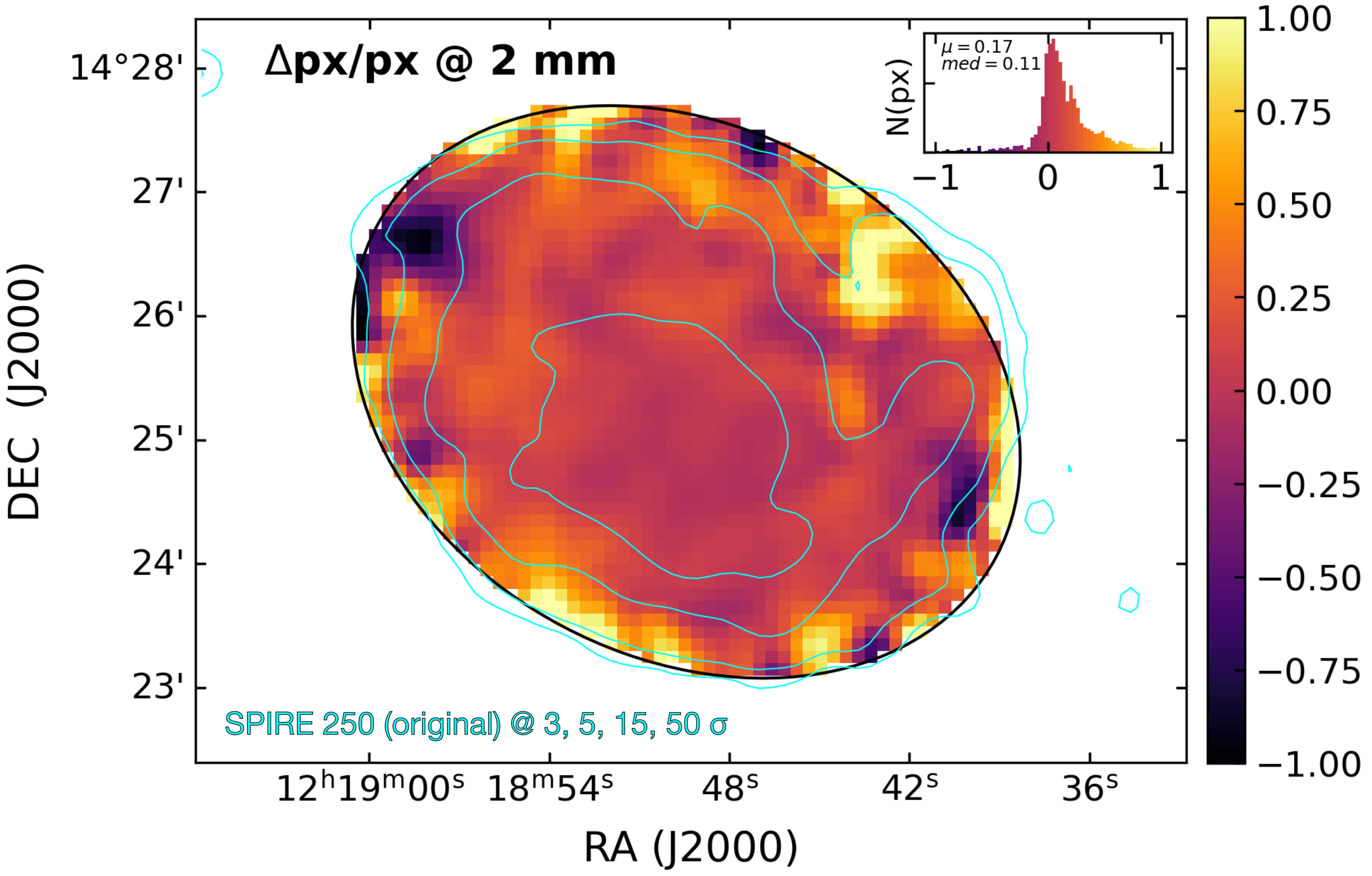

Error = 10% of the global flux

added in quadrature to the statistical error (sky_rms in Scanam_nika header).

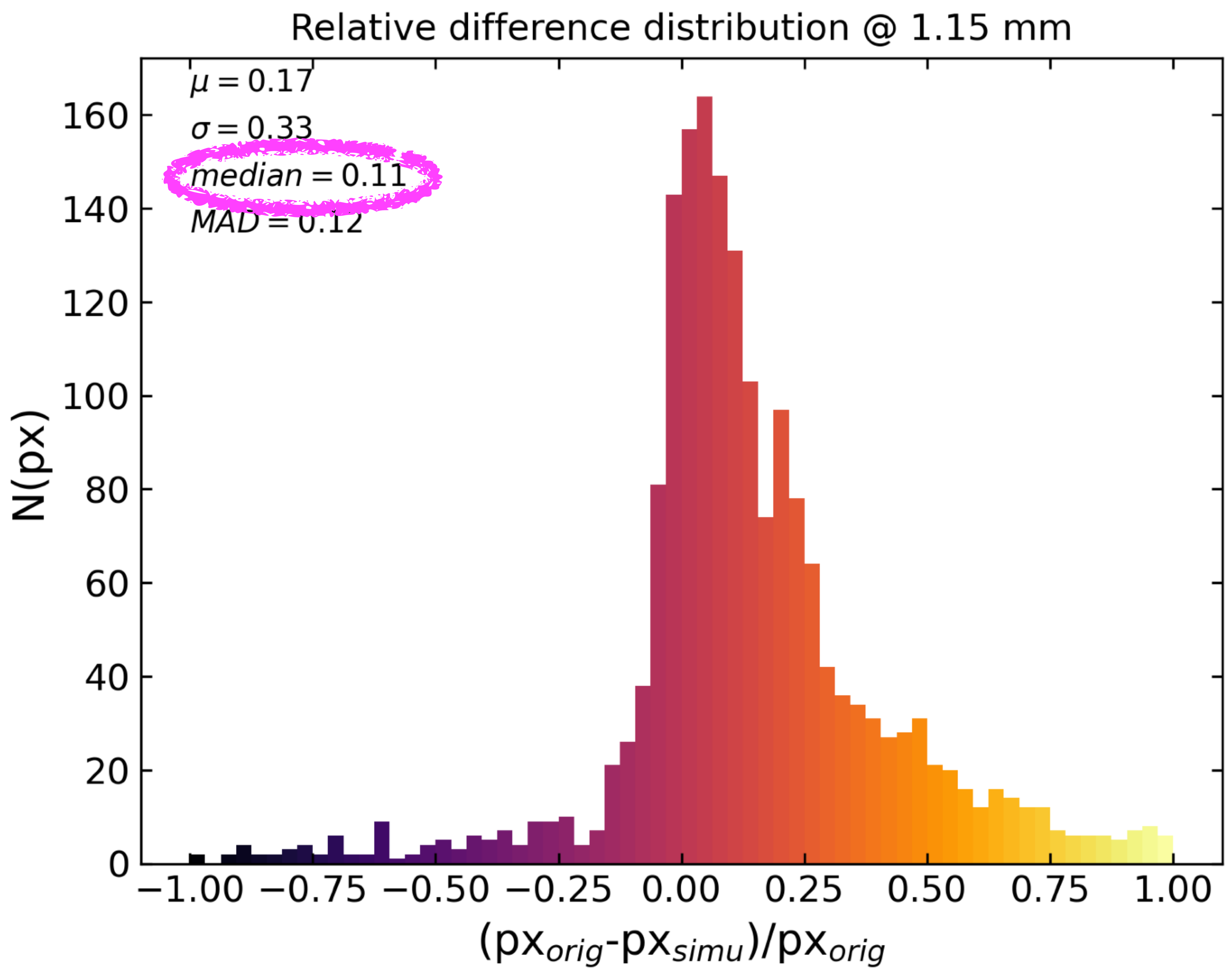

Scanam_nika maps: filtering

- How to include this evidence in our **uncertainty** budget?

PX SCALE (1.15 mm)

Error = 10% of the NIKA2 flux matching the 3σ simu

added in quadrature to the statistical error map (sky_rms in Scanam_nika header).

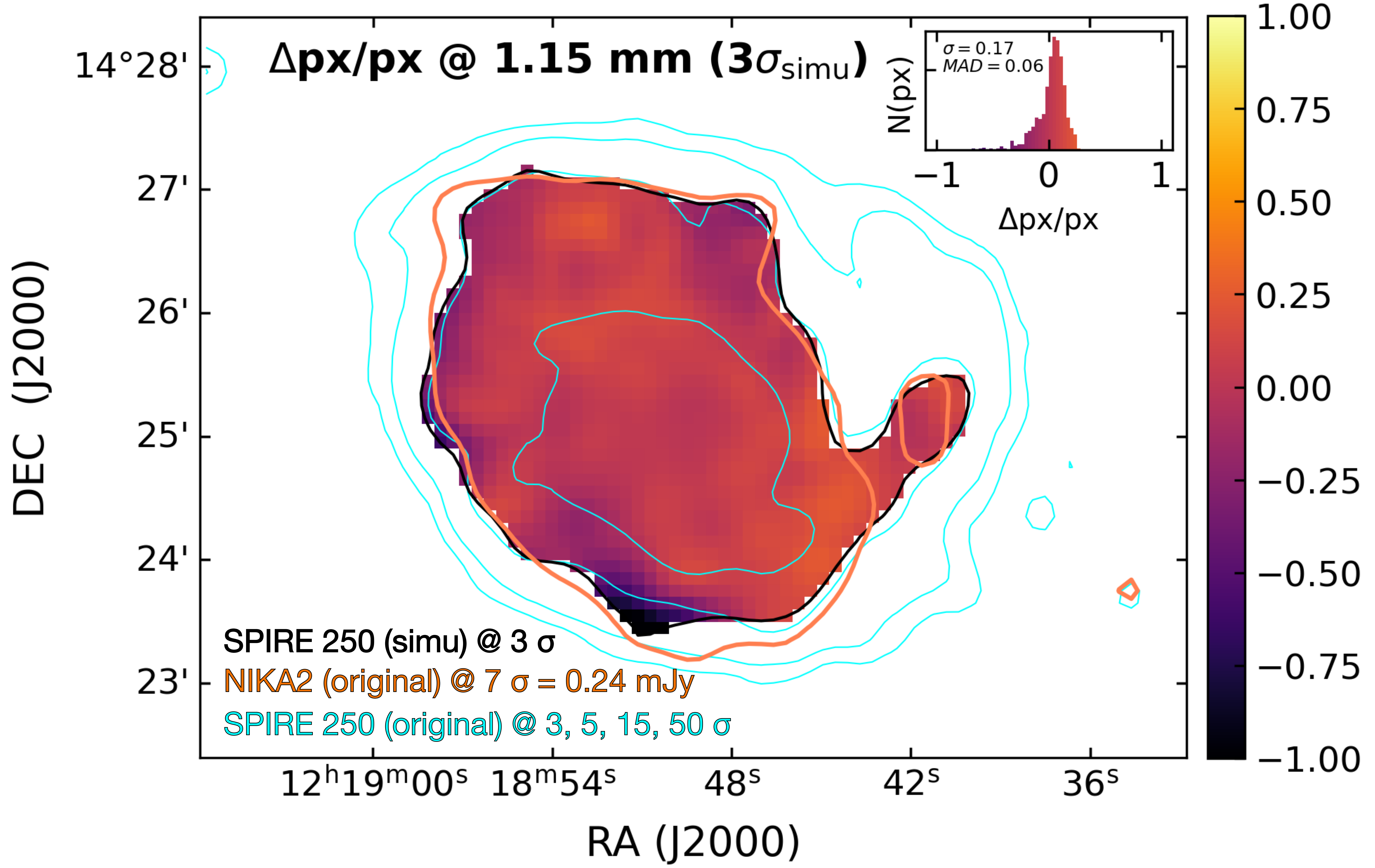

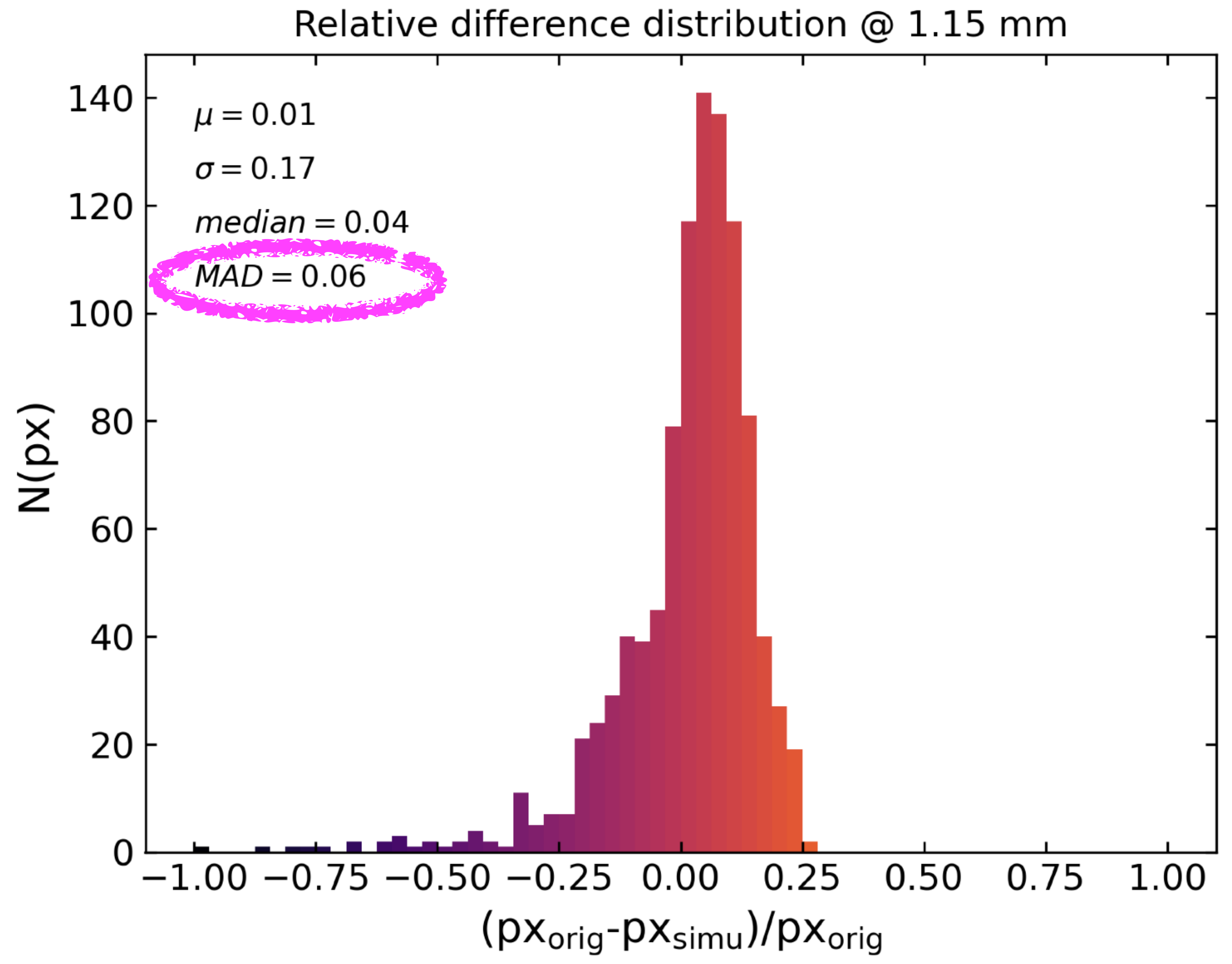

Scanam_nika maps: filtering

- How to include this evidence in our **uncertainty** budget?

Error = 10% of the NIKA2 flux matching the 3σ simu

added in quadrature to the statistical error map (sky_rms in Scanam_nika header).

PX SCALE (2 mm)

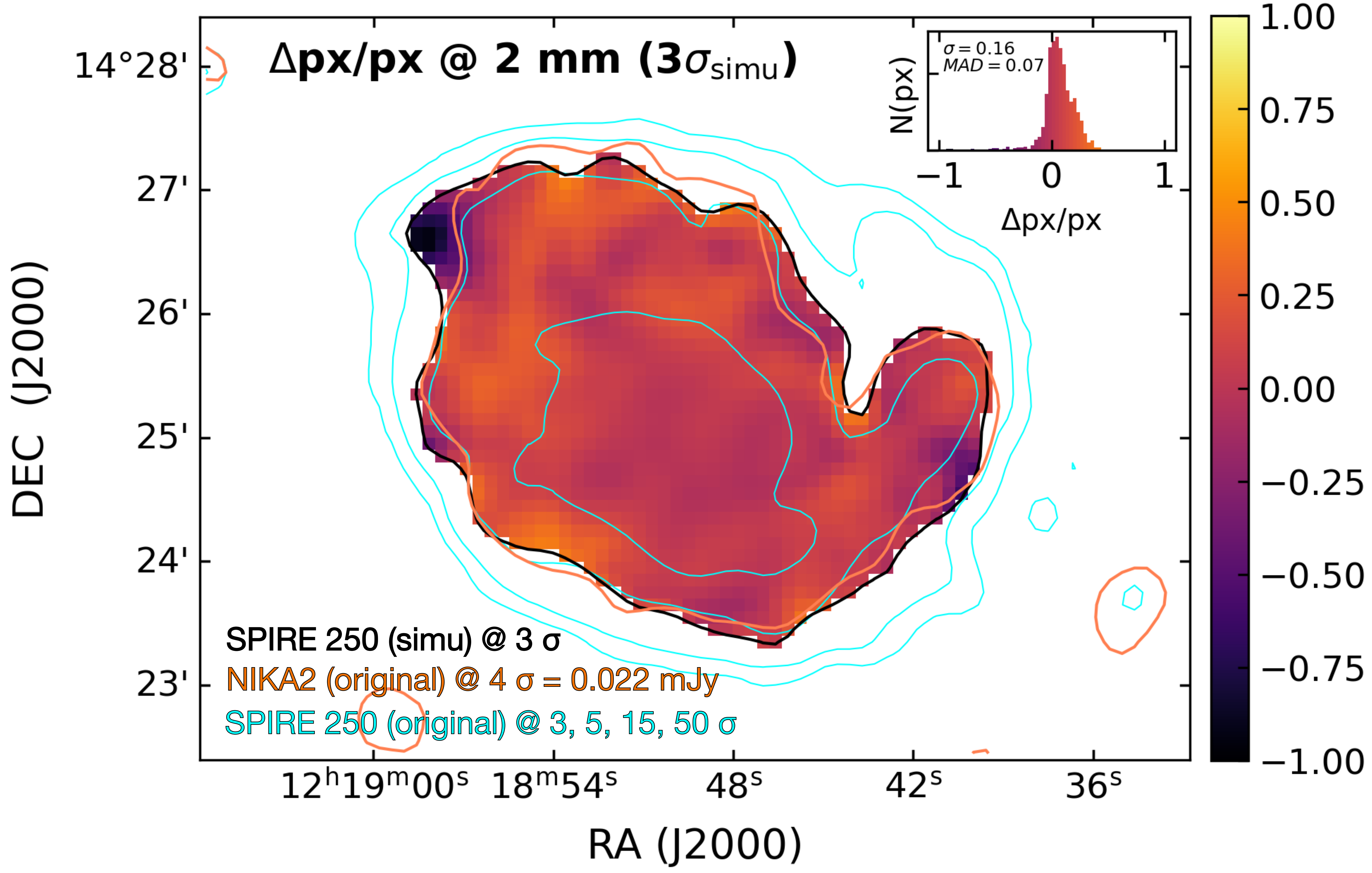

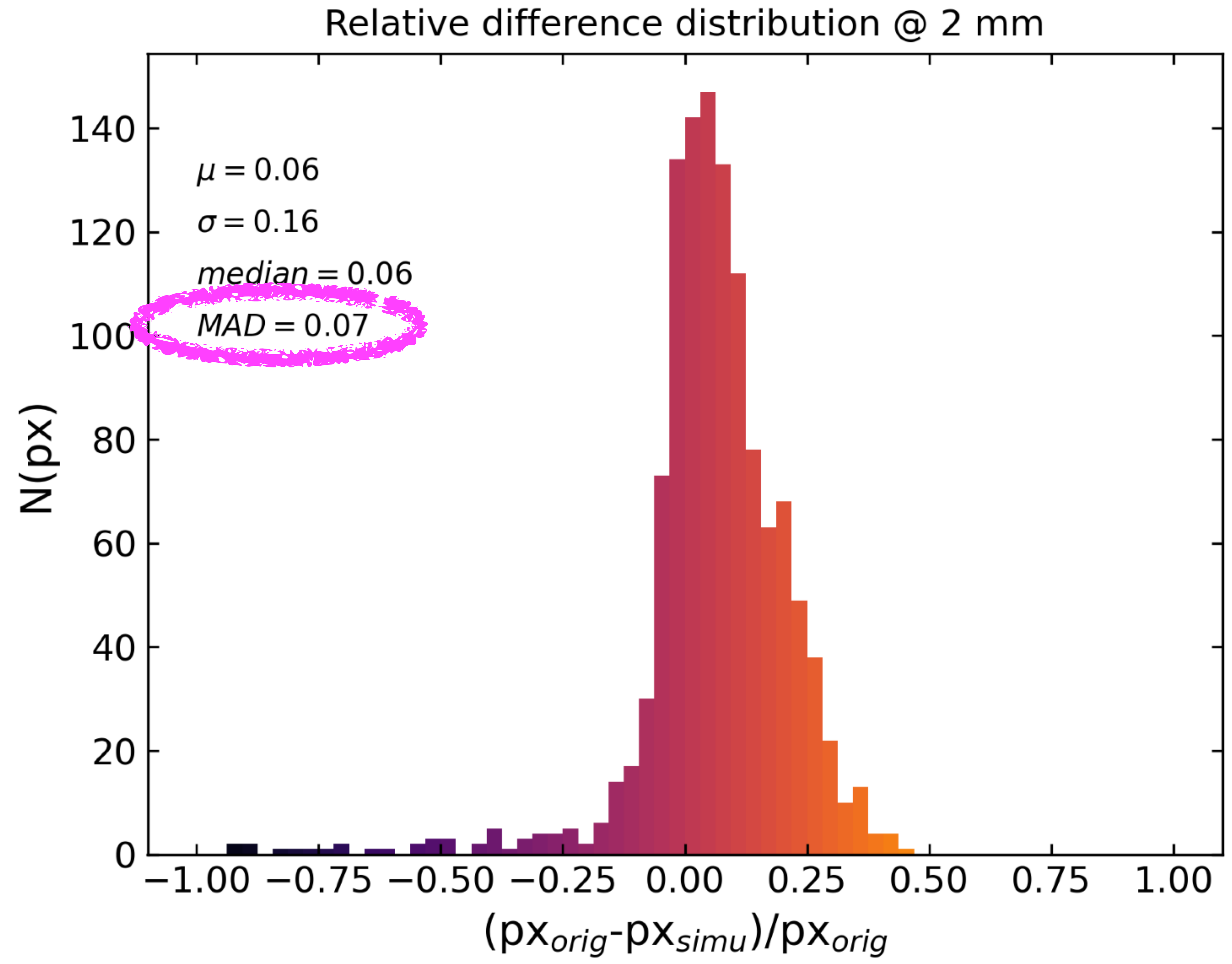

Data

Used for computing the **SFR** surface density & **stellar mass** maps.

Used for computing the total **gas mass** and **subtract CO** from NIKA2 and Planck.

IRAC images are calibrated for **point sources**. IRAC flux densities must be multiplied by 0.91, 0.94, 0.66, and 0.74 for the 3.6 µm, 4.5 µm, 5.8µm, and 8 µm bands respectively.

Telescope/Instrument	λ_{obs} [μm]	θ_{res}^{FWHM} [″]	Pixel size [″]	Calibration factor [%]	SED fitting	Calibrators	Ref.
GALEX/FUV	0.153	4	3	4.5		✓	*a*
GALEX/NUV	0.227	5.6	3	2.7		✓	*a*
Spitzer/IRAC	3.6	1.66	0.6	10.2	✓	✓	*a*
Spitzer/IRAC	4.5	1.72	0.6	10.2	✓		*a*
Spitzer/IRAC	5.2	1.88	0.6	10.2	✓		*a*
Spitzer/IRAC	8	1.98	0.6	10.2	✓		*a*
Spitzer/MIPS	25	6	1.5	4	✓	✓	*a*
Herschel/PACS	70	9	2	5.4	✓		*a*
Herschel/PACS	100	10	3	5.4	✓		*a*
Herschel/PACS	160	13	4	5.4	✓		*a*
Herschel/SPIRE	250	18	6	5.9	✓		*a*
Herschel/SPIRE	350	25	8	5.9	✓		*a*
Hersc	500	36	12	5.9	✓		*a*
IRAM A2	1150	12	3	7.7	✓		*c*
Planc	1380	300	103	1	✓		*c*
IRAM-30m/NIKA2	2000	18	3	5.8	✓		*c*
X-VLA+Effelsberg	3000	15	1	5	✓		*b*
C-VLA+Effelsberg	6000	15	1	5	✓		*b*
L-VLA	20000	4.5	0.7	3	✓		*d*

Table 2. Multi-wavelength continuum maps used in this work. In the order, we list (increasing wavelengths): the telescope and instrument name; the central wavelength; the angular resolution (FWHM); the pixel size; and the calibration factor. Finally, we indicate whether the map was used for SED fitting and/or as a calibrator. References: (*a*) Dustpedia archive; (*b*) Chyży et al. (2007); (*c*) this work; (d) Eric Koch and Karin Sandstrom. The reference for the GALEX-to-SPIRE calibration factors is Galliano et al. (2021) and references therein. For NIKA2 see Ejlali et al. (2025, their Appendix A1) for uncertainty on the beam solid angle (i.e. 5.8% at 1.15 mm and 2.9% at 2 mm), Perotto et al. (2020) and reference therein for uncertainty on Uranus model (i.e. 5%). For VLA+Effelsberg see Tabatabaei et al. (2017); Chemin et al. (2016) and for VLA see Perley & Butler (2015) and the official VLA NRAO website: https://science.nrao.edu/facilities/vla/.

Transition	Telescope	λ_{rest} [mm]	θ_{res}^{FWHM} [″]	Pixel size [″]
CO(2 – 1) [a]	IRAM–30m	1.3	13.4	2
CO(1 – 0) [b]	IRAM–30m	2.6	25.6	4
HI [c]	VLA	210	30	5

Table 3. Spectral line intensity maps used to compute the gas surface density of NGC4254 and correct the millimeter continuum for CO line emission contamination.
[a] HERACLES program (Leroy et al. 2009).
[b] EMPIRE program (Jiménez-Donaire et al. 2019).
[c] VIVA VLA Atlas (Chung et al. 2009).

Include 5% uncertainty on Uranus model (see Perrotto+20 and references therein)

CO(2-1) contamination in the mm continuum

$$\frac{C}{\mathrm{mJy\,beam^{-1}\,per\,K\,km\,s^{-1}}} = \frac{F_\nu}{\int T_{MB}\,\mathrm{d}v} = \frac{2k\nu^3}{c^3}\frac{g_\nu(\mathrm{line})}{\int g_\nu\,\mathrm{d}v}\Omega_b$$

(Drabek et al. 2012)

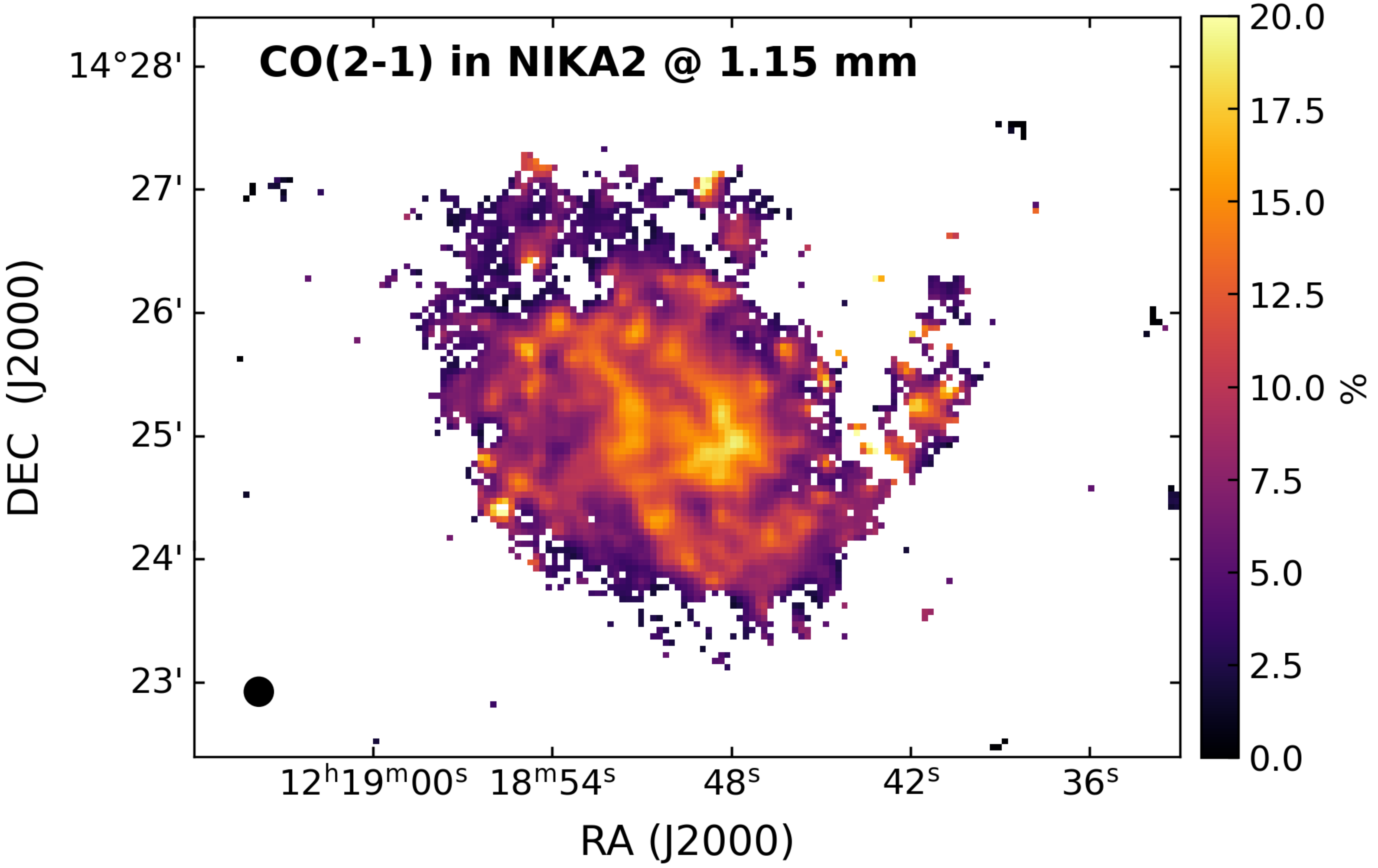

NIKA2 @ 1.15 mm:

C = 0.0476
CO flux = 9%
CO-sub flux = 0.59 ± 0.04 Jy

Planck @ 1.38 mm (HFI4):

C = 50.3
CO flux = 5%
CO-sub flux = 0.35±0.07 Jy

Integrated photometry

Photometry consistent with **Dustpedia** values (Clark et al. 2018), **KINGFISH** photometry presented in Aniano et al. (2020), and the IR photometry by **Chang** et al. (2020).

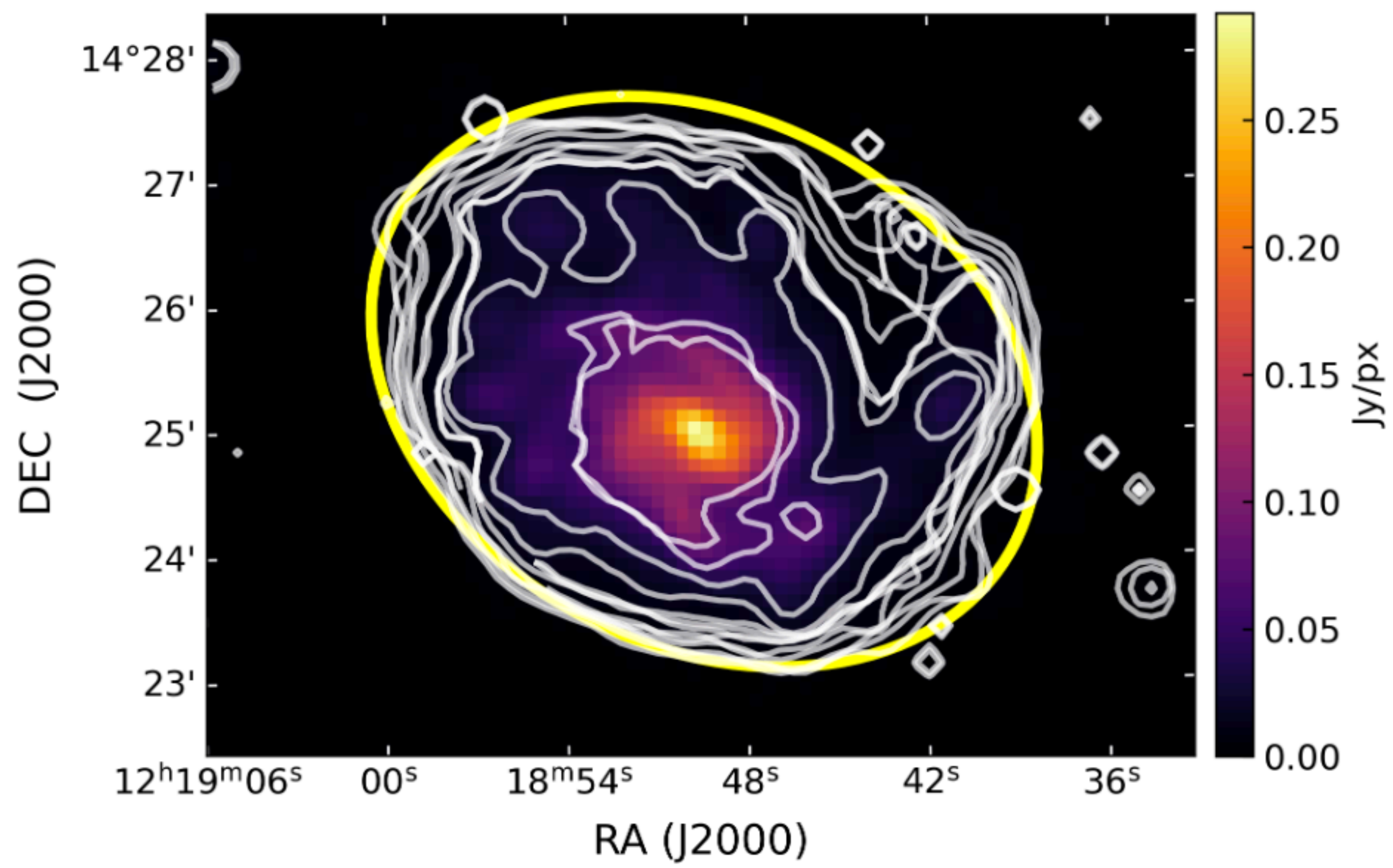

Fig. 5. SPIRE 250 μm $8' \times 6'$ cutout of NGC 4254, overlaid with the ellipse we use for computing the aperture photometry of the galaxy (yellow solid line). For reference, we show the multi-wavelength 5σ contours (white solid lines) of NGC 4254 of the bands listed in Tab. 5 at native angular resolution and pixel size.

Instrument	Luminosity [$10^7\ L_\odot$]	Flux [Jy]	Error [Jy]	Rms [mJy]
IRAC 3.6 μm	370	0.68	0.07	2
IRAC 4.5 μm	200	0.47	0.05	1.4
IRAC 5.2 μm	435	1.3	0.1	4
IRAC 8 μm	950	3.9	0.4	3
MIPS 25 μm	340	4.2	0.2	6
PACS 70 μm	1625	59	3	140
PACS 100 μm	2160	112	6	150
PACS 160 μm	1530	126	7	220
SPIRE 250 μm	475	61	4	204
SPIRE 350 μm	137	25	2	100
SPIRE 500 μm	32	8.3	0.5	55
NIKA2 1.15 mm	0.99	0.59	0.046	30
HFI4 1.38 mm	0.49	0.35	0.07	68
NIKA2 2 mm	0.089	0.092	0.016	14
X-VLA+Eff. 3 cm	0.0056	0.087	0.004	0.04
C-VLA+Eff. 6 cm	0.0048	0.148	0.007	0.3
L-VLA 20 cm	0.004	0.41	0.01	2

Table 5. Multi-band integrated photometry of NGC 4254 computed using HIP. The NIKA2 1.15 and Planck/HFI4 global fluxes are measured on the CO-subtracted maps (see Sect. 3.6). The NIKA2 rms includes the contribution from the scatter driven by large scale filtering (cf. Appendix A). All the maps were sky-flattened. Monochromatic luminosities (i.e. νS_ν) listed in the second column were computed assuming a distance of 14.4 Mpc (see Tab. 1).

Spiral arms, bulge and disk - photometry

Up to 18″ resolution to have a good morphological sampling.

Instrument	Spiral arms Flux [Jy]	Disk Flux [Jy]	Bulge Flux [Jy]	Total Flux [Jy]
IRAC 3.6 μm	0.50 ± 0.05 (0.04)	0.12 ± 0.01 (0.04)	0.058 ± 0.006 (0.002)	0.68
IRAC 4.5 μm	0.35 ± 0.04 (0.05)	0.082 ± 0.008 (0.06)	0.039 ± 0.004 (0.003)	0.47
IRAC 5.2 μm	1.0 ± 0.1 (0.2)	0.24 ± 0.02 (0.2)	0.076 ± 0.008 (0.015)	1.3
IRAC 8 μm	3.1 ± 0.3 (0.3)	0.72 ± 0.07 (0.4)	0.21 ± 0.02 (0.04)	4.0
MIPS 24 μm	3.4 ± 0.1 (0.7)	0.67 ± 0.03 (0.6)	0.28 ± 0.01 (0.2)	4.3
PACS 70 μm	48±3 (74)	8.4 ± 0.5 (43)	5.1 ± 0.3 (8)	61
PACS 100 μm	92 ± 5 (54)	17 ± 1 (62)	8.8 ± 0.5 (8)	117
PACS 160 μm	103 ± 6(48)	23 ± 1 (43)	8.5 ± 0.5 (8)	126
SPIRE 250 μm	46±3	12.6 ± 0.7	3.4 ± 0.2	62
NIKA2 1.15 mm	0.41 ± 0.02 (0.8)	0.17 ± 0.01 (0.8)	0.018 ± 0.001 (0.06)	0.6
NIKA2 2 mm	0.068 ± 0.001 (0.3)	0.0247 ± 0.0008 (0.4)	0.0031 ± 0.0001 (0.04)	0.095
X-VLA+Eff. 3 cm	0.066 ± 0.003 (0.02)	0.0188 ± 0.0009 (0.02)	0.0034 ± 0.0002 (0.0008)	0.088
C-VLA+Eff. 6 cm	0.107 ± 0.005 (0.03)	0.036 ± 0.002 (0.03)	0.0051 ± 0.0003 (0.001)	0.148
L-VLA 20 cm	0.285 ± 0.009 (0.04)	0.127 ± 0.004 (0.04)	0.0113 ± 0.0003 (0.002)	0.42

Table 8. Multi-band photometry of spiral arms, disk and bulge of NGC 4254, computed using HIP on the images degraded to 18″ resolution (i.e. beam FWHM of SPIRE 250 μm and NIKA2 2 mm). Notice that all the maps were sky-flattened. Fluxes (in Jy) are given along with the associated error which includes the flux calibration uncertainty. For reference, we report in brackets the statistical uncertainty (i.e., rms), in units of mJy. NIKA2 1.15 mm fluxes are measured on the CO-subtracted map (see Sect. 3.6). The NIKA2 rms values include the contribution from the scatter driven by large scale filtering (cf. Appendix A). The last column reports the sum of the three components, which is consistent with the global photometry reported in Tab. 5.